

الجمهورية الجزائرية الديمقراطية الشعبية
République algérienne démocratique et populaire
وزارة التعليم العالي والبحث العلمي
Ministère de l'enseignement supérieur et de la recherche scientifique
جامعة عين تموشنت بلحاج بوشعيب
Université –Ain Temouchent- Belhadj Bouchaib
Faculté des Sciences et de la Technologie
Département de Génie Civil et Travaux Publics



Projet de Fin d'Etudes
Pour l'obtention du diplôme de Master en : Structure.
Domaine : Science et Technologie
Filière : Génie Civil.
Spécialité : Structure.
Thème

**Comportement mécanique des nanostructures
fonctionnellement graduées reposant sur fondation élastique**

Présenté Par :

- 1) Mr. Bensaoula Sidahmed
- 2) Melle. ABDELHAKEM Chaimaa Racha

Devant le 04 /06/2024 devant le jury composé de :

Mme. ABDELBARI	MCA	UAT.B.B (Ain Temouchent)	Présidente
Mr. AMARA	Professeur	UAT.B.B (Ain Temouchent)	Examineur
Mme. ATTIA	MCA	UAT.B.B (Ain Temouchent)	Encadrant

Année Universitaire 2023/2024

الجمهورية الجزائرية الديمقراطية الشعبية
People's Democratic Republic of Algeria
وزارة التعليم العالي والبحث العلمي
Ministry of Higher Education and Scientific Research
جامعة عين تموشنت بلحاج بوشعيب
University of Ain Temouchent - Belhadj Bouchaib
Faculty of Science and Technology
Department of Civil Engineering and Public Works



Final Year Project
For the Master's Degree in: Structure
Field: Science and Technology
Major: Civil Engineering
Specialization: Structure
Topic

Mechanical behavior of functionally graded porous nanostructures resting on Elastic foundation

Presented By :

1. Mr. Bensaoula Sidahmed
2. Ms. ABDELHAKEM Chaimaa Racha

On 04/06/2024 before the jury composed of:

Mrs. ABDELBARI	MCA	UAT.B.B (Ain Temouchent)	President
Mr. AMARA	Professor	UAT.B.B (Ain Temouchent)	Examiner
Mrs. ATTIA	MCA	UAT.B.B (Ain Temouchent)	Supervisor

Academic Year 2023/2024

DEDICATION

To my dear father.

To my dear mother,

To my brothers Mohamed and Abdelrahim,

To my friends Yasmin, Hanaa, Chahra Zed, Noussaiba,

To all those who encouraged me throughout this work,

Abdelhakem Chaimaa Racha

DEDICATION

I dedicate this thesis to everyone who believed in me, stood by me, and helped me in my journey.

To my mother and father who always encouraged me and supported me in my path.

*To my dear brother **Farouk** and my dear sisters **Sophia** and **Amina**.*

*To my friends and fellow colleagues **Djawed**, **Amin**, **Sofian**, **Mohamed** and **Amina**.*

To all the teachers who contributed to shaping me into the man I am today with guidance and education.

Bensaoula Sidahmed

ACKNOWLEDGMENTS

We wish to express our profound gratitude to God, the Almighty and Merciful, who supported us with His strength and patience throughout the completion of this work.

This work was accomplished at the Laboratory of Engineering and Sustainable Development at Ain Temouchent University, under the supervision of Dr. **Attia Amina**. We would like to express our profound gratitude to her for her encouragement throughout the preparation of this thesis. Her valuable advice greatly helped us in successfully completing this work.

We are also grateful to the jury members Mme **ABDELBARI Salima** and Mr. **AMARA Khaled** who kindly agreed to be part of the jury and examine our work.

A special thank you is dedicated to Mr. **Bennacer Hamid**, who provided us with the training opportunity.

We do not forget our **parents**, whose love, sacrifice, and encouragement have been the pillars of our success. We extend our sincerest thanks to them, as well as to our friends, who supported us morally throughout the completion of this work

Abstract

The goal of this work is to use a first order shear deformation theory (FSDT) with four variables in the displacement field to investigate the static and dynamic behavior of functionally graded plates sitting on Winkler / Pasternak foundations-type. This study also examined the various forms of porosity in the FG plates that develop during the melting or mixing phases. The Navier's solution is used to solve the obtained differential equations. The Hamilton principle was also utilized to derive the equations of motion for the plates in this work, and using local theories and Eringen theories on continuum mechanics (non-local). The resulting numbers are contrasted with those found in other studies. Through a number of examples, a thorough parametric analysis was created to demonstrate how foundation parameters, porosity distributions, power indices, and geometry affect both perfect and imperfect FG plates.

Keywords:

Functionally graded material, Elastic foundation, First order shear deformation theory (FSDT), Porosity, Dynamic analysis. Local and non-local theories. Perfect and imperfect FG plates

Résumé

Ce travail vise à mettre en œuvre une théorie de déformation par cisaillement du premier ordre (FSDT) qui utilise quatre variables dans le champ de déplacement. Afin d'analyser les propriétés statiques et dynamiques des plaques fonctionnellement graduées qui sont basées sur des fondations de type Winkler / Pasternak. Les différentes formes de porosité présentes dans les plaques FG lors des phases de fusion ou de mélange ont également été étudiées dans cette étude. Les équations différentielles obtenues sont résolues à l'aide de la solution de Navier. Et en utilisant des théories locales et des théories de Eringen (non locales). Dans cette étude, on a également employé le principe de Hamilton pour dériver les équations de mouvement des plaques, et les résultats obtenus diffèrent de ceux présents dans d'autres études. Plusieurs illustrations ont été utilisées pour illustrer l'impact des paramètres de fondation, des distributions de porosité, des indices de puissance et de la géométrie sur les plaques FG parfaites et imparfaites.

Mots clés :

Matériau fonctionnellement classé, Fondation élastique, Théorie de la déformation par cisaillement du premier ordre (FSDT), Porosité, Analyse dynamique. Plaques FG parfaites et imparfaites. Théories locales et non locales.

المخلص

الهدف من هذا العمل هو دراسة السلوك الديناميكي والسكوني للصفائح المتدرجة وظيفيا المرتكزة على هياكل من نوع اساسات وينكلر / باسترناك باستخدام نظرية انحناء التشوه من الدرجة الاولى مع أربع متغيرات في مجال التشوه. تم ايضا استكشاف انواع مختلفة من الثقوب التي تظهر في الألواح ذات التركيب الوظيفي اثناء مراحل الانصهار او الخلط تم حل المعادلات التفاضلية التي يتم انتاجها باستخدام حل نافيه واستخدم نظريات إيرينجن في ميكانيكا الاستمرارية (نظريات غير محلية). قمنا باشتقاق معادلات الحركة للألواح في هذا العمل باستخدام مبدأ هاملتون ثم تمت مقارنة الارقام الناتجة مع تلك التي تم الابلاغ عنها في الادبيات. تم تطوير دراسة معمقة باستخدام عدة حالات لإظهار كيفية تأثير الاساس وتوزيع الثقوب ومؤشرات الطاقة والهندسة على كل من الألواح ذات تركيب الوظيفي المثالية وغير مثالية.

الكلمات المفتاحية:

المواد المتدرجة وظيفيا، الأساس المرن، نظرية تشوه القص من الدرجة الأولى المسامية، لوحات مثالية وغير المثالية، التحليل الديناميكي. النظريات المحلية وغير المحلية.

Table of Contents

ACKNOWLEDGMENTS

Abstract

List of Tables

List of Figures

Tables of contents

List of notations and symbols

General Introduction 1

CHAPTER 1: FUNCTIONALLY GRADED MATERIAL 3

I. Introduction:..... 3

I.1. The Concept of FGMs: 3

I.2. The Definition of Functionally Graded Material: 5

I.3. The Definition of Composite Materials: 6

I.4. The Difference Between FGM and Composite Materials: 7

I.5. Classification: 8

I.5.1. Structure-based Classification 8

I.5.2. Type-based Classification 9

I.5.3. Process-based Classification 9

I.6. Applications of FGMs:..... 10

I.6.1. Civil Engineering:..... 11

I.6.2. The importance of FGMs in civil engineering: 12

I.7. Advantages and Disadvantages of Functionally Graded Materials (FGM)..... 13

I.7.1. Advantages of FGM..... 13

I.7.2. Disadvantages of FGM 14

I.8. FGM Manufacturing Processes: 14

I.8.1. Physical Vapor Deposition (PVD)..... 15

I.8.2. Chemical Vapor Deposition (CVD)	15
I.8.3. Powder Metallurgy	15
I.8.4. Centrifugal Method	15
I.8.5. Tape Casting Method	15
I.8.6. Slip Casting	15
I.8.7. Solid Freeform Fabrication Method (SFF)	15
I.8.8. Directed Energy Deposition	16
I.8.9. Plasma Spraying	16
I.8.10. Sintering and Infiltration	16
I.9. Conclusion:	19
CHAPTER II: THEORIE OF PLATES	20
II. Introduction	20
II.1. The analytical models of FGM plates.	20
II.1.1. Classical Plate Theory of Love-Kirchhoff	20
Various applications of classical thin plate theory (CPT)	22
II.1.2. First-Order Shear Deformation Theory (FSDT)	23
Various applications of First-Order Shear Deformation Theory (FSDT):	24
II.1.3. High-order shear deformation theories (HSDT):	25
Various applications of High-order shear deformation theories (HSDT):	26
II.1.4. The different models of high-order theory:	27
II.2. The material properties of FGM plates:	29
II.2.1. The power law mixing law or material property of a P-FGM structure (power law)	30
II.2.2. Sigmoid mixing law or material property of an S-FGM structure (sigmoid law):	32
II.2.3. Exponential mixing law or material property of an E-FGM structure (exponential law):	34
II.3. Conclusion	35
CHAPTER III: ANALYTICAL STUDY OF FG PLATE	36
III. Introduction	36
III.1. Background and Motivation	36
III.2. Research Objectives	38
III.3. Geometry and concept of the functionally graduated plate (P-FGM)	39
III.4. Functionally graded porous plates:	40

III.5. Types of porosity distribution:	41
III.5.1. FGM plates with porosity type I (even porosities):	41
III.5.2. FGM plates with porosity type II (uneven porosities)	41
III.5.3. FGM plates with porosities type III (logarithmiques- uneven porosities)	42
III.5.4. FG plate with type IV porosities (density):	42
III.5.5. FGM plates with porosity type V:	43
III.6. The four-variable first-order theory FSDT improved:	43
III.6.1. Cinematic:	44
III.7. Nonlocal Theory and Constitute Relations:	45
III.8. Movement Equation:	46
III.9. The Navier method:	49
III.10. Conclusion:	52
CHAPTER IV: RESULT AND DISCUSSION	53
IV. Introduction	53
IV.1. Presentation and Analysis of Results:	53
IV.1.1. Mechanical Analysis of Macroscopic Functionally Graded Material (FGM) Plates	53
IV.1.2. Dynamic Analysis of Macroscopic Functionally Graded Material (FGM) Plates	61
A- Perfectly Supported FG Plate	61
B- The perfect FG plates resting on an elastic foundation (Winkler-Pasternak)	66
C- Perfect and imperfect FG plates resting on the Winkler-Pasternak elastic foundation	68
IV.1.3. Dynamic analysis of free FG nano-plates at the nanoscale	70
A- Perfectly Supported Nano-FG Plate	70
B- Perfect and imperfect FG nano-plates resting on the Winkler-Pasternak elastic foundation	71
IV.2. Conclusion:	82
GENERAL CONCLUSION	83
Bibliographic references	85

List of Figures

Figure I. 1:Materials development towards FGM ((Mahamood and al., 2012))	5
Figure I. 2: Classification of composite materials.	6
Figure I. 3:Characteristics of FGM Composite Materials Compared to Conventional Composite	7
Figure I. 4:Functionally graded materials with different gradient forms [(Zhang et al., 2019)]. a Discrete/discontinuous FGM with interface. b Continuous FGM without interface. c, f Composition gradient. d, g Orientation gradient. e, h Fraction gradient	9
Figure I. 5:Typical example of three different types of FGM gradient (Popoola et al., 2016)	10
Figure I. 6:Applications of FGMs.	11
Figure I. 7:Commonly used processing techniques for the production of FGMs (ADDOU, 2021)	18
Figure II.1: Schematization of plate deformations by the classical theory «CPT» (Reddy, 1997)	21
Figure II 2: Representation of the Reissner-Mindlin plate (Reddy, 1997)	24
Figure II 3: High-order plate representation (Reddy, 1997)	25
Figure II 4: Plate model of functionally graded materials (FGM)	30
Figure II 5: Variation of the volume fraction in a P-FGM plate	31
Figure II 6 :Variation of the volume fraction in an S-FGM plate	33
Figure II 7: Variation of Young's modulus in an E-FGM plate.	34
Figure III. 1: FG plaques supported on elastic foundations.	39
Figure III. 2:Presentation of various representations of porosity variations.	40

Figure IV. 1:Variation of transverse shear stress as a function of $z/hz/h$ for a square FGM plate on elastic supports with $a/h=10$, $p=2$: (a) $K_0 =10$; (b) $K_1=10$	57
Figure IV. 2:Variation of normal stress as a function of $z/hz/h$ for a square FGM plate on elastic supports with $a/h=10$, $p=2$, (a) $K_0 =10$. (b) $K_1 =10$	59
Figure IV. 3:Variation of the shear stress as a function of z/h for a square FGM plate on elastic supports with $a/h=10$, $p=2$: (a) $K_0=10$; (b) $K_1=10$	60
Figure IV. 4:The variation of the first five modes of the nondimensional frequency $\omega *$ of simply supported isotropic square FG plates.	74
Figure IV. 5: The variation of the nondimensional frequency ω of AL/AL2O3 FG square plates as a function of the power index parameter.	75
Figure IV. 6: The variation of the nondimensional frequency ω of rectangular FG plates as a function of the power index parameter.....	75
Figure IV. 7:the effect of the elastic foundation and the power index on the nondimensional frequency ω of plates with $a/h = 10$	76
Figure IV. 8:The variation of the nondimensional frequency ω of imperfect FG plates, resting on a Pasternak elastic foundation as a function of the porosity index for even porosities.	77
Figure IV. 9: The variation of the nondimensional frequency " ω " of imperfect FG plates, resting on a Pasternak elastic foundation as a function of the porosity index for uneven porosities.....	78
Figure IV. 10:the variation of the nondimensional frequency ω of perfect and imperfect FG plates resting on a Pasternak elastic foundation, as a function of different porosity variations with $\xi = 0.2$	79
Figure IV. 11 The effect of non-local parameter (with μ values less than 0.5) on the variation of nondimensional frequencies of nano-plates without a foundation for different power index values.	80
Figure IV. 12: The effect of non-local parameter (with μ values ranging from 0 to 2.5) on the variation of nondimensional frequencies of nano-plates without a foundation for different power index values.	80
Figure IV. 13: the variation of the dimensionless frequency of nano-plates ($h/a=0.1$). based on different types of foundations. depending on non-local parameters, (with $\xi = 0.2$, $p = 1$).	81

Liste of tables

Table I. 1: A comparison between ceramic and metal properties.	5
Table II. 1: Different shear functions used in plate theories isotropic and FGM (Boukhari, 2016)	27
Table IV. 1: Comparison of non-dimensional deflections and transverse shear stresses of an FGM plate under sinusoidal loading.	55
Table IV. 2: Comparison of non-dimensional deflections of a homogeneous plate under uniform loading resting on a Winkler foundation for $a/h=100$.	55
Table IV. 3: Comparison of non-dimensional deflections of a homogeneous plate under uniform loading resting on a Winkler-Pasternak elastic foundation for $a/h=100$.	56
Table IV. 4: The first five dimensionless fundamental frequencies ω^* of a simply supported	62
Table IV. 5: The first two nondimensional fundamental frequencies $\hat{\omega}$ of square Al/Al₂O₃ plate.....	63
Table IV. 6: The first four nondimensional frequencies $\bar{\omega}$ of a rectangular plate ($b/a=2$)	64
Table IV. 7: Fundamental nondimensional frequencies « ω » of isotropic and square FG plates resting on Winkler-Pasternak foundations.	67
Table IV. 8: Variations of the frequency parameters « ω » of perfect and imperfect square FG plates with respect to the stiffness of Winkler-Pasternak foundations ($p=1$).	69
Table IV. 9: The first four nondimensional frequencies ω of rectangular nano-plates (with ($b/a=2$ et $a/h=10$))	71
Table IV. 10: Variations of the frequency parameters "ω^-" of perfect and imperfect square FG nano-plates with respect to the stiffness of Winkler-Pasternak foundations ($p=1$) and ($h/a=0.1$).	72

List of notations and symbols

a	Length of the plate
b	Width of the plate
h	Thickness of the plate
z	Origin at the mid-surface of the beam and in the thickness direction
u, v, w	Displacements in the x, y, z directions
u_0, v_0, w_0	Displacements on the mid-plane of the plate
w_b	Transverse displacement due to bending
w_s	Transverse displacement due to shear
θ	Rotation
$\varphi_x, \varphi_y,$	Rotations around the x, y axes
$f(z)$	Transverse shear function
E	Young's modulus
E_C	Young's modulus of the ceramic
E_M	Young's modulus of the metal
ν	Poisson's ratio
$E(z)$	Young's modulus as a function of "z"
$\rho(z)$	Density as a function of "z"
$\nu(z)$	Poisson's ratio as a function of "z"
$V(z)$	Volume fraction
P	Material index
m_0, m_1	Real and apparent mass density
ξ	Porosity index
φ	Porosity distribution type parameter
$\sigma_x, \sigma_y, \sigma_z$	Components of normal stresses
$\tau_{xz}, \tau_{yz}, \tau_{xy}$	Components of tangential stresses
$\varepsilon_x, \varepsilon_y, \varepsilon_z$	Strains in the x, y, z directions
$\gamma_{xz}, \gamma_{yz}, \gamma_{xy}$	Distortions in the x, y, z directions

δ	Variation
$\delta u_0, \delta v_0, \delta w_0, \delta \theta$	Virtual displacement field
$\delta \varepsilon_x, \delta \varepsilon_y, \delta \varepsilon_z$	Virtual longitudinal strain field
$\delta \gamma_{xz}, \delta \gamma_{yz}, \delta \gamma_{xy}$	Virtual transverse strain field
μ	Non-local parameter
δU	Variation of strain energy
δV	Variation of external work
δK	Variation of kinetic energy
δU	Variation of foundation deformation energy
N_x, N_y, N_{xy}	Normal forces
M_x, M_y, M_{xy}	Bending moments
Q_{xz}, Q_{yz}	Shear force
K_w	Winkler parameter
G_p	Pasternak parameter
$U_{mn}, V_{mn}, W_{mn}, X_{mn}$	Arbitrary parameters
ω	Natural frequency
∂	Partial derivative
i, j	Natural numbers
C_{ij}	Stiffness coefficients
A_{ij}	Membrane stiffness terms
B_{ij}	Coupling stiffness terms
D_{ij}	Bending stiffness terms
I_0, I_1, I_2	Moment of inertia components
∇	Laplace
$\{ \}$	Column vector
$[]$	Matrix
$[K]$	Stiffness matrix
$[M]$	Mass matrix

General Introduction

General Introduction

Functionally Graded Materials (FGM) are an advanced form of composite materials which usually consists of metal and ceramic which makes it possible to customize and modify the characteristic of the result material thus resulting in improving its mechanical behavior, and although it was originally created in order to create a barrier against high temperatures but its uses have evolved and is being employed in several sectors such as aerospace, automotive, nuclear energy and civil engineering ((Sofiyev & Avcar, 2010),(Bessaim and al, 2013), (Naebe & Shirvanimoghaddam, 2016), (Ebrahimi and al, 2017), (Zidi and al, 2017),(El-Haina and al, 2017), (Avcar and al, 2018),(Zarga and al, 2019),(Karami and al, 2019), (Hellal and al., 2021)). There are different types of conventional continuum theories and each theory has its properties and qualities and uses like where the classical plate theory (CPT) can only be used on thin plates since it ignores transverse shear deformation making it less accurate when using any other plates, while the first-order shear deformation theory (FSDT) takes into consideration transversal shear deformation so it can be used on both thin and medium plates, Lastly The higher-order shear deformation theory (HSDT) it doesn't need a shear correction coefficient which in itself depends on the variables of geometry, load and boundary conditions and thickness of plates thus making higher-shear deformation theory (HSDT) a more reliable shear deformation theory than classical plate theory and first shear deformation theory (FSDT) and can be used on thin, medium as well as thick plates.((Al-Basyouni and al, 2015), (Bouderba, Houari, & Tounsi, 2013),(M. Avcar, 2016), (Youcef and al, 2018), (Draoui and al, 2019)). While the classical structural theories (local theories) are founded on the assumption that stress at a specific point is solely influenced by the strain at that same point. The non-classical continuum mechanics (nonlocal), states that stress at a point is influenced by strains across the entire continuum ((Reddy and al,2008)(Lu and al, 2007), (Heireche and al, 2008), (Benzair and al., 2008), (Amara and al, 2010)). Porosities are a result of divergent solidification temperatures of the material elements, thus creating micro voids during the sintering process during the process of manufacturing Functionally Graded Materials (FGMs). These tiny spaces, are what referred to as porosities, the introduction of air bubbles into the matrix during the melting or mixing stages is one of the main causes for these micro-voids. Furthermore, water vapor may develop on particle surfaces during the solidification process, which aids in the creation of micro gaps in the material structure. In order to minimize porosity and guarantee the appropriate material integrity and functionality, careful control and optimization of manufacturing parameters like temperature, pressure, and atmosphere are required. These porosities (micro voids) have the potential to significantly affect

General Introduction

the mechanical properties and overall performance of the FGM. A number of foundation models have been introduced to better define the interaction between the plate and the foundation as a result of the growing interest in the study of integrated structures, there various model to which are used among them are the Winkler model and the Pasternak model, the Winkler model which operates on utilizing springs alone and the Pasternak model in which it enhances the Winkler model by adding a shear layer to it with a two-parameter substrate resulting in a much more reliable model in the representation of mechanical interactions, especially when it comes to flexible plates ((Wang and al, 2005). (Winkler,1867); (Kolahchi and al, 2016). (Pasternak, 1954).(Akhavan and al, 2009), (Hsu, 2010), (Baferani and al, 2011), (Lü and al, 2009), (Bouderba et al., 2013), (Bounouara and al, 2016), (Sobhy, 2013). (Kneifati, 1985)).

The first chapter concentrates mainly on Functionally Graded Material's FGM, what they are, from what they are made of and what are the various field of applications for it, this chapter mainly focuses on introducing the reader to the concept.

The second chapter delves deeper into the subject, we discuss the different types of theories that are used for researching the mechanical behavior of FGM plates which they are, first the classical plate theory (CPT), the second one is first order shear deformation theory (FSDT), and lastly the high order shear deformation theory (HSDT).

In the third chapter, we explained what porosities are and how they are created and conducted research on a functionally graded metal-ceramic nano plate (P-FGM) that was resting on an elastic foundation of the Winkler-Pasternak type by using first order shear deformation theory (FSDT) with four Unknown's as well as Eringen continuum mechanics (non-local theories).

Chapter 4 will have a thorough parametric analysis and discussion of the ways in which the porosity parameter, power index, stiffness of the number of modes and shape and the foundation parameters affect the behaviors under consideration.

And a general conclusion on the entirety of our work by which it will allow us to discuss our findings on FGM throughout our thesis.

CHAPTER 1
Functionally graded material

I.Introduction:

Functionally Graded Materials (FGMs) offer customized engineering opportunities to satisfy the unique requirements of many applications, marking an important milestone in the field of advanced materials. One characteristic that sets FGMs apart is their capacity to display intentional and progressive changes in their characteristics across their structure. Because of this special quality, which opens the door to the best performance possible, FGMs are a crucial material category in the context of modern technology. FGMs are utilized in a variety of industries, including shipbuilding, civil engineering, automotive, and aerospace. They provide benefits including high strength, light weight and resistance to corrosion, and the capacity to manufacture complicated shapes. Because of their distinct qualities and capacity to adapt to many media formats, they are continually changing and becoming more and more used in a variety of sectors. Because of their unique qualities and capacity to adapt to many media formats, they are continually changing and becoming more and more used in a variety of different sectors. Y. Koizumi first proposed the idea of functionally graded materials (FGMs) in 1984.

I.1. The Concept of FGMs:

Functional Gradient Materials (FGMs) are a class of heterogeneous materials that exhibit controlled spatial variation in their chemical and/or structural characteristics in at least one direction. This gradual variation in properties is achieved through deliberate modification of chemical composition, microstructure, or atomic order depending on the position within the material.

FGMs are often composed of a mixture of ceramic and metal, with a ceramic-rich surface and a metal-rich surface (Table I.1), between which a gradual change in volume fractions is observed (Reddy, 2000). This technology, which mimics the structural complexity of natural materials such as bones, teeth and bamboo ((Bakar and al, 2018) ; (Sato and al, 2017)), was first proposed in 1972 for composites and polymer materials ((Bohidar and al, 2014)). However, it was in 1984 in Japan that FGMs were applied in an innovative way during the design of a space shuttle (Ashwinkumar, 2017), aiming to create a material capable of withstanding temperature variations of around 1000°C. (Figure I.1).

FGMs represent a significant advance in the field of materials science, offering solutions to the limitations inherent in homogeneous materials. For example, a homogeneous material with excellent thermal resistance might lack ductility, while a ductile material might not withstand high temperatures. FGMs, however, enable a combination of properties that were previously considered mutually exclusive. Creating FGMs requires a thorough understanding of materials chemistry, thermodynamics, materials mechanics, and manufacturing processes. Manufacturing techniques for FGMs are diverse and include methods such as physical vapor deposition (PVD), chemical vapor deposition (CVD), gradient sintering, powder metallurgy, and computer-aided extrusion. These techniques must be meticulously controlled to ensure a precise and efficient gradient of functional properties.

The application of FGMs extends to many fields, ranging from aerospace, where they are used for heat shields and engine components, to the biomedical industry, where they are integrated into implants for better integration with bone tissue. In the energy sector, FGMs contribute to improving the performance of gas turbines thanks to their resistance to high temperatures and thermal gradients. Additionally, in electronics, FGMs enable the development of substrates for circuits that can withstand significant thermal stress without compromising electrical conductivity. Innovation in the field of FGMs continues to grow, with ongoing research to develop even more resistant materials adapted to extreme environments. Scientists are also exploring the possibility of integrating nanotechnologies to further refine property gradients and pave the way for revolutionary applications.

In conclusion, functionally gradient materials represent a fascinating and constantly evolving area of materials science. They offer almost unlimited possibilities for the design of advanced systems and structures. With their ability to mimic complex natural materials and withstand extreme conditions, FGMs have the potential to transform many industrial sectors and become a pillar of technological innovation. The history of FGMs, from their initial design to their application in cutting-edge projects, Figure I.1 shows the development of the materials towards FGM (Mahamood and al, 2012).

Table I. 1:A comparison between ceramic and metal properties.

<i>Ceramics</i>	<i>At the Hight of Temperature</i>	<ul style="list-style-type: none"> • <i>Good thermal Resistance</i> • <i>Good resistance to oxidation</i> • <i>Low thermal conductivity</i>
<i>Ceramic-Metal</i>	<i>Continuity of Material from point to point</i>	<ul style="list-style-type: none"> • <i>Elimination of the interface problem</i> • <i>Relax thermal stress</i>
<i>Metal</i>	<i>At the low of Temperature</i>	<ul style="list-style-type: none"> • <i>Good mechanical stress</i> • <i>High thermal conductivity</i> • <i>Very good toughness</i>

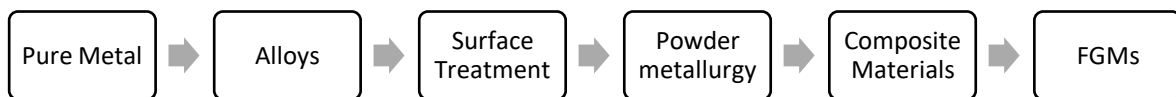


Figure I. 1:Materials development towards FGM (Mahamood and al., 2012)

I.2. The Definition of Functionally Graded Material:

A manufactured material that varies purposefully and systematically in composition, microstructure, or structural qualities is known as functionally graded material. Materials that have been functionally graded (FGM) are intentionally designed to display various, continuous gradients that are optimized for one or more properties. Basically, anything that is purposefully made to have structural modifications on a regular basis is considered functionally designed. Differentiating functionally designed materials from more homogeneous ones is the ability to purposefully increase the number of materials in order to improve specific performance

characteristics. Products that are efficiently employed to meet needs across applications will have more possibilities as a result of this customization (Li and al., 2020).

I.3. The Definition of Composite Materials:

A composite material is a material that combines two or more separate materials with varying properties. These constituents, occasionally denoted as component phases, retain their unique properties inside the ultimate structure of the composite. Together, these components create a unique mixture that has better properties than either one alone. Because of their versatility and ability to provide customized features, compounds are highly sought in a wide range of industries. Because of their capacity to provide mechanical flow ahead, composites are highly sought after in applications demanding long-term and permanent performance. The materials are often referred to as the matrix (continuous phase) and the reinforcement (dispersed phase).

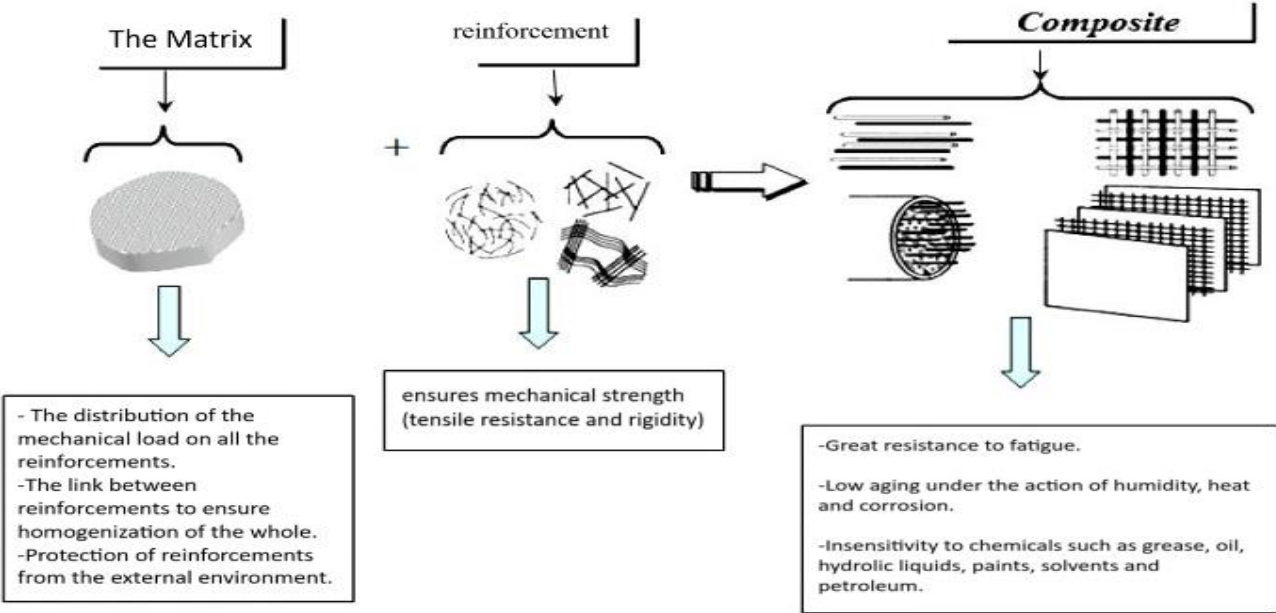


Figure I. 2: Classification of composite materials.

I.4. The Difference Between FGM and Composite Materials:

Composite materials are manufactured by combining two or more different materials to form a new material with improved properties. These materials typically consist of distinct layers, such as fibers embedded in a matrix. Composites are widely used in applications such as aerospace, automotive, construction, and sporting goods due to their high strength, lightweight nature, and tailored properties.

On the other hand, Functionally Graded Materials (FGM) are materials that exhibit a gradient in their composition, microstructure, or properties. This means that the material changes gradually from one end to the other, rather than having distinct layers. FGMs are often used in engineering applications where a smooth transition of properties is needed, such as in thermal barrier coatings, dissimilar material joints, or components for extreme environments.

It's important to note that FGMs can be considered as a specific category of composite materials, but with a more continuous structure and property gradient. FGMs offer advantages such as reduced interfacial shear stresses and improved resistance to delamination compared to traditional composites ((J. Wang, 1999); (Chawla, 2012). Materials.(Koizumi, 1997)

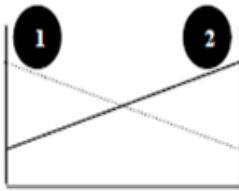
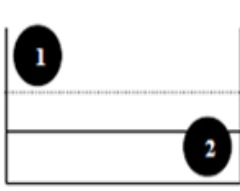
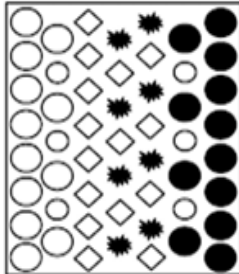
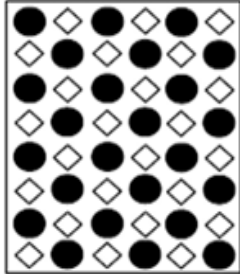
Property	<p>1 -Mechanical resistance.</p> <p>2 -Thermal conductivity.</p>		
Structure	<p>-Elements:</p> <p>ceramic ○</p> <p>metal ●</p> <p>microprosite ○</p> <p>fiber ◇</p>		
Material	Example	FGM	NON-FGM

Figure I. 3:Characteristics of FGM Composite Materials Compared to Conventional Composite

I.5. Classification:

Functionally Graded Materials (FGM) have undergone significant classification over time due to the advancement of applications and technologies aimed at producing FGM at various scales. In this article, we will delve into three primary classification criteria: structure, type, and application domain of FGM.

I.5.1. Structure-based Classification

FGM can be classified based on their structural characteristics, primarily into two groups: continuous gradient materials and discontinuous gradient materials (Figuer I.4) (Makwana and al., 2014); (Zhang and al., 2019).

- **Continuous Gradient Materials:** Continuous gradient materials exhibit a smooth transition in properties without distinct interfaces.
- **Discontinuous Gradient Materials:** Discontinuous gradient materials showcase abrupt changes in composition or microstructure, often categorized into different types based on the nature of the gradient.

In addition, these materials can also be classified into three gradient types:

- Gradient of composition (Figure. I.4 c, f).
- Gradient of orientation (Figure. I.4 d, g).
- Gradient of fraction (Figure. I.4 e, h).

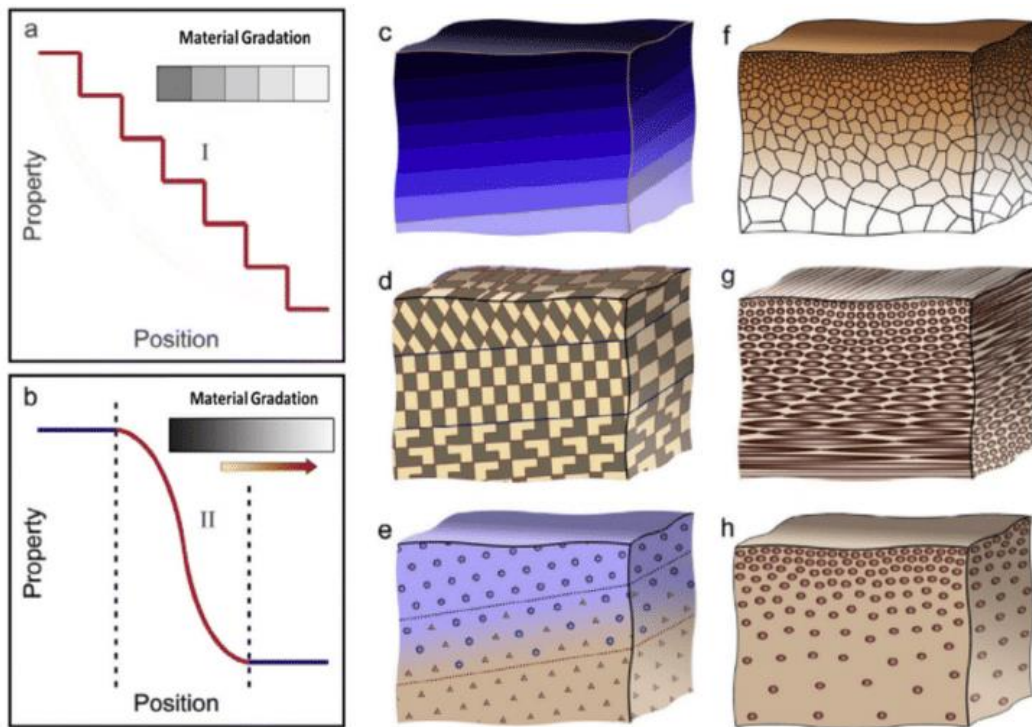


Figure I. 4:Functionally graded materials with different gradient forms [(Zhang et al., 2019)]. a Discrete/discontinuous FGM with interface. b Continuous FGM without interface. c, f Composition gradient. d, g Orientation gradient. e, h Fraction gradient

I.5.2. Type-based Classification

FGM classification based on type considers three primary gradients : composition, microstructure, and porosity (Figure I.5) (ELMASCRI, 2020).

- Composition Gradient: This type of FGM classification focuses on variations in material composition, leading to diverse chemical structures.
- Microstructure Gradient: in FGM are obtained during the solidification process, resulting in varied surface and internal microstructures.
- Porosity Gradient: within FGM change with spatial location, affecting the material's properties and performance.

I.5.3. Process-based Classification

Another classification criterion involves categorizing FGM production processes into constructive and transport processes.

- Constructive Process: involve layer-by-layer fabrication, enabling precise control over gradient (Ngo and al., 2018)
- Transport Process: rely on physical methods such as fluid flow, diffusion, or thermal conduction to create gradients within structures (K. Wang and al., 2012), (Kaushal and al., 2018).

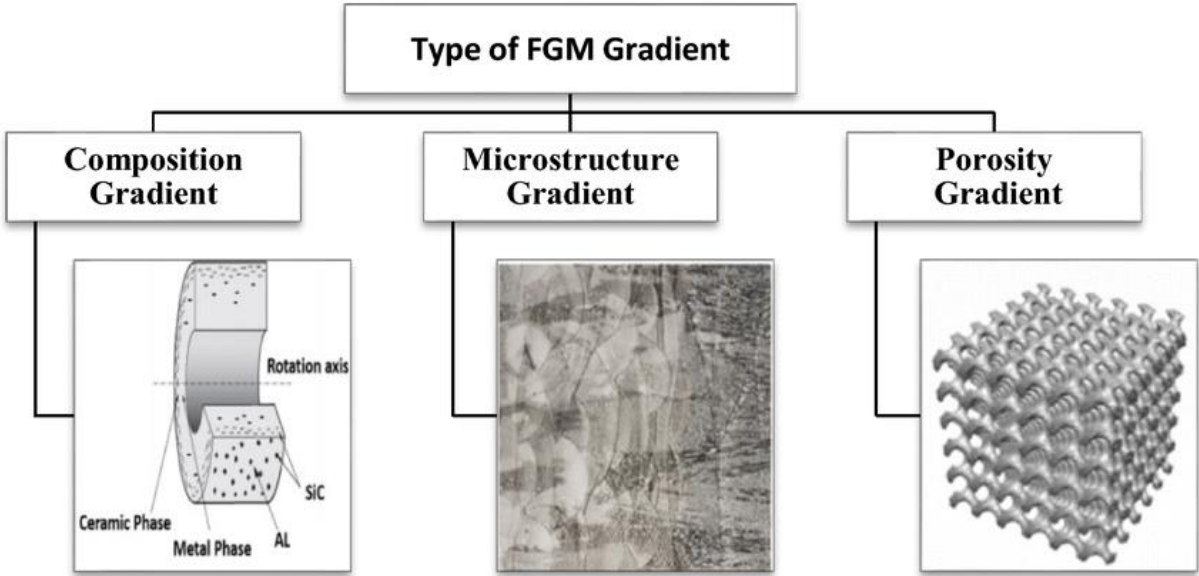


Figure I. 5: Typical example of three different types of FGM gradient (Popoola et al., 2016).

I.6. Applications of FGMs:

Functionally graduated materials (FGM) can be used in various fields, as shown in Figure I.6. They offer the possibility of combining contradictory properties such as conductivity and thermal insulation in the same material, which allows them to be used in different areas. Although the concept was originally developed for the aviation industry, it is now applicable to a wide range of fields.

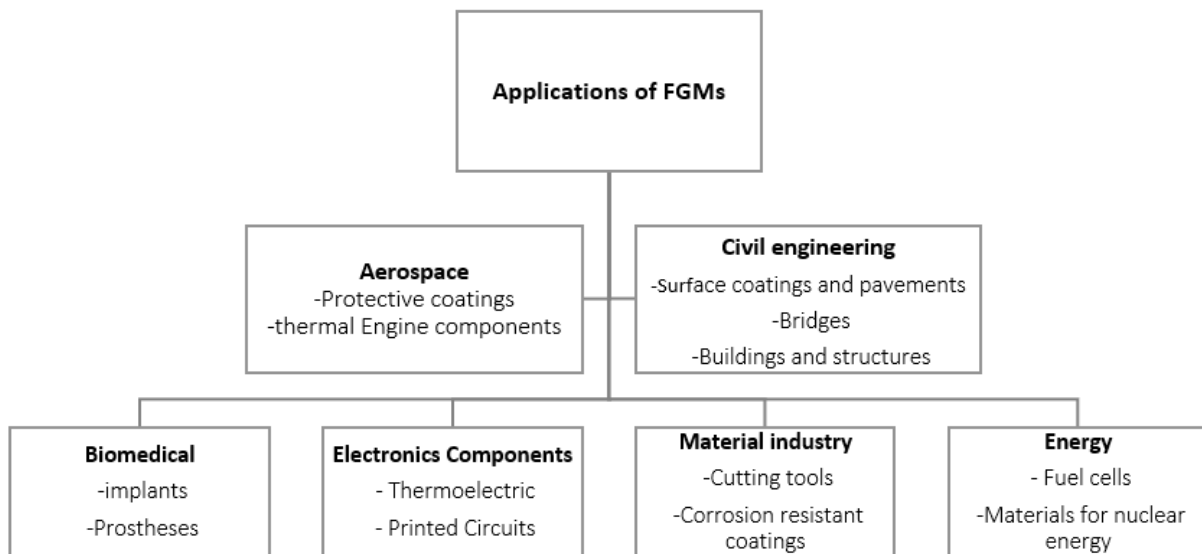


Figure I. 6:Applications of FGMs.

The use of FGMs is particularly interesting when the service conditions of an application require hardware properties that vary spatially. This flexibility makes it possible to design systems and structures that are both more efficient and more durable.

I.6.1. Civil Engineering:

Functionally Graded Materials (FGMs) herald a revolution in the realm of civil engineering, promising significant advancements in the design of structures that are not only more robust and durable, but also precisely tailored to the unique challenges of each project. And making an impact in several sectors such as:

1. **Road and Pavement Construction:** Envision lighter, more cost-effective yet equally sturdy roads. Through FGM, this vision could become a reality. These innovative materials could transform the road infrastructure, making it both more sustainable and economical (SAID, 2016).
- 2- **Geotechnical Engineering and Foundations:** In the delicate domain of geotechnical engineering, FGMs opens the door to revolutionary foundations. They promise to enhance the stability of soils and foundations, offering new possibilities for design and construction to adeptly address geotechnical challenges.

- 3- **Retaining Structures:** When it comes to stabilizing soils, particularly in areas where stability is a concern, FGMs emerges as an innovative solution. They enable the construction of more resilient retaining walls, providing a creative response to engineering challenges.
- 4- **Piles and Foundation Pillars:** FGMs also revolutionizes the design of piles and pillars, offering increased strength, durability, and performance. This could significantly enhance the load-bearing capacity of foundations, a major asset in numerous civil engineering applications.
- 5- **Coastal Protection and Maritime Engineering:** Confronting the rigors of the marine environment, FGMs offers reinforcement solutions for coastal and maritime structures. These materials could play a crucial role in increasing the resilience of infrastructure to extreme environmental conditions (BENSALAH, 2022).
- 6- **Thermal and Acoustic Insulation:** FGMs extends beyond mechanical strength; they also offer significant advantages in terms of thermal and acoustic insulation. Their use could contribute to the design of more environmentally friendly and energy-efficient buildings and infrastructure.

In summary, FGMs are positioned as key players in the future of civil engineering, promising more efficient, durable, and cost-effective structures. Their ability to adapt to specific mechanical and thermal constraints, reduce transitional stresses between different materials, optimize overall infrastructure performance, and lower manufacturing and maintenance costs, marks a significant evolution in how we conceive and build. (Amitrano and al,2020).

I.6.2. The importance of FGMs in civil engineering:

Functional gradient materials (FGMs) play a critical role in civil engineering due to their ability to offer optimized mechanical and thermal properties, making them particularly suitable for many applications in infrastructure construction.

The importance of FGMs in this area manifests itself in several ways (Iakovidis and al., 2022); (Halbe, 2021) :

- **Durability and resistance:** FGMs enable the design of materials that adapt to the specific mechanical constraints encountered in infrastructures, thus improving their durability and resistance to various loads and environmental conditions.

- **Reduction of transition stresses:** FGMs can be used to minimize transition stresses between different materials, thereby reducing the risk of failure and cracking within structures.
- **Performance optimization:** The use of functional gradient materials makes it possible to optimize the performance of infrastructures by adapting the properties of the materials to the specific requirements of each component.
- **Cost reduction:** FGMs also contribute to reducing costs related to the manufacturing and maintenance of infrastructure by using more efficient and durable materials, thus promoting better use of available resources.

I.7. Advantages and Disadvantages of Functionally Graded Materials (FGM)

Functionally Graded Materials (FGM) are an intriguing class of materials that offer unique properties owing to their graded composition. Understanding the advantages and disadvantages of FGM is crucial for various applications across industries (ELLALI, 2019).

I.7.1 Advantages of FGM

Functionally Graded Materials provide several advantages over conventional materials:

- **Decreased Thermal Stresses:** One significant advantage of FGM is the reduction of thermal stresses resulting from differences in thermal expansion coefficients of constituent materials.
- **Enhanced Stress Control:** The absence of a distinct interface in FGM allows for better overall stress control, leading to improved material performance.
- **Improved Material Cohesion:** FGM facilitates better cohesion between different materials, such as metals and ceramics, enhancing overall structural integrity.
- **Expansion of Functional Region:** FGM enables the expansion of the functional region before reaching the limit of plastic deformation, enhancing the material's versatility.
- **Prevention of Delamination:** The absence of sharp interfaces in FGM helps in preventing delamination, which is common in traditional composite materials.
- **Increased Fracture Toughness:** FGM exhibits higher fracture toughness, contributing to improved durability and reliability in various applications.

- **Reduction of Stress Singularities:** FGM eliminates stress singularities at different locations, including free surfaces, corners, and crack tips, leading to enhanced structural performance.

I.7.2. Disadvantages of FGM

Despite their advantages, Functionally Graded Materials present several challenges:

- **Complex Manufacturing Process:** The fabrication of FGM is intricate due to the need for precise property gradients, leading to complex manufacturing processes.
- **Inadequate Property Matching:** Matching properties of different materials within an FGM can be challenging, leading to issues such as poor adhesion and undesired material phases.
- **Formation of Undesired Phases:** During fabrication, undesired phases may form within the FGM, impacting its mechanical and functional properties.
- **Cost Implications:** The manufacturing of FGM often requires specialized equipment and techniques, leading to higher production costs compared to traditional materials.

Functionally Graded Materials offer a unique set of advantages, including reduced thermal stresses, improved material cohesion, and enhanced fracture toughness. However, challenges such as complex manufacturing processes and inadequate property matching must be addressed for wider adoption.

I.8. FGM Manufacturing Processes:

Functionally graduated materials (FGM) are composite materials whose properties gradually vary in the volume of the material. This gradual variation is generally designed to respond to changes in environmental or operational constraints, thus optimizing material performance for specific applications. FGMs may have gradients in composition, microstructure, mechanical, thermal, electrical, magnetic, etc. Some manufacturing processes used for functionally graded materials include (ADDU, 2021):

I.8.1. Physical Vapor Deposition (PVD)

PVD involves the deposition of material atoms onto a substrate through physical processes such as evaporation or sputtering. This technique allows precise control over film thickness and composition, facilitating the creation of graded structures in FGMs

I.8.2. Chemical Vapor Deposition (CVD)

CVD enables the synthesis of FGMs by depositing thin films of different materials onto substrates through chemical reactions in the vapor phase. This method offers versatility in material selection and deposition conditions, ensuring uniformity across the graded layers

I.8.3. Powder Metallurgy

Powder metallurgy involves the consolidation of metal powders through processes like compaction and sintering. By blending powders with varying compositions, FGMs with tailored properties can be fabricated, making them ideal for aerospace and automotive applications.

I.8.4. Centrifugal Method

The centrifugal method utilizes centrifugal force to distribute materials radially within a mold, resulting in graded structures with controlled composition gradients. This technique is particularly advantageous for producing FGMs with high throughput and uniformity.

I.8.5. Tape Casting Method

Tape casting involves the deposition of ceramic slurries onto flexible substrates, followed by layer stacking and densification. This method is suitable for fabricating thin, flexible FGMs used in electronics and medical devices.

I.8.6. Slip Casting

Slip casting utilizes a slurry of ceramic particles suspended in a liquid medium, which is poured into molds and allowed to solidify. By adjusting the composition of the slurry, FGMs with graded microstructures can be produced, offering enhanced mechanical properties.

I.8.7. Solid Freeform Fabrication Method (SFF)

SFF encompasses various additive manufacturing techniques like 3D printing, enabling the layer-by-layer deposition of materials to create complex FGM geometries. This method offers design flexibility and rapid prototyping capabilities.

I.8.8. Directed Energy Deposition

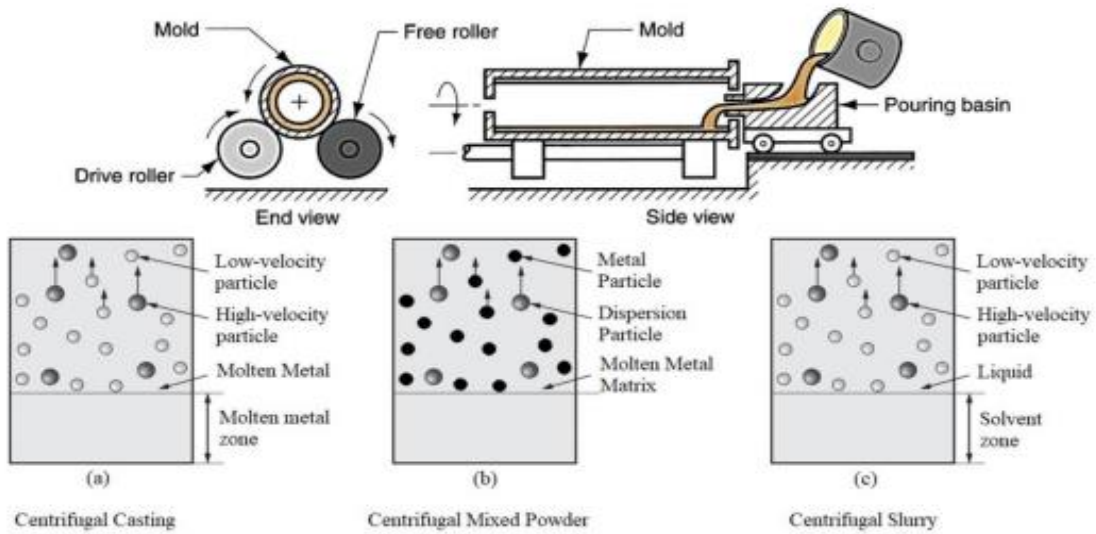
Directed Energy Deposition (DED) involves the focused delivery of energy, such as laser or electron beams, to melt and fuse materials onto a substrate. By controlling deposition parameters, FGMs with gradient compositions and structures can be achieved.

I.8.9. Plasma Spraying

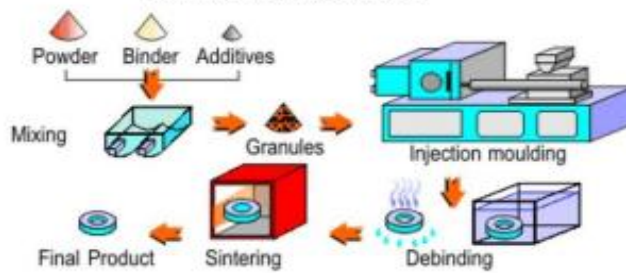
Plasma spraying utilizes a plasma torch to melt and propel feedstock material onto a substrate, forming a dense coating. This technique is commonly employed for thermal barrier coatings in aerospace applications, showcasing the versatility of FGMs.

I.8.10. Sintering and Infiltration

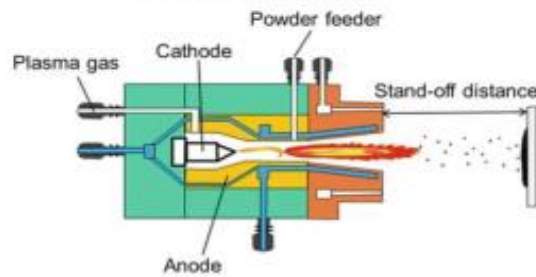
Sintering involves the heating of powdered materials to bond particles together, while infiltration involves the impregnation of porous substrates with molten metal. Combined, these techniques enable the fabrication of FGMs with tailored porosity and mechanical properties.



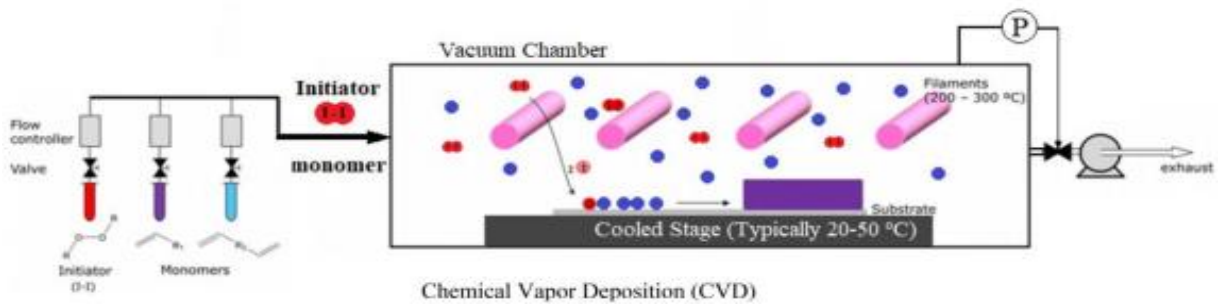
Centrifugal Casting Methods



Powder Metallurgy (PM)



Plasma Spray Forming (PSF)



Chemical Vapor Deposition (CVD)

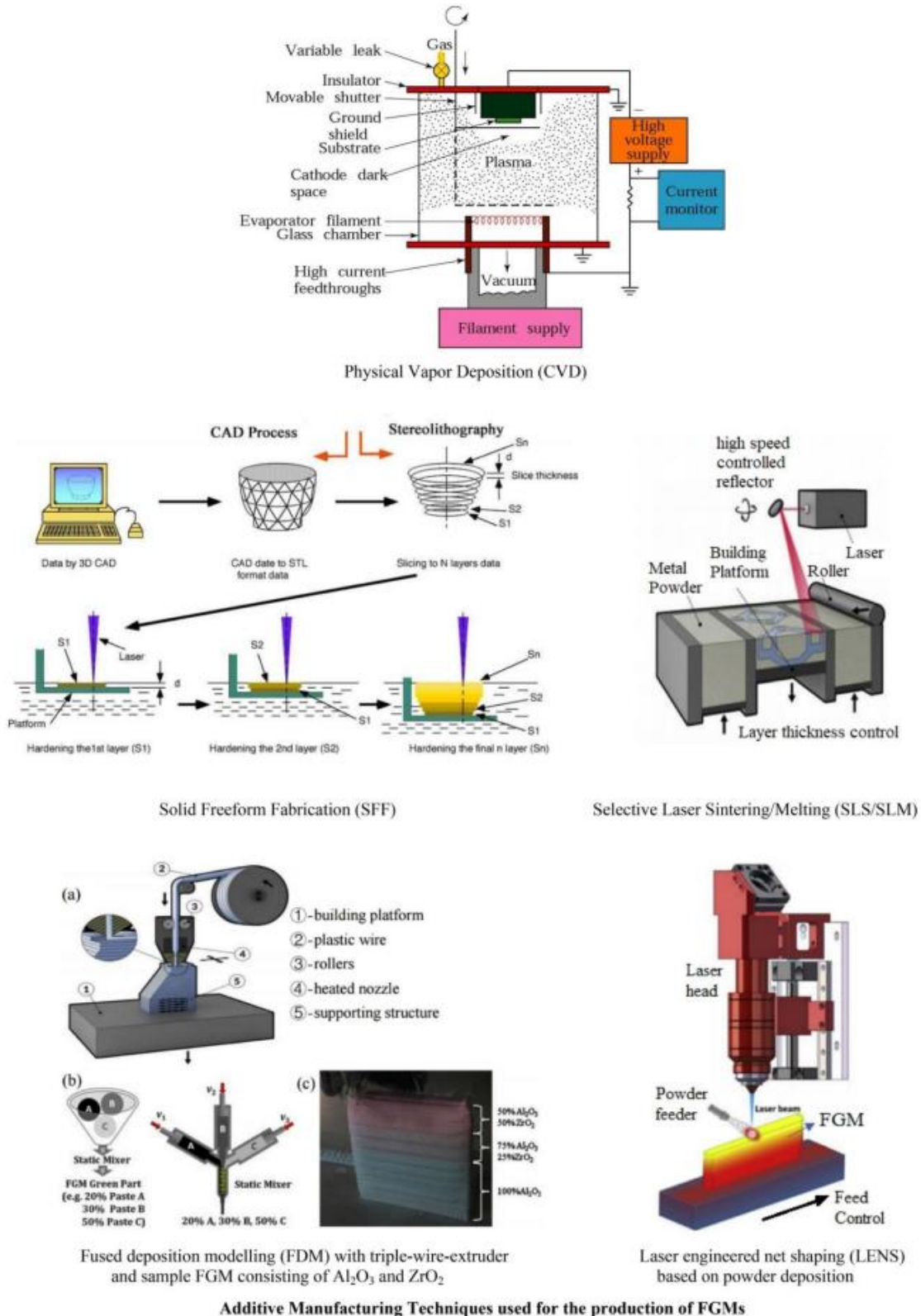


Figure I. 7: Commonly used processing techniques for the production of FGMs (ADDYOU, 2021)

I.9. Conclusion:

In this chapter, we have defined functionally graded materials "FGMs," the concept of their development, their properties, their areas of application, and their main manufacturing methods.

The spatial and progressive variation of the properties of functionally graded materials allows for the creation of innovative structures that can be exploited in numerous areas of application in special civil engineering structures.

Chaptre II

Theorie of plates

II. Introduction

The study of the static and dynamic behaviors of FGM plate structures or beams often involves resorting to different theories and methods to effectively solve associated problems. Over time, several theories have been developed to model plate behavior, each with its own assumptions and application domains.

In 1888, Love introduced a theory of thin plates, based on the assumptions of Gustav Kirchhoff and inspired by Euler-Bernoulli's assumptions. This theory, also known as the classical theory or Kirchhoff-Love theory, provided an important basis for thin plate analysis carried out by researchers such as Timoshenko (1921), (Reissner, 1945), and Uflyand (1948). Subsequently, Mindlin contributed to strengthening the theory of semi-thick plates, also known as the first-order deformation theory. This theory takes into account the effects of plate thickness on its behavior, thus offering more precise modeling in certain situations.

However, when the plate thickness becomes significant, an improvement of the assumptions of classical and first-order theories is necessary. It is at this stage that higher-order theories come into play to account for additional effects such as transverse curvature and transverse shear.

Therefore, the choice of the right theory and appropriate method will depend on the specific characteristics of the structure under study, the plate thickness, and the expected effects on its static and dynamic behavior. Each theoretical approach offers its own advantages and limitations, and it is crucial to select the most suitable method based on the application requirements.

II.1. The analytical models of FGM plates.

II.1.1. Classical Plate Theory of Love-Kirchhoff

Classical Plate Theory, also known as Love-Kirchhoff theory, is a fundamental framework used in the analysis of thin plates subjected to loads and deformations. It serves as a cornerstone in understanding the behavior of structures made from functionally graded materials. This theory provides a comprehensive approach to studying the mechanical

properties and behaviors of such materials, offering valuable insights into their design and application.

This theory is based on several assumptions (Figure II.1):

- **Planarity Assumption:** This assumption states that the middle plane of the plate, which is equivalent to the average curve of beams, is initially flat. This means that any point in this plane will only move in the vertical direction and not in the plane itself.
- **Non-Deformation Assumption:** This assumption implies that the middle layer of the plate, which is equivalent to the neutral fiber of beams, does not undergo deformation within its plane. In other words, the length and shape of any line in the middle plane remain unchanged during the deformation.
- **Transverse Displacement Assumption:** This assumption considers only the transverse displacement 'w' of points in the middle layer. It means that any point in the middle plane of the plate can move up or down, but not in the plane itself.

These assumptions simplify the mathematical model and make it possible to analyze the stresses and deformations in thin plates under the effect of loads

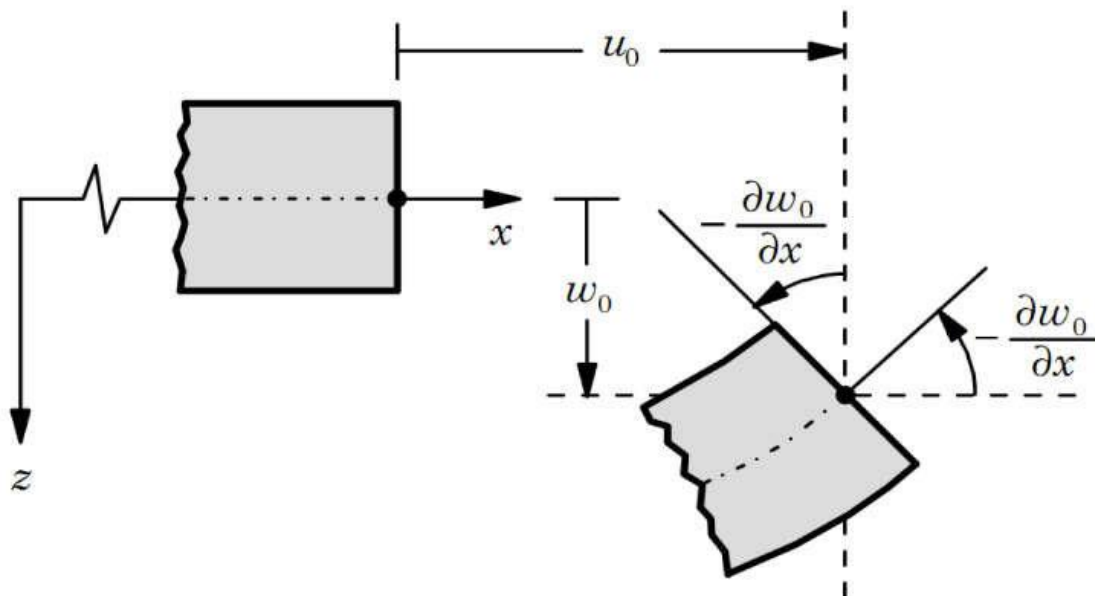


Figure II.1: Schematization of plate deformations by the classical theory «CPT» (Reddy, 1997).

This model of plate can be referred to the works of Timoshenko and Woinowsky-Krieger (Timoshenko, 1959) ; (L. Wang and al., 2017) ; (Reddy, 1999).

The displacement field in Kirchhoff-Love theory has the form of equations (II.1):

$$\begin{aligned} u(x, y, z) &= u_0(x, y) - z \frac{\delta w_0}{\delta x} \\ v(x, y, z) &= v_0(x, y) - z \frac{\delta w_0}{\delta y} \\ w(x, y, z) &= w_0(x, y) \end{aligned} \quad (\text{II.1})$$

Where:

u_0 and v_0 are membrane displacements in x and y directions respectively.

w_0 is the arrow of the plate.

$\frac{\delta w_0}{\delta x}$ and $\frac{\delta w_0}{\delta y}$ are rotations due bending (without shearing).

Various applications of classical thin plate theory (CPT)

- **Leissa (1973):** This study used the CPT to study free vibration of thin isotropic rectangular plates.
- **Hu and Zhang (2011):** They applied the assumptions of the CPT and Von Karman to analyze the vibration and stability of FGM (Functionally Graded Material) plates. They also studied the influence of certain parameters on these vibrations.
- **Chakraverty and Pradhan (2014):** These researchers combined the CPT and the Rayleigh-Ritz method to analyze plate vibrations in FGM. In their work, the plate rested on the elastic foundation of Winkler with different boundary conditions. They analyzed the influence of certain foundation parameters, boundary conditions and geometric properties.

This work demonstrates the versatility and effectiveness of the CPT for the analysis of plate vibrations in various contexts.

II.1.2. First-Order Shear Deformation Theory (FSDT)

The First-Order Shear Deformation Plate Theory (FSDT), also known as the Mindlin Plate Theory (Mindlin 1951), and it is based on the displacement field (II.2):

$$\begin{aligned} u(x, y, z) &= u_0(x, y) - z\varphi_x(x, y) \\ v(x, y, z) &= v_0(x, y) - z\varphi_y(x, y) \\ w(x, y, z) &= w_0(x, y) \end{aligned} \quad (\text{II.2})$$

Where φ_x and φ_y denote rotations about the y and x axes, respectively.

This theory extends the Classical Thin Plate Theory (CPT) by including transverse shear deformation in its kinematic assumptions. Here are the key points:

- **Transverse Shear Deformation:** Unlike the CPT, which assumes that planes perpendicular to the mid-plane before deformation remain perpendicular after deformation, the FSDT allows for transverse shear deformation. This means that these planes can become non-perpendicular due to shear deformation.
- **Shear Correction Factors:** The FSDT introduces shear correction factors to account for the discrepancy between the actual transverse shear force distributions and those computed using the kinematic relations of the FSDT. These correction factors help to more accurately predict the behavior of the plate under various conditions.
- **Dependence on Geometric Parameters and Conditions:** The shear correction factors in the FSDT depend not only on the geometric parameters of the plate but also on the loading and boundary conditions. This makes the FSDT a more versatile and accurate model for analyzing plate behavior under a wider range of conditions.

FSDT is particularly useful for thick and thin FGM plates as it can provide a more accurate prediction of their behaviour (Wang et al, 2001).

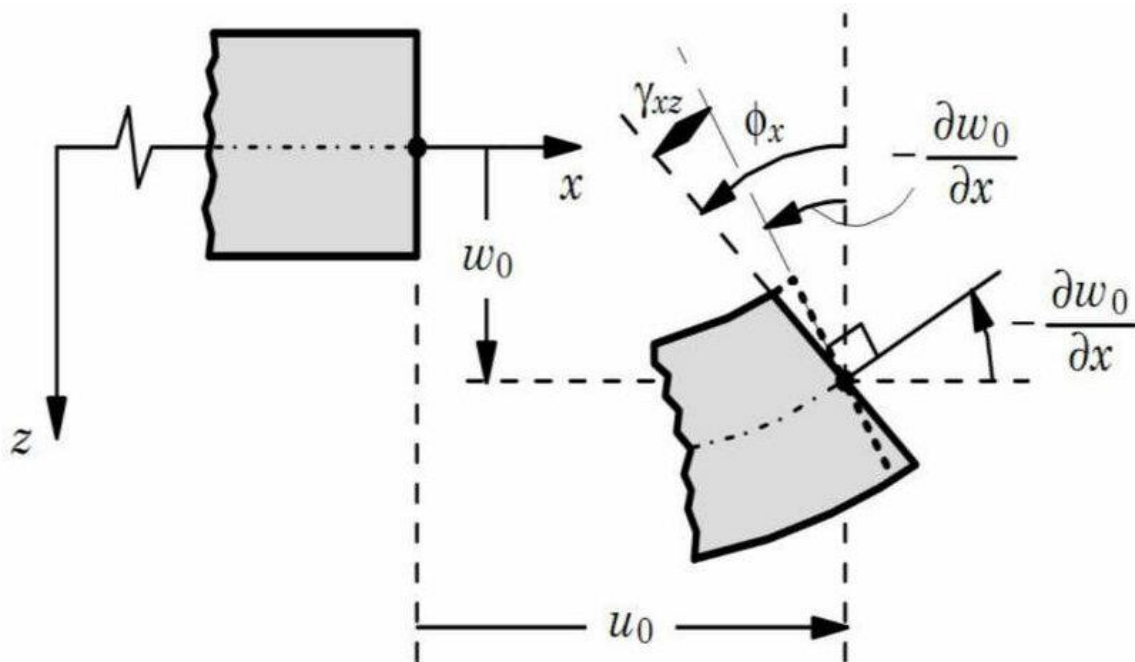


Figure II 2: Representation of the Reissner-Mindlin plate (Reddy, 1997)

Various applications of First-Order Shear Deformation Theory (FSDT):

- **Liew, Xiang and Kitipornchai (1993):** They applied Mindlin plate theory to analyze the vibration of thick rectangular plates with different boundary conditions.
- **Croce and Venini (2004):** They applied FSDT to study the bending behavior of FGM plates under mechanical load in a thermal environment.
- **Fallah, Aghdam and Kargarnovin (2013):** They used the FSDT and the extended Kantorovich method to analyze the free vibration of moderately thick FGM plates resting on an elastic foundation.
- **Hosseini-Hashemi, Fadaee and Atashipour (2011):** They developed and proposed a new precise analytical approach based on Reissner-Mindlin plate theory to analyze the free vibration of FGM rectangular plates.
- **Nguyen, Sab and Bonnet (2008):** They developed a new FSDT model for FGM plate analysis.

This work demonstrates the versatility and effectiveness of FSDT and Mindlin plate theory for the analysis of plate vibration and bending behavior in various contexts.

II.1.3. High-order shear deformation theories (HSDT):

Are based on a nonlinear distribution of displacement fields in plate thickness, taking into account the effects of transverse shear deformation and/or normal transverse deformation. Unlike classical and first-order theories, HSDT models do not require correction factors for the shear effect. Several authors have proposed high-order shear deformation theories to analyze the mechanical behavior of thick plates, especially those that are functionally graduated. The HSDT developed by Reddy in 2000 was used by many researchers to study static bending, free vibration and buckling of FGM plates, including (Hildebrand and al., 1949); (Naghdi, 1957); (Reddy, 1984); (Kant & Swaminathan, 2002); (Liberescu L., 1967).

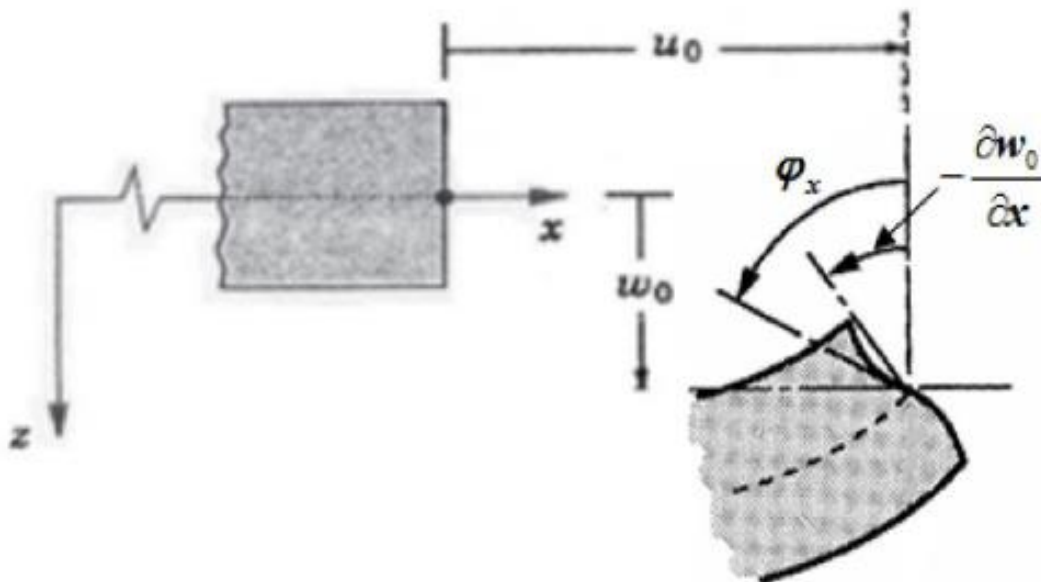


Figure II 3: High-order plate representation (Reddy, 1997).

The displacement field in High-order shear deformation theories (HSDT) has the form of equations (II.3):

$$u(x, y, z) = u_0(x, y) - z \frac{\delta w_0}{\delta x} + f(z) \varphi_x(x, y)$$

$$v(x, y, z) = v_0(x, y) - z \frac{\delta w_0}{\delta y} + f(z) \varphi_y(x, y)$$

$$w(x, y, z) = w_0(x, y)$$

Where:

(u_0, v_0) and (φ_x, φ_y) are membrane displacements and rotations in x and y directions respectively. ($\varphi_x = \frac{\delta w_0}{\delta x} + \varphi_x$; $\varphi_y = \frac{\delta w_0}{\delta y} + \varphi_y$)

f (z) is a transverse shear (shape) function characterizing theories in contrast to Love-Kirchhoff's theory where f (z)= 0 , while in the Reissner-Mindlin theory f (z)= z .

Various applications of High-order shear deformation theories (HSDT):

- **Javaheri and Eslami, 2002:** They applied the theory of third-order shear deformation (TSDT) and the Navier solution to study the thermal buckling of simply supported FGM plates.
- **Shen, 2002:** Shen performed a non-linear analysis of FGM plates subjected to transverse loads in the thermal environment using TSDT34.
- **Yang, Liew and Kitipornchai, 2004:** They studied buckling, free vibration and dynamic stability of laminated FGM plates using HSDT56.
- **Belkhouja et al., 2020:** They studied an exponential-trigonometric theory of higher-order shear deformation (HSDT) for the analysis of bending, free vibration and buckling of plates in FGM78.
- **Rabhi et al., 2020:** They studied the buckling and free vibration of exponential gradient sandwich plates resting on elastic foundations under various boundary conditions by applying a new HSDT at 3 unknowns910.

This research has all contributed to the advancement of understanding and analysis of thick plates and composite materials. They improved existing models and proposed new approaches to solving complex problems in this area.

II.1.4. The different models of high-order theory:

Shear functions $f(z)$ are mathematical functions used in high-order models to describe the distribution of transverse shear stresses in a material. Several authors have proposed different shear functions $f(z)$ to model this complex phenomenon.

The distribution of transverse shear stresses in the thickness of a material can take different forms, such as parabolic, sinusoidal, hyperbolic or exponential. Each form of stress distribution has its own characteristics and implications for the mechanical behavior of the material.

the shear functions $f(z)$ are powerful tools to model the distribution of transverse shear stresses in high-order materials. The shape of the stress distribution chosen can have a significant impact on the results of mechanical analyses and must be carefully selected according to the properties of the material studied and the mechanical phenomena to be taken into account.

Table II. 1:Different shear functions used in plate theories isotropic and FGM (Boukhari, 2016)

Theory	Titled	Shear function $f(z)$	Distribution of γ_{xz} and γ_{yz} according to z	Correction and shear coefficient	Domain of validity
CPT.Kirchoff [Kirchoff, 1850a] and [Kirchoff, 1850b]	Classical plate theory	0	Thin plates
FSDT Midlin [Midlin, 1951]	Deformation theory of 1st order plates	z	constant	Required	Thin and medium plates thick

Ambartsumian [Ambartsumian, 1958]	Theory of order superior	$\frac{z}{2} \left(\frac{h^2}{4} - \frac{z^2}{3} \right)$	Linear	Not Required	Thin plates and moderately thick
Reissner [Reissner, 1975]	Theory of order superior	$\frac{5}{2}z \left(1 - \frac{4z^2}{3h^2} \right)$	Parabolic		Thin plates and thick
TSDPT, Touratier [Touratier, 1991]	Theory of trigonometric deformation plates	$\frac{h}{\pi} \sin\left(\frac{\pi z}{h}\right)$			
ESDPT Karama and al. [Karama, 2003]	Theory of deformation exponential of plates	$ze^{-2(z/h)^2}, \alpha > 0$			
PSDPT, Levinson [Levinson, 1980], Reddy [Reddy, 1984]	Theory of deformation parabolic of plates	$z \left(1 - \frac{4z^2}{3h^2} \right)$			
Aydogdu [Aydogdu, 2003]	Theory of deformation exponential of plates	$z\alpha^{\frac{2(z/h)^2}{\ln(\alpha)}}, \alpha > 0$			
Elmeiche, Tounsi and al [Elmeiche, 2011]	Refined theory plates	$\frac{\left(\frac{h}{\pi}\right) \sin\left(\frac{hz}{\pi}\right) z}{\cosh\left(\frac{\pi}{2}\right) - 1}$			

Aite atmane and al [Aite atmane, 2010]	Refined theory plates	$\frac{\cosh\left(\frac{\pi}{2}\right)}{\cosh\left(\frac{\pi}{2}\right) - 1} z$ $- \frac{\frac{h}{\pi} \sinh\left(\frac{\pi z}{h}\right)}{\cosh\left(\frac{\pi}{2}\right) - 1}$			
Shimpi [Shimpi, 2002]	Refined theory plates	$h \left[\frac{1}{4} \left(\frac{z}{h} \right) - \frac{5}{3} \left(\frac{z}{h} \right)^3 \right]$			

II.2. The material properties of FGM plates:

Graded functional materials (FGM) represent a significant advancement in the field of multiphase materials, allowing the design of structures with gradual properties by continuously modifying the components according to a predetermined profile. FGMs are characterized by their non-uniform microstructures that lead to continuous gradient macroscopic properties, enabling the exploration of a wide range of innovative applications.

A typical FGM is characterized by a progressive variation of material properties throughout its structure. This gradation can be described using various mathematical functions such as power law, exponential function, or sigmoid function to determine the volume fractions of constituents. These functions allow for precise and controlled definition of phase distribution within the material, thereby influencing its overall properties. Let's take the example of an elastic rectangular plate to illustrate the concept of FGM in figure II.4. The coordinates x and y define the plane of the plate, while the z-axis is perpendicular to its mid-surface in the thickness direction.(ADDU, 2021)

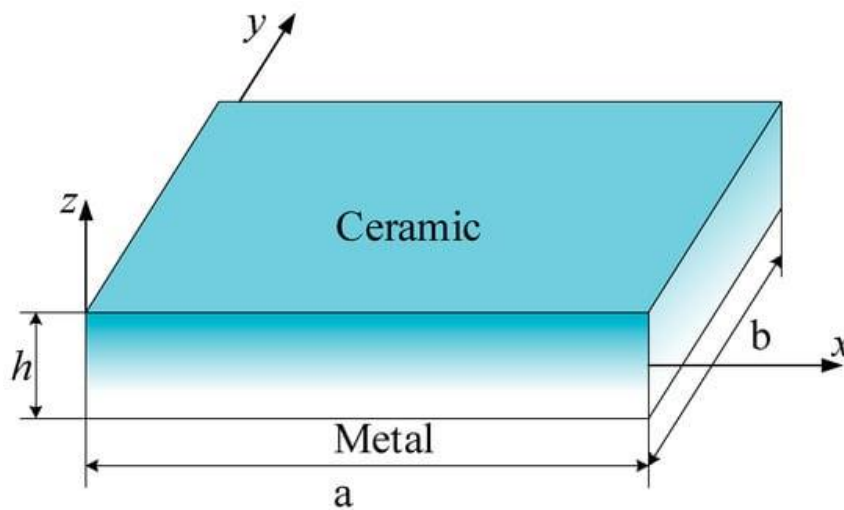


Figure II 4: Plate model of functionally graded materials (FGM).

The properties of the material, such as Young's modulus and Poisson's ratio, play a crucial role in the performance of structures. These properties may vary between the upper and lower surfaces of materials but are carefully defined based on specific requirements.

It is interesting to note that Young's modulus and Poisson's ratio of plates generally only vary in the thickness direction, represented by the z -axis. Previous studies, such as Delale and Erdogan in 1983, highlighted that the impact of Poisson's ratio on deformation is less compared to Young's modulus. Thus, the Poisson's ratio of plates is often considered constant.

However, Young's moduli can vary along the thickness of plates in the case of functionally graded materials (FGMs). These variations can follow functions such as power laws (P-FGM), exponential functions (E-FGM), or sigmoid functions (S-FGM), thereby influencing the mechanical properties of materials.

II.2.1. The power law mixing law or material property of a P-FGM structure (power law)

is defined by the volume fraction of the FGM which corresponds to a power law function. This volume fraction is determined by the equation (II.6)

$$V(z) = \left(\frac{z}{h} + \frac{1}{2} \right)^2$$

where p is the material parameter and h is the thickness of the plate.

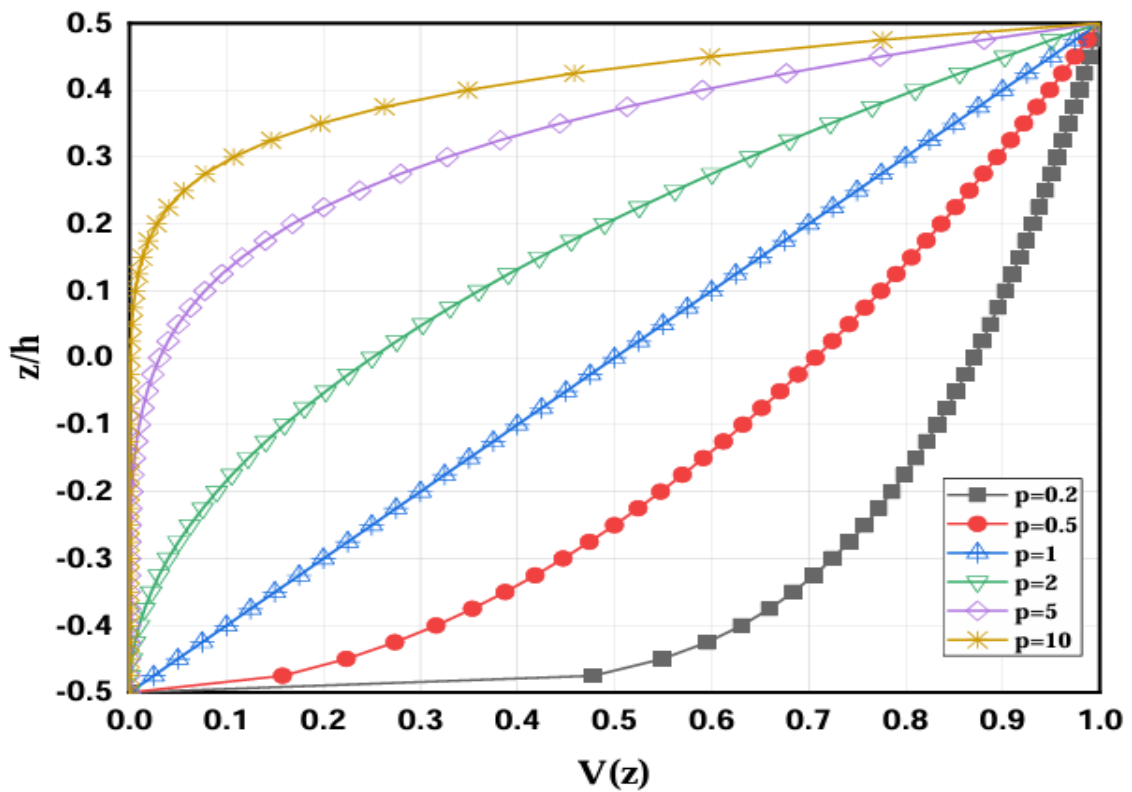


Figure II 5: Variation of the volume fraction in a P-FGM plate.

Once the local volume fraction $V(z)$ is defined, the material properties of a P-FGM can be calculated using the mixing law expressed by equation (II.7) according to (Bao & Wang, 1995).

$$E(z) = E_m + (E_c - E_m)V(z)$$

Where $m E$ and $c E$ are respectively the Young's moduli of the lower surface ($z = -h/2$) and upper surface ($z = h/2$) of the FGM plate, Figure II.5 illustrates the variation of Young's modulus in the direction of the thickness of the P-FGM plate, showing that Young's modulus changes rapidly near the lower surface for $p > 1$ and increases rapidly near the upper surface for $p < 1$. This variation is essential for understanding the mechanical behavior of P-FGM structures and for designing composite materials with specific properties

II.2.2. Sigmoid mixing law or material property of an S-FGM structure (sigmoid law):

is a method used to express variations in the properties of FGM materials. This approach is often used to overcome stress concentrations that occur in FGMs due to interfaces where the material changes rapidly.

(Chung, 2001) introduced the sigmoid volume fraction S-FGM, composed of two power law functions defined by specific relationships.

$$V_1(z) = \frac{1}{2} \left(\frac{h/2+z}{h/2} \right)^P \quad \text{For} \quad -h/2 \leq z \leq 0$$

$$V_1(z) = 1 - \frac{1}{2} \left(\frac{h/2+z}{h/2} \right)^P \quad \text{For} \quad 0 \leq z \leq h/2$$

By applying the mixing rule, the Young's modulus of the FGM-S can be calculated using equations

$$\text{For} \quad -h/2 \leq z \leq 0$$

$$E_1(z) = V_1(z)E_c + [1 - V_1(z)]E_m$$

$$\text{For} \quad 0 \leq z \leq h/2$$

$$E_1(z) = V_2(z)E_c + [1 - V_2(z)]E_m$$

these equations allow determining the Young's modulus as a function of the volume fraction of sigmoid distributions illustrated in Figure II.6.

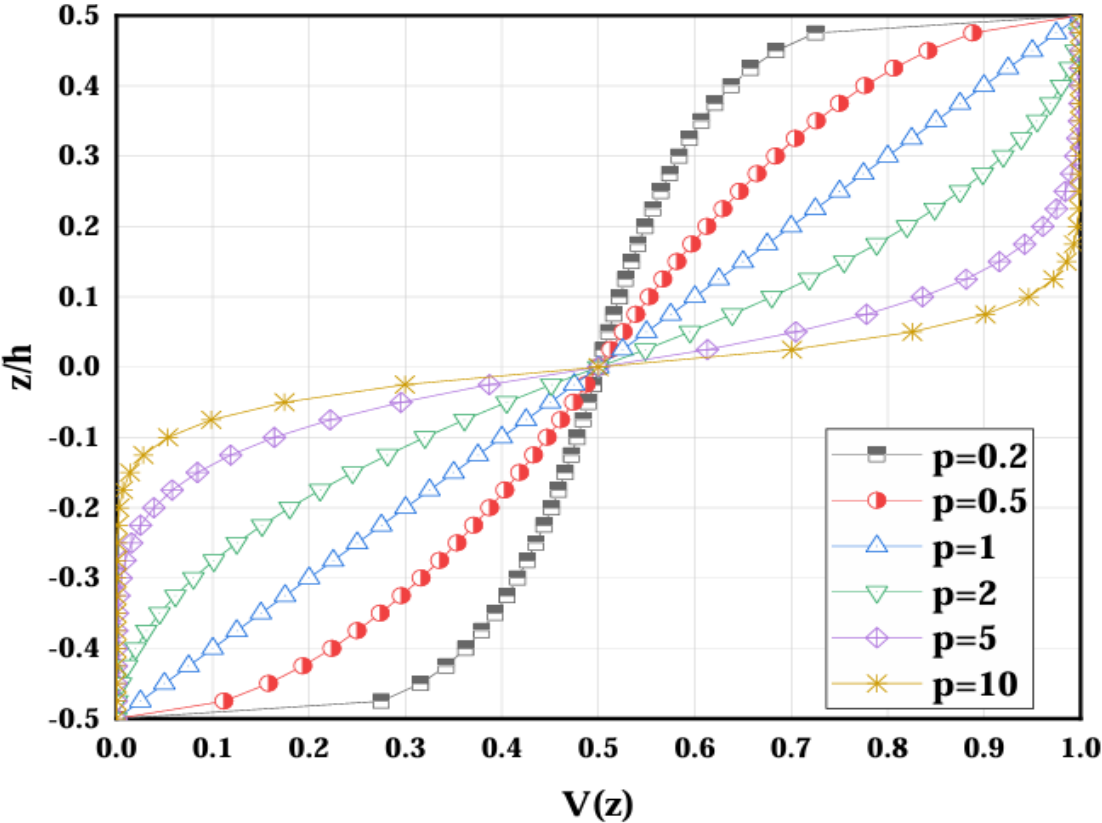


Figure II 6 :Variation of the volume fraction in an S-FGM plate

II.2.3. Exponential mixing law or material property of an E-FGM structure (exponential law):

This law is used to describe the material properties of FGMs using an exponential function and is given by equation II.10: (Delale & Erdogan, 1983).

$$E(z) = E_m e^{B(z+h/2)} , B = \frac{1}{2} \ln \frac{E_c}{E_m}$$

The variation of Young's modulus across the thickness of E-FGM plates is depicted in Figure II.7

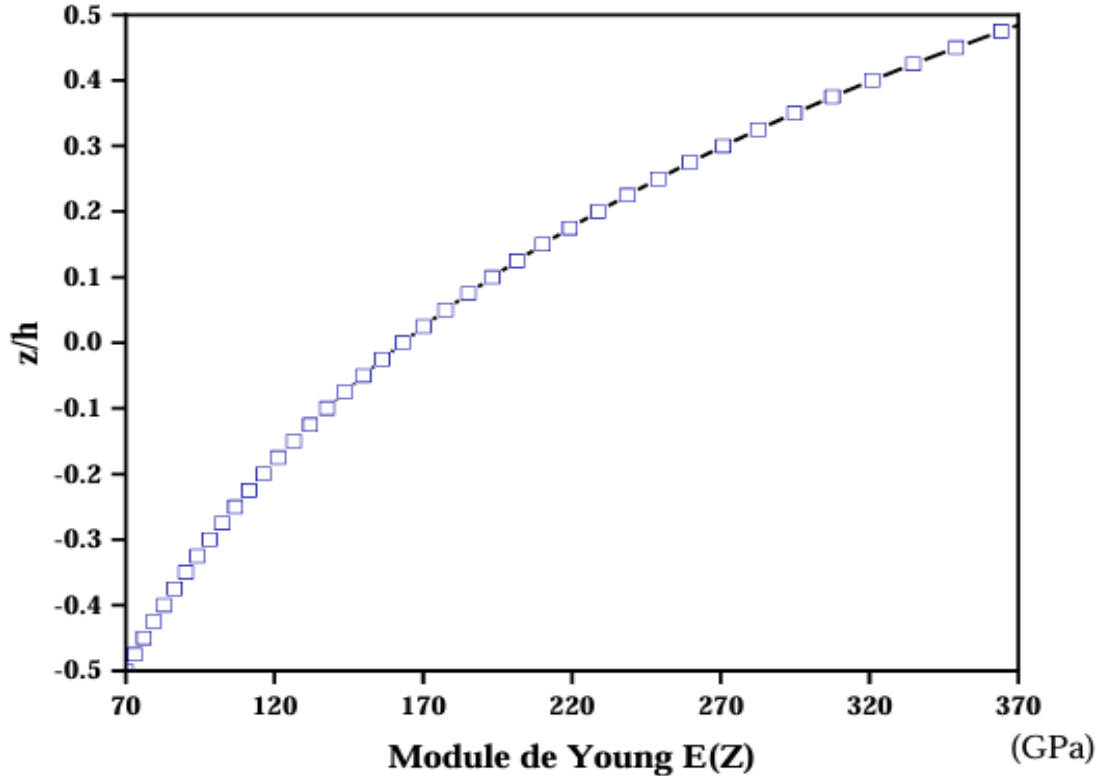


Figure II 7: Variation of Young's modulus in an E-FGM plate.

II.3. Conclusion

In this chapter, we have given a general overview of the different theories of plates, including the classical theory (CPT) of Love-Kirchhoff used for the study of thin plates, the theory of deformation in shear order one (FSDT) which takes into account the transverse shear effect. To obtain accurate results by this theory, most often a correction coefficient is used.) and high-order shear theory (HSDT). We also presented a synthesis on the different models of high-order theory and the authors' work on models

Chapter III
Analytical study of
FG plate

III. Introduction

There are several techniques to prepare FGMs by using most of the materials, as described by researchers. Researchers in recent times have developed major techniques of porosity, and different materials have been used as per different applications regularly. The suitability of these plate like systems can be used in the diversified field, such as in aerospace (air plane, rocket), nanocomposites, chemical biomedical devices, capacitors, microelectronics, oxide fuel cells, photo catalysts, resistor, turbine blades; and also in engineering and technological applications. In the field of flexible electronics, the nucleus of these plate like systems, such as in electronic skins, and smart textiles have acquired immense interest for future compliance with human bodies and robots. Hence, they were used in solar cells, biocompatible strategies in orthopedics, drug delivering nanocontainers, and biofuel cells, microfluidic applications including high efficiency cancer therapy and advanced photothermal therapy (Penna and al., 2022)

The efficient employment of more advanced and multifunctional composite, smart, and hybrid structures made of advanced materials with properly designed porosity patterns in the realm of modern diversified engineering applications is not only a challenging task but also a keen interest around the globe. To enter a strike in the modern scenario of structural designing technology, an engineered functional and multifunctional gradation in porosity and variously distributed microstructural defects in the lattice structure may be in great demand (Jalali and al., 2021). The grade and distribution of porosity are mainly adopted to regulate the thermomechanical properties of materials and also to tailor the mechanical, thermal, diffusion, and enhancement properties of various advanced materials such as thermoelectric systems, piezoelectric materials, semiconductive structures, and other multifunctional materials. The most widespread NP production technique includes reducing or coating the solid phase from the liquid or solution phase. This method is mainly used to prepare metal and metal alloy NPs (Valencia et al., 2022)

III.1. Background and Motivation

Some researchers further argue that their superposition will give most accurate predictions because a close match for their predictions was achieved with respect to experiments. Being a junior perspective researchers, we kept our further investigation on the idea of nonlocal theory, plate-type functionally graded material, linearized theory and free

bending of the plate is done. It is concluded that with respect to classical model, nonlocal theory gives increased adhesive's maximum bending power, and faster I-degradation of additional non-s of nonlocal theory increases the plate's bending power. Because two nonlo-cal parameters make the situation much more complex, the authors simplify the free bending prob-blems, as proposed by different researchers in the past. They considered the nonlocal theory effect only in sandwiched structure. The plate models are useful for mechanical analysis of quasi zero axial deformation, lower dimensional solid structures such as plate and sandwich structures. The state-of-the-art in modeling of plates in mechanics involves nonlocal hyperelastic and linearized theories, thus higher order theories. All of them are implemented. Implanted in functionally graded mechanism, the modern plate mechanics become too complex to incorporate each and every noninertial effect. To fabricate such green products, the people from academia are striving for the tools to probe the ecofriendly structural design strategies for green materials. Particular attention is paid to the effect of classical and nonlocal small scale parameters.

Research on micro-electromechanical systems and nano-electromechanical systems has increased due to their small volume, light weight, and excellent performance in various fields (Tang et al., 2022). When material structure are reduced to micro-nano levels, their mechanical behavior differs significantly from macro dimension levels. As the materials possess dimensionality from micrometer to nanometer, it is important to account for the characteristic length scale of the materials into the governing equation. Such types of models are known in the literature as nonclassical models. Classical model give incorrect evaluation of such characteristic length scale material in case. It is reasoned that micro-structural in their aspect, stresses and displacements are needed but classical model gives constant stress power law over the entire body's volume. It gives a finite stress on the body's surface (Monaco and al., 2021). This is the main reason such models are known as classical, because we have no reasons to believe that materials retain such behaviour. It is quite clear that these models can give us wrong predictions for internal stresses and hence for the boundary inhomogeneity. Classical model predictions also depend on the response of the body's geometric size. In many different ways to deal with the said issues, the classical model result to ill-posed predictions. The surface elasticity and nonlocal theory non-classical theory are the accurate models that account for these effects, separately (Thakur et al., 2021).

III.2. Research Objectives

(Monaco et al., 2021) This research aims to explore mechanical behaviors of FGPNs resting on EF using gradient theory. According to Eringen's higher order continuum theory, the general classical Euler–Bernoulli beam theory cannot accurately describe the mechanical behaviors at nanoscale because of the size-dependent behaviors and nonlocal surface energetics. In this theory, several dimensions such as micro-continuum, nonlocal, gradient and nanoscale continuum, are taken into consideration. Through compounding the surface elasticity and the nonlocal distribution of the stress tensor, one can approach the real behavior of materials in discontinuities as in interfaces and surfaces. It is worth mentioning, as a relevant concept, that Liebscher observed that, by resolving the experimental stresses, the razor blade can be sharpened to some nanometers by the Szillat–Gogler method. This method makes use of a lumped interface in the edge zone and a notched distribution of the elastic constants being in conformity with an integration procedure based on the principle of momentum of Liu. Many researchers have expanded the idea of Eringen's theory, among them the most popular are Toupin, Mindlin, Henzias, Yugang Gao, and their several followers. Many of these researchers are not only eager to challenge the conventional continuum mechanics, but also owing to the fact that the classical theory becomes simply invalid for solving the multiscale bar/beam-like body problems, they have proposed a governing equation without any need to comprehensively recall balance equations for varied modifications of the continuum mechanics. (Penna and al., 2021) Recently, Timoshenko beam theory has been enriched by the presence of two nonlocal deformation parameters. Tagantsev's gradient theory comes to facilitate our objective utilization for the first time for our numerical validation. We are just persuaded to delve into the nonlocal derivative to scrutinize bending and stretching of elastomeric thin film crystalline systems. The proposed relation between these compatible surfaces to exhibit some compatibility of the elastic mechanics in nonlocal beam theory is also appealing. The same general trend on the dependence of thermal vibrations properties on values of the nonlocal parameter is obtained for nonisopotency, Hookean plateau and Hookean yard. The consequences of Wood in capability of temperature are also discussed. During the presentation, we are reviewing paper for the first time. Moreover, we disclose an essential achievement that for CNTs under hygrothermal variation; the thermal vibration response (frequency and amplitude) is being at the extreme domain. We also explore possible improvements of preconceived available theoretical data in which the thermal response of RW and FWs appears

more tangible and might be approved by employing more advanced gradient theories like nonlocal and stress gradient theory.

III.3. Geometry and concept of the functionally graduated plate (P-FGM)

In the framework of this study, we conducted research on a functionally graded metal-ceramic nano plate (P-FGM) that was resting on an elastic foundation of the Winkler-Pasternak type and had dimensions of "a" for length, "b" for width, and "h" for thickness in the x y coordinate system (Figure III.1). It is assumed that the FG plate's material properties, including mass density, Poisson's ratio, and Young's modulus, will continuously change with thickness in accordance with a power-law distribution.

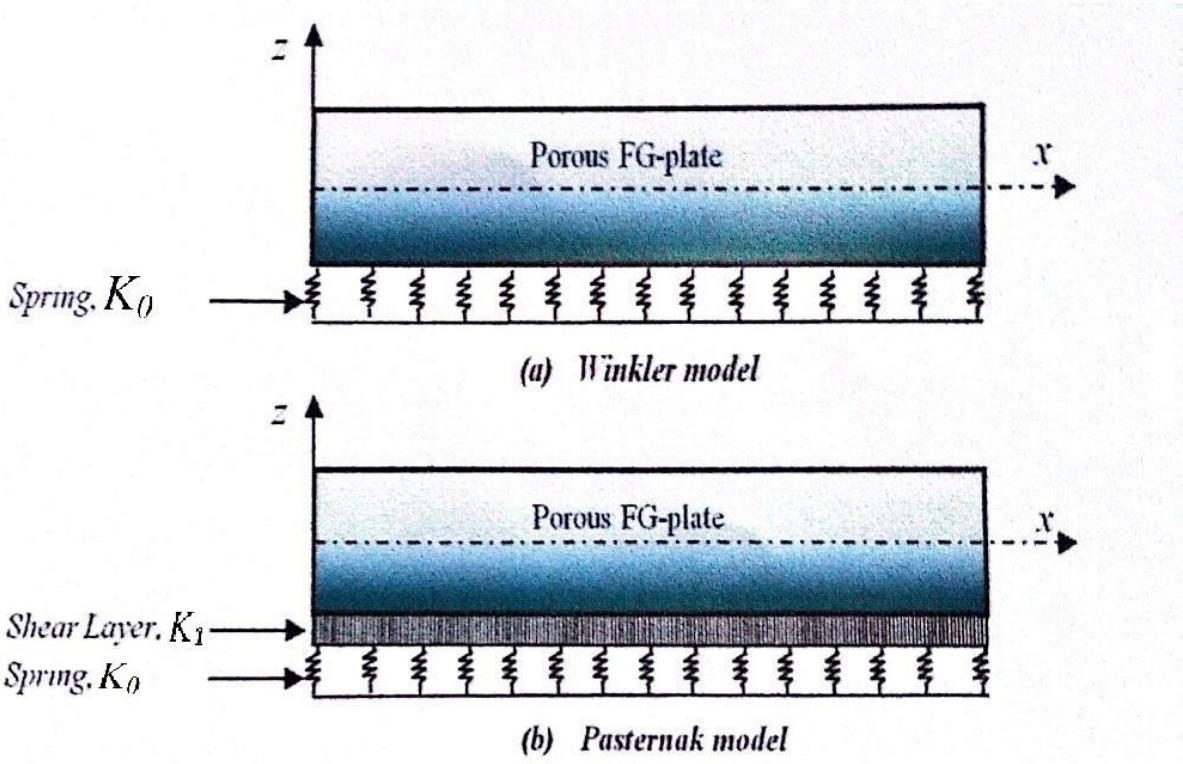


Figure III. 1: FG plaques supported on elastic foundations.

The variation of material properties across plate thickness is shown in the following equation:

$$p(z) = P_m + (P_c - P_m) \left(\frac{z}{h} + \frac{1}{2}\right)^p \quad (\text{III.1})$$

Where P_m and P_c are the properties of metallic and ceramic materials respectively. p is the power index.

This equation shows how the material properties of the plate changes as a function of position within the thickness of the plate. Variation in material properties will lead to massive result on the mechanical and thermal behavior of the plate.

III.4. Functionally graded porous plates:

The existence of empty spaces in the material's structure is referred to as the porosity of FGM plates. This porosity may develop throughout the FGM plate manufacturing process, to more precise during the sintering phase or component material consolidation phase of the manufacturing process. FGM plates can have uniform, non-uniform, logarithmic-non-uniform, or density-based porosity, not to mention other possible varieties. Porosity in FGM plates has the possibility to massively affect the mechanical and thermal characteristics of the material in question.

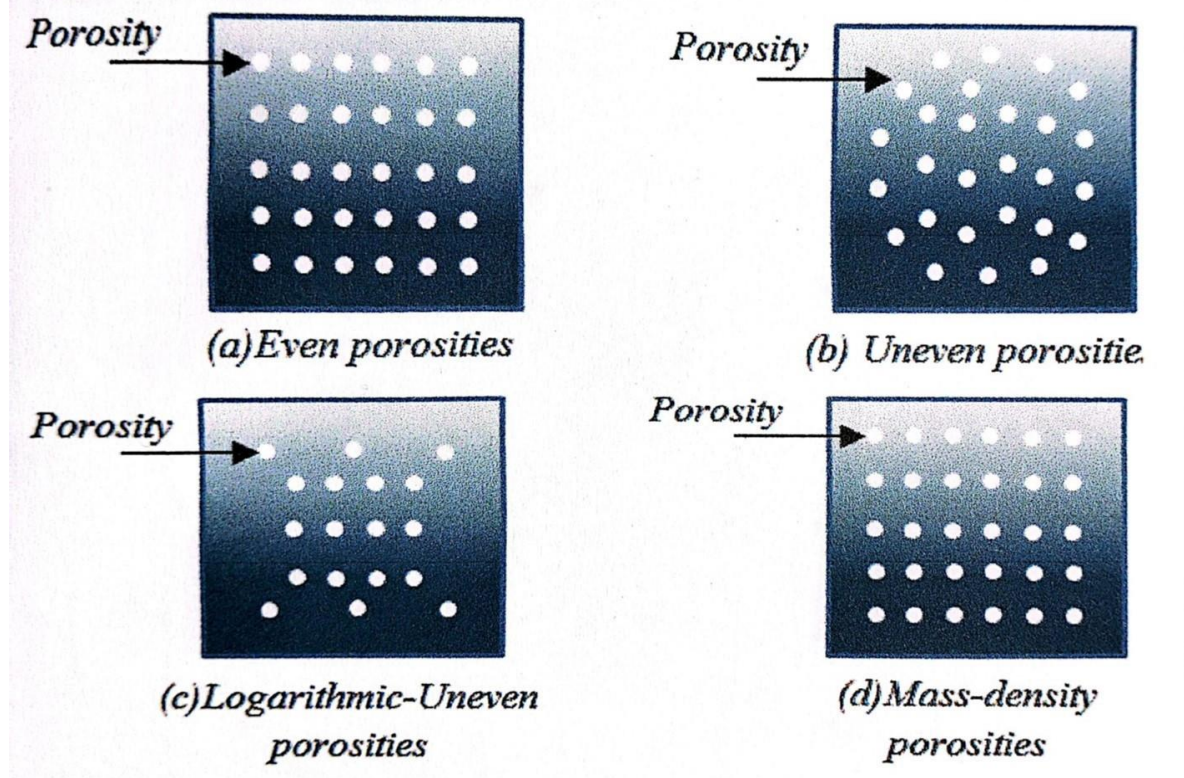


Figure III. 2: Presentation of various representations of porosity variations.

III.5. Types of porosity distribution:

III.5.1. FGM plates with porosity type I (even porosities):

Even porosity throughout the FGM plate's thickness can be seen in the first porosity distribution model. According to (Wattanasakulpong & Ungbhakorn, 2014) model, porosity remains constant throughout the plate's thickness (Fig. III.2a). Equations that take this uniform porosity distribution into account are used to derive the effective material properties (III.2).

$$P(z) = P_c \left(\left(\frac{1}{2} + \frac{z}{h} \right)^p - \frac{\xi}{2} \right) + P_m \left(1 - \left(\frac{1}{2} + \frac{z}{h} \right)^p - \frac{\xi}{2} \right) \quad (III.2)$$

Where ξ is the parameter which takes into account the effect of porosity.

Formulation of young's module $E(z)$ (III.3a), masse density $\rho(z)$ (III.3c) and poison's ratio $\nu(z)$ (III.3b) can be obtained by applying the equation (III.2) (Wattanasakulpong & Ungbhakorn, 2014):

$$E(z) = (E_c - E_m) \left(\frac{z}{h} + \frac{1}{2} \right)^p + E_m - \frac{\xi}{2} (E_c + E_m) \quad (III.3a)$$

$$\nu(z) = (\nu_c - \nu_m) \left(\frac{z}{h} + \frac{1}{2} \right)^p + \nu_m - \frac{\xi}{2} (\nu_c + \nu_m) \quad (III.3b)$$

$$\rho(z) = (\rho_c - \rho_m) \left(\frac{z}{h} + \frac{1}{2} \right)^p + \rho_m - \frac{\xi}{2} (\rho_c + \rho_m) \quad (III.3c)$$

III.5.2. FGM plates with porosity type II (uneven porosities)

Uneven porosity presents obstacles to material infiltration, especially in the intermediate zone, which in itself increase the risk of creating micro-voids. On the other hand, the upper and lower free surfaces of the plate allow for easier material infiltration; nevertheless, this also increases the risk of micro-void developing. Wattanasakulpong and Ungbhakorn's created a different porosity distribution model in which porosity varies with thickness, taking these factors into account. Equations define the effective properties of materials having an odd distribution, as seen in Figure III.2 (b). (III.4).

$$E(z) = (E_c - E_m) \left(\frac{z}{h} + \frac{1}{2} \right)^p + E_m - \frac{\xi}{2} (E_c + E_m) \left(1 - \frac{2|z|}{h} \right) \quad (IVI.4a)$$

$$\nu(z) = (\nu_c - \nu_m) \left(\frac{z}{h} + \frac{1}{2} \right)^p + \nu_m - \frac{\xi}{2} (\nu_c + \nu_m) \left(1 - \frac{2|z|}{h} \right) \quad (VI.4b)$$

$$\rho(z) = (\rho_c - \rho_m) \left(\frac{z}{h} + \frac{1}{2}\right)^p + \rho_m - \frac{\xi}{2}(\rho_c + \rho_m) \left(1 - \frac{2|z|}{h}\right) \quad (\text{VII.4c})$$

III.5.3. FGM plates with porosities type III (logarithmiques- uneven porosities)

Gupta and Talha (2018) created a model based on the porosity's logarithmic changes over plate thickness. In contrast to even or uneven distributions, this method provides a unique porosity distribution that affects material qualities in a different way.

$$E(z) = (E_c - E_m) \left(\frac{z}{h} + \frac{1}{2}\right)^p + E_m - \log\left(1 + \frac{\xi}{2}\right) (E_c + E_m) \left(1 - \frac{2|z|}{h}\right) \quad (\text{VIII.5a})$$

$$v(z) = (v_c - v_m) \left(\frac{z}{h} + \frac{1}{2}\right)^p + v_m - \log\left(1 + \frac{\xi}{2}\right) (v_c + v_m) \left(1 - \frac{2|z|}{h}\right) \quad (\text{VIII.5b})$$

$$\rho(z) = (\rho_c - \rho_m) \left(\frac{z}{h} + \frac{1}{2}\right)^p + \rho_m - \log\left(1 + \frac{\xi}{2}\right) (\rho_c + \rho_m) \left(1 - \frac{2|z|}{h}\right) \quad (\text{IXI.5c})$$

III.5.4. FG plate with type IV porosities (density):

The density-based FG porosity model with type IV porosities is based on the concepts of true and apparent density. These concepts are defined by the following equations:

$$m_0 = \int_h \rho(z) dz \quad \text{and} \quad \xi = 0 \quad \text{and} \quad m_1 = \int_h \rho(z) dz \quad \text{at} \quad \xi > 0 \quad (\text{III.6})$$

Or

$$\rho(z) = (\rho_c - \rho_m) \left(\frac{h}{z} + \frac{1}{2}\right)^p + \rho_m - \frac{\xi}{2}(\rho_c + \rho_m) \quad (\text{III.7})$$

Here, m_0 real mass density and m_1 apparent mass density. Considering that the model of elasticity depends on the density of the material, the expression for Young's model, as proposed by (Eltaher and al.), the following equation shows that:

$$E(z) = (E_c - E_m) \left(\frac{h}{z} + \frac{1}{2}\right)^p + E_m - \frac{m_0 - m_1}{m_0} - (E_c + E_m) \quad (\text{III.8})$$

With consideration for differences in elastic models as a function of density as well as both true and apparent densities, this model offers a more precise method for evaluating porosity in materials.

III.5.5. FGM plates with porosity type V:

A two-parameter porosity (type V) Although it allows for a greater range of porosity distributions, the addition of a two-parameter porosity model complicates the study. Different porosity distributions can be obtained by altering parameters like ξ and φ , which offers diversity in material design and optimization.

$$E(z) = (E_c - E_m)\left(\frac{z}{h} + \frac{1}{2}\right)^P + E_m - \frac{\xi}{2}(E_c + E_m)\left(1 - \frac{2|z|}{h}\right)^\varphi \quad (\text{III.9a})$$

$$\rho(z) = (\rho_c - \rho_m)\left(\frac{z}{h} + \frac{1}{2}\right)^P + \rho_m - \frac{\xi}{2}(\rho_c + \rho_m)\left(1 - \frac{2|z|}{h}\right)^\varphi \quad (\text{III.9b})$$

III.6. The four-variable first-order theory FSDT improved:

A crucial topic for the design and modeling of composite structures is the investigation of transverse shear stresses through the thickness of composite plates. Analytical analysis of these restrictions can be done precisely and effectively by using first-order theory with four variables.

This method is based on the analytical solutions for cross-stacked and balanced antisymmetric laminated composite plate structures provided by Hamilton's principle and Navier's method. When compared to higher-order theories and three-dimensional elasticity models, the four-variable first-order theory is distinguished by its precision and capacity to give dependable numerical findings.

For the examination of laminated composite plates' natural frequencies, the outcomes derived from this theory are essential. To ensure the stability and longevity of composite structures, accurate knowledge of transverse shear stresses through plate thickness is crucial. (BOUNOUARA, 2016)

Two terms can be identified in the transverse displacement component (w): bending is represented by term (w_b) and cross-sectional shear by term (w_s). These two elements are expressed as follows and solely rely on the x and y coordinates:

$$w = w_b + w_s \quad (\text{III.10})$$

III.6.1. Cinematic:

The simplified hypotheses in this study are based on an already existing FSDT theory, the difference in this theory is the number of unknown variables has been reduced to four.

The displacement field of the old FSDT is indicated by:

$$\begin{aligned}
 u(x, y, z) &= u_0(x, y) + z \frac{\delta w}{\delta x} - z \varphi_x(x, y) \\
 v(x, y, z) &= v_0(x, y) + z \frac{\delta w}{\delta y} - z \varphi_y(x, y) \\
 w(x, y, z) &= w_0(x, y)
 \end{aligned} \tag{III.11}$$

$(u_0, v_0, w_0, \varphi_x$ et $\varphi_y)$ are five unknown displacement functions of the midplane of the plate; and h represents the thickness of the plate. By dividing the transverse displacement w into two, bending and shear (meaning $w = w_b + w_s$) and by adding another hypothesis that is represented by this equation $\varphi_x = \frac{\delta w_b}{\delta x}$ et $\varphi_y = \frac{\delta w_b}{\delta y}$ the new displacement field of the present theory can be rewritten in a simpler form such that:

$$\begin{aligned}
 u(x, y, z) &= u_0(x, y) - z w_{b,1} \\
 v(x, y, z) &= v_0(x, y) - z w_{b,2} \\
 w(x, y, z) &= w_b(x, y) + w_s(x, y)
 \end{aligned} \tag{III.12}$$

The constraints linked to the displacement fields are:

$$\begin{Bmatrix} \varepsilon_x \\ \varepsilon_y \\ \gamma_{xy} \\ \gamma_{xz} \\ \gamma_{yz} \end{Bmatrix} = \begin{Bmatrix} u_{0,1} - z w_{b,11} \\ v_{0,2} - z w_{b,22} \\ u_{0,2} + v_{0,1} - 2z w_{b,22} \\ w_{s,1} \\ w_{s,2} \end{Bmatrix} \tag{III.13}$$

Assuming a linear distribution of shear stress throughout the plate's thickness, the basic theory of FSDT, or "First-order Shear Deformation Theory," was created. But in order to prevent shear-lock, this method needed a constant shear correction coefficient. A novel distributed shear function theory was put forth in an effort to enhance the basic FSDT theory. By using this method, discontinuities at the top and bottom surfaces are eliminated and shear

stress is distributed parabolically across the plate's thickness. This enhancement allows for a better consideration of the shear strain vector in plate analysis. (Nguyen and al, 2019) .

$$\begin{Bmatrix} \gamma_{xz}^c \\ \gamma_{yz}^c \end{Bmatrix} = f(z) \begin{Bmatrix} \gamma_{xz} \\ \gamma_{yz} \end{Bmatrix} \quad (III.14)$$

Transverse shear strain distribution through plate thickness is given by the shear distribution function $f(z)$. The following requirements were met by selecting this function: The shear strain is distributed parabolically across the thickness and is equal to zero on the plate's top and lower surfaces; the integration throughout the thickness of the plate roughly corresponds to the FSDT's constant shear correction factor (5/6). Inspired by the research of (Zenkour, 2006). The shear distribution function can be chosen as follows:

$$f(z) = \frac{5}{4} \cos\left(\frac{\pi z}{h}\right) \quad (III.15)$$

The constraints linked to the displacement fields are:

$$\begin{Bmatrix} \varepsilon_x \\ \varepsilon_y \\ \gamma_{xy} \end{Bmatrix} = \begin{Bmatrix} u_{0,1} \\ v_{0,2} \\ u_{0,2} + v_{0,1} \end{Bmatrix} - z \begin{Bmatrix} w_{b,11} \\ w_{b,22} \\ w_{b,22} \end{Bmatrix}, \quad \begin{Bmatrix} \gamma_{xz}^c \\ \gamma_{yz}^c \end{Bmatrix} = f(z) \begin{Bmatrix} \gamma_{xz} \\ \gamma_{yz} \end{Bmatrix} \quad (III.16)$$

III.7. Nonlocal Theory and Constitute Relations:

An interesting alternative to conventional physics theories is offered by Eringen. In actuality, there are often more restrictions on the application of classical concepts than one may believe, leading to inconsistent or a rather disparate kind of results from experimental findings. The non-local approach, which lies in between atomic theories and classical mechanics, considers the influence of the microstructure on the behavior of the material. This approach generalizes classical theories by considering that behavior at a given point depends on the state of the material at that location. In order to more thoroughly explain elastic behavior, these theories' mathematical formulation takes long-range interactions into account and include a unique internal length of the material. Said another way, constitutive relations and non-local theory offer a fresh perspective on understanding material behavior in a more refined way. (BOUNOUARA, 2016)

the study of Eringen (1983), the tensor of stresses not localized at the point is represented by:

$$\sigma - \mu \nabla^2 \sigma = \tau$$

In the two-dimensional case of a material with functional gradient, the nonlocal behavior relation in equation (III-16) is in the following forms:

$$\begin{pmatrix} \sigma_x \\ \sigma_y \\ \tau_{xy} \\ \tau_{xz} \\ \tau_{yz} \end{pmatrix} - \mu \left(\frac{\partial^2}{\partial x^2} + \frac{\partial^2}{\partial y^2} \right) \begin{pmatrix} \sigma_x \\ \sigma_y \\ \tau_{xy} \\ \tau_{xz} \\ \tau_{yz} \end{pmatrix} = \begin{bmatrix} C_{11} & C_{12} & 0 & 0 & 0 \\ C_{12} & C_{22} & 0 & 0 & 0 \\ 0 & 0 & C_{66} & 0 & 0 \\ 0 & 0 & 0 & C_{55} & 0 \\ 0 & 0 & 0 & 0 & C_{44} \end{bmatrix} \begin{pmatrix} \varepsilon_x \\ \varepsilon_y \\ \gamma_{xy} \\ \gamma_{xz} \\ \gamma_{yz} \end{pmatrix} \quad (III.16)$$

($\sigma_x, \sigma_y, \tau_{xy}, \tau_{xz}, \tau_{yz}$) and ($\varepsilon_x, \varepsilon_y, \gamma_{xy}, \gamma_{xz}, \gamma_{yz}$) are the components of stresses and strains, respectively. And C_{ij} can be given by:

$$C_{11} = C_{22} = \frac{E(z)}{1-\nu^2} ; C_{12} = \frac{\nu E(z)}{1-\nu^2} ; C_{44} = C_{55} = C_{66} = \frac{E(z)}{2(1+\nu)} \quad (III.17)$$

III.8. Movement Equation:

Hamilton's principle is used to derive equations of motion in our study It can be formulated analytically:

$$0 = \int_0^T (\delta U + \delta U_f - \delta K) dt \quad (III.18)$$

$\delta U, \delta U_f$ and δK are the variations, of strain energy, energy of work done by external forces and kinetic energy, respectively.

*** The variations in the strain energy are calculated by:**

$$\delta U = \int_A \int_{-h/2}^{h/2} (\sigma_x \delta \varepsilon_x + \sigma_y \delta \varepsilon_y + \tau_{xy} \delta \gamma_{xy} + \tau_{xz}^c \delta \gamma_{xz}^c + \tau_{yz}^c \delta \gamma_{yz}^c) dz dA \quad (III.19)$$

$$\begin{aligned} \delta U = \int_A [& N_x \delta U_{,1} - M_y \delta w_{b,11} + N_y \delta U_{f,2} + M_y \delta w_{b,22} + N_{xy} (\delta u_{,2} + \delta U_{f,1}) - 2M_{,xy} \delta w_{b,12} \\ & + Q_x^c \delta w_{s,1} + Q_y^c \delta w_{s,2}] dA \end{aligned}$$

N, M and Q^c are the resulting constraints defined by:

$$(N_x, N_y, N_{xy}) = \int_{-h/2}^{h/2} (\sigma_x, \sigma_y, \sigma_{xy}) dz \quad (III.20a)$$

$$(M_x, M_y, M_{xy}) = \int_{-h/2}^{h/2} (\sigma_x, \sigma_y, \sigma_{xy}) z dz \quad (III.20b)$$

$$(Q_x^c, Q_y^c) = \int_{-h/2}^{h/2} (\tau_{xz}^c, \tau_{yz}^c) f(z) dz \quad (III.20c)$$

* The expression of the variation of work energy δU_f is:

$$\delta U_f = - \int_V (U_{Winkler} + U_{Pasternak}) dV \quad (III.21)$$

- **Winkler Model:**

$$q_{Winkler} = K_0 W$$

- **Pasternak Model:**

$$q_{Pasternak} = k_0 W - k_1 \nabla^2 W$$

k_1 Is the shear stiffening and ∇^2 is the reongulair carttesian coordinates

The Laplace differential operator:

$$\nabla^2 = \frac{\partial^2}{\partial x^2} + \frac{\partial^2}{\partial y^2}$$

* The change in strain energy is calculated by:

$$\delta K = \int_V (\dot{u}\delta\dot{u} + \dot{v}\delta\dot{v} + \dot{w}\delta\dot{w}) \rho(z) dV \quad (III.22)$$

After integration by part in the direction of the thickness, equation (III.23) becomes:

$$\delta K = \int_A \{ I_0 [\dot{u}\delta\dot{u} + \dot{v}\delta\dot{v} + (\dot{w}_b + \dot{w}_s)\delta(\dot{w}_b + \dot{w}_s)] - I_1 (\dot{u}\delta\dot{w}_{b,1} + \dot{w}_{b,1}\delta\dot{u} + \dot{v}\delta\dot{w}_{b,2} + \dot{w}_{b,2}\delta\dot{v}) + I_2 (\dot{w}_{b,1}\delta\dot{w}_{b,1} + \dot{w}_{b,2}\delta\dot{w}_{b,2}) \} dA$$

The superscript symbol (.) indicates differentiation with respect to the time variable (t).

The density of the material is represented by the symbol (ρ).

(I_0, I_1, I_2) Represent the mass inertias defined by:

$$(I_0, I_1, I_2) = \int_{-h/2}^{h/2} (1, z, z^2) \rho(z) dz \quad (III.23)$$

By substituting the expressions of the variations $\delta U, \delta V$ and δK are given by the equations (III.19), (III.20) and (III.21) in equation (III.16) and by carrying out the integration by parts, then by grouping the coefficients or terms of $\delta u, \delta v, \delta w_b$ and δw_s .

we obtain the following equations of motion of the present theory:

$$\begin{aligned} \delta u: N_{x,1} + N_{xy,2} &= I_0 \ddot{u} - I_1 \ddot{w}_{b,1} \\ \delta v: N_{y,2} + N_{xy,1} &= I_0 \ddot{v} - I_1 \ddot{w}_{b,2} \\ \delta w_b: M_{x,11} + M_{y,22} + 2M_{xy,12} - q_{Winkler} - q_{Pasternak} \\ &= I_0 (\ddot{w}_b + \ddot{w}_s) + I_1 (\ddot{u}_{,1} + \ddot{v}_{,2}) - I_2 (\ddot{w}_{b,11} + \ddot{w}_{b,22}) \\ \delta w_s: Q_{x,1}^c + Q_{y,2}^c &= I_0 (\ddot{w}_b + \ddot{w}_s) \end{aligned} \quad (III.24)$$

By substituting equation (III.13 and 14) into equation (III-16) and the subsequent results into equation (III-20), the constraint resultants are determined as follows:

$$\begin{Bmatrix} N_x \\ N_y \\ N_{xy} \end{Bmatrix} - \mu \left(\frac{\partial^2}{\partial x^2} + \frac{\partial^2}{\partial y^2} \right) \begin{Bmatrix} N_x \\ N_y \\ N_{xy} \end{Bmatrix} = \begin{bmatrix} A_{11} & A_{12} & 0 \\ A_{12} & A_{22} & 0 \\ 0 & 0 & A_{66} \end{bmatrix} \begin{Bmatrix} u_{,1} \\ v_{,2} \\ u_{,2} + v_{,1} \end{Bmatrix} + \begin{bmatrix} B_{11} & B_{12} & 0 \\ B_{12} & B_{22} & 0 \\ 0 & 0 & B_{66} \end{bmatrix} \begin{Bmatrix} -w_{b,11} \\ -w_{b,22} \\ -2w_{b,12} \end{Bmatrix} \quad (III.25a)$$

$$\begin{Bmatrix} M_x \\ M_y \\ M_{xy} \end{Bmatrix} - \mu \left(\frac{\partial^2}{\partial x^2} + \frac{\partial^2}{\partial y^2} \right) \begin{Bmatrix} M_x \\ M_y \\ M_{xy} \end{Bmatrix} = \begin{bmatrix} B_{11} & B_{12} & 0 \\ B_{12} & B_{22} & 0 \\ 0 & 0 & B_{66} \end{bmatrix} \begin{Bmatrix} u_{,1} \\ v_{,2} \\ u_{,2} + v_{,1} \end{Bmatrix} + \begin{bmatrix} D_{11} & D_{12} & 0 \\ D_{12} & D_{22} & 0 \\ 0 & 0 & D_{66} \end{bmatrix} \begin{Bmatrix} -w_{b,11} \\ -w_{b,22} \\ -2w_{b,12} \end{Bmatrix} \quad (III.25b)$$

$$\begin{Bmatrix} Q_{xz}^c \\ Q_{yz}^c \end{Bmatrix} - \mu \left(\frac{\partial^2}{\partial x^2} + \frac{\partial^2}{\partial y^2} \right) \begin{Bmatrix} Q_{xz}^c \\ Q_{yz}^c \end{Bmatrix} = \begin{bmatrix} Aa_{55} & 0 \\ 0 & Aa_{444} \end{bmatrix} \begin{Bmatrix} w_{s,1} \\ w_{s,2} \end{Bmatrix} \quad (III.25c)$$

nonlocal theory equations of motion:

$$\begin{aligned}
 \delta u: N_{x,1} + N_{xy,2} &= (1 - \mu \nabla^2)(I_0 \ddot{u} - I_1 \ddot{w}_{b,1}) \\
 \delta v: N_{y,2} + N_{xy,1} &= (1 - \mu \nabla^2)(I_0 \ddot{v} - I_1 \ddot{w}_{b,2}) \quad (III.26) \\
 \delta w_b: [M_{x,11} + M_{y,22} + 2M_{xy,12}] &+ (1 - \mu \nabla^2)(k_0 W - k_1 \nabla^2 W) \\
 &= (1 - \mu \nabla^2)(I_0(\ddot{w}_b + \ddot{w}_s) + I_1(\ddot{u}_{,1} + \ddot{v}_{,2}) - I_2(\ddot{w}_{b,11} + \ddot{w}_{b,22})) \\
 \delta w_s: Q_{x,1}^c + Q_{y,2}^c &= (1 - \mu \nabla^2)(I_0(\ddot{w}_b + \ddot{w}_s))
 \end{aligned}$$

III.9. The Navier method:

The Navier method can be displayed in double trigonometric functions as follows:

$$\begin{cases} u(x, y, t) \\ v(x, y, t) \\ w_b(x, y, t) \\ w_s(x, y, t) \end{cases} = \sum_{m=1}^{\infty} \sum_{n=1}^{\infty} \begin{cases} U_{mn} e^{i\omega t} \cos \alpha_m x \sin \beta_n y \\ V_{mn} e^{i\omega t} \sin \alpha_m x \cos \beta_n y \\ W_{bmn} e^{i\omega t} \sin \alpha_m x \sin \beta_n y \\ W_{smn} e^{i\omega t} \sin \alpha_m x \sin \beta_n y \end{cases} \quad (III.27)$$

Where U_{mn} , V_{mn} , W_{bmn} and W_{smn} are arbitrary parameters to be determined, ω is the eigenfrequency associated with (m,n) the eigenmode, and $\alpha = m\pi / a$ and $\beta = n\pi / b$.

$$q(x) = \sum_{m=1,3,5}^{\infty} \sum_{N=1,3,5}^{\infty} Q_{mn} \sin \alpha x \sin \beta y \quad (III.28)$$

For a sinusoidally distributed load, we have:

$$m = n = 1 \quad \text{and} \quad Q_1 = q_0 \quad (III.29)$$

The analytical solutions can be derived for any fixed value of 'm' and 'n' by substituting Equations (III.27) and (III.28) into Equation (III.26).

Free vibration:

$$([K] - \omega^2 \lambda [M]) \{\Delta\} = \{0\} \quad (III.30 a)$$

Static problems:

$$[K]\{\Delta\} = \{F\} \quad (\text{III.30 b})$$

where

$$[K] = \begin{bmatrix} a_{11} & a_{12} & a_{13} & a_{14} \\ a_{12} & a_{22} & a_{23} & a_{24} \\ a_{13} & a_{23} & a_{33} & a_{34} \\ a_{14} & a_{24} & a_{34} & a_{44} \end{bmatrix}, \quad (\text{III.31 a})$$

$$[M] = \begin{bmatrix} m_{11} & 0 & m_{13} & m_{14} \\ 0 & m_{22} & m_{23} & m_{24} \\ m_{13} & m_{23} & m_{33} & m_{34} \\ m_{14} & m_{24} & m_{34} & m_{44} \end{bmatrix}, \quad (\text{III.31 b})$$

and

$$\{\Delta\} = \begin{Bmatrix} U_m \\ V_m \\ W_{bm} \\ W_{sm} \end{Bmatrix}, \quad \{F\} = \begin{Bmatrix} 0 \\ 0 \\ Q_m \\ Q_m \end{Bmatrix} \quad (\text{III.31 c})$$

with

$$\begin{aligned}
a_{11} &= -\alpha^2 A_{11} - \beta^2 A_{66} \\
a_{12} &= -\alpha\beta(A_{12} + A_{66}) \\
a_{13} &= \alpha[\alpha^2 B_{11} + (B_{12} + 2B_{66})\beta^2] \\
a_{14} &= 0 \\
a_{22} &= -\alpha^2 A_{66} - \beta^2 A_{22} \\
a_{23} &= \beta[\beta^2 B_{22} + (B_{12} + 2B_{66})\alpha^2] \\
a_{24} &= 0 \\
a_{33} &= -[D_{11}\alpha^4 + 2(D_{12} + 2D_{66})\alpha^2\beta^2 + D_{22}\beta^4] - \lambda\alpha[k_0 + (\beta^2 + \alpha^2)k_1] \\
a_{34} &= 0 \\
a_{44} &= -[A_{55}^s\alpha^2 + \beta^2 A_{44}^s] - \lambda\alpha[k_0 + (\beta^2 + \alpha^2)k_1]
\end{aligned}$$

$$\begin{aligned}
m_{11} &= I_1 \\
m_{12} &= 0 \\
m_{13} &= -I_2\alpha \\
m_{14} &= 0 \\
m_{22} &= I_1 \\
m_{23} &= -I_2\beta \\
m_{24} &= 0 \\
m_{33} &= I_1 + I_3(\beta^2 + \alpha^2) \\
m_{34} &= I_1 \\
m_{44} &= I_1 \\
\lambda &= 1 + \mu(\beta^2 + \alpha^2)
\end{aligned} \tag{III.32}$$

III.10. Conclusion:

In this chapter, a first order shear deformation theory (FSDT) with four unknowns was used to provide a dynamic behavior analysis of perfect and imperfect FG-plates. The research was done on a functionally graded metal-ceramic nano plate (P-FGM) that was resting on an elastic foundation of the Winkler-Pasternak type. The porosity effect in graded material properties is described by five different models of porosity distributions. Using the Navier equation and Hamilton's equation, as well as nonlocal theory which was provided by Eringen work, the equations of motion was established.

Chapter IV

Results and discussion

IV. Introduction

In this chapter, our goal is to present the numerical results obtained to demonstrate the effectiveness and accuracy of the proposed theory regarding the static and free vibration responses of isotropic homogeneous plates and functionally graded material (FGM) plates at different scales.

These plates are simply supported, with or without the presence of Winkler or Pasternak elastic foundations. The material properties of FGM plates vary according to different porosity distributions. Our study aims to evaluate the impact of material index, porosity index, geometric ratio, non-local parameter, and elastic foundation parameters on the vibrational characteristics of these plates.

IV.1. Presentation and Analysis of Results:

IV.1.1. Mechanical Analysis of Macroscopic Functionally Graded Material (FGM) Plates

Here, we use a new shear deformation theory to give numerical findings for the static response analysis of a simply supported Functionally Graded Material (FGM) plate subjected to uniform and sinusoidal stress, sitting on a Winkler-Pasternak elastic foundation. Solutions from the literature are compared and contrasted. This chapter presents a number of numerical examples to confirm the accuracy of this theory.

The numerical results are presented for a ceramic/metal graded plate that has been evaluated. The material properties are given as follows:

Ceramic Properties:

- Young's Modulus (E_c): 380 GPa
- Poisson's Ratio (ν_c): 0.3
- Density (ρ_c): 3,800 kg/m³

Metal Properties:

- Young's Modulus (E_m): 70 GPa
- Poisson's Ratio (ν_m): 0.3
- Density (ρ_m): 2,702 kg/m³

The parameters non-dimensional form:

$$\bar{w} = \frac{10h^3 E_c}{a^4 q_0} w \left(\frac{a}{2}, \frac{b}{2} \right)$$

$$\bar{\sigma}_x = \frac{h}{aq_0} \sigma_x \left(\frac{a}{2}, \frac{b}{2}, \frac{h}{2} \right)$$

$$\bar{\tau}_{xy} = \frac{h}{aq_0} \tau_{xy} \left(0, 0, -\frac{h}{3} \right)$$

$$\bar{\tau}_{xz} = \frac{h}{aq_0} \tau_{xz} \left(0, \frac{b}{2}, 0 \right)$$

$$K_0 = k_0 a^4 / D \text{ et } K_1 = k_1 a^2 / D.$$

$$\text{where } D = Eh^3 / 12(1-\nu^2)$$

A comparison of the transverse shear stresses and non-dimensional deflections of a simply supported square FGM plate is shown in **Table IV.1**. A comparison is made between the outcomes and the findings derived from the Sinusoidal Shear Deformation Theory (SSDT) (Touratier, 1991).

Table IV. 1: Comparison of non-dimensional deflections and transverse shear stresses of an FGM plate under sinusoidal loading.

a/h	p	\bar{w}		$\bar{\tau}_{xz}$	
		SSDT	present	SSDT	present
2	0	0,6668	0,6696	0,2414	0,2291
	1	1,2152	1,2198	0,2414	0,2291
	4	2,1353	2,1261	0,1975	0,1838
	10	2,7205	2,7215	0,2136	0,2003
10	0	0,2960	0,2960	0,2462	0,2321
	1	0,5889	0,5889	0,2462	0,2321
	4	0,8819	0,8810	0,2029	0,1873
	10	1,0089	1,0083	0,2198	0,2042

The results produced by the current approach are in good agreement with those reported by SSDT, as Table IV.1 demonstrates. Table IV.1 further illustrates how the material parameter p affects the deflections and stresses.

The non-dimensional deflections of a thin isotropic plate sitting on a Winkler-Pasternak elastic foundation are compared with those reported in the literature in order to justify the current approach.

A comparison of the deflections of a square homogenous plate with simple support that is resting on a Winkler elastic foundation under uniform loading is shown in **Table IV.2**. The deflections are compared to those reported by (Lam and al., 2000) and (Kobayashi and Sonoda, 1989), where a good degree of agreement was seen between the findings.

Table IV. 2: Comparison of non-dimensional deflections of a homogeneous plate under uniform loading resting on a Winkler foundation for a/h=100.

K ₀	$\frac{Dw(0,5a,0,5a)10^3}{qa^4}$		
	[Kobayashi 1989]	[Lam et al. 2000]	present
1	4,052	4,053	4,052
3 ⁴	3,347	3,349	3,347
5 ⁴	1,506	1,507	1,506

A comparative analysis of the deflections of a square homogenous plate with simple support put on an elastic foundation made of Winkler-Pasternak under uniform loading is shown in **Table IV.3**. The current theory's results (four variables) are in close agreement with those of ((Lam and al., 2000)).

Table IV. 3: Comparison of non-dimensional deflections of a homogeneous plate under uniform loading resting on a Winkler-Pasternak elastic foundation for $a/h=100$.

K ₀	K ₁	$\frac{Dw(0,5a, 0,5a)10^3}{qa^4}$	
		[Lam et al.2000]	present
1	1	3,853	3,853
	3 ⁴	0,763	0,763
	5 ⁴	0,115	0,115
3 ⁴	1	3,210	3,210
	3 ⁴	0,732	0,732
	5 ⁴	0,115	0,115
5 ⁴	1	1,476	1,476
	3 ⁴	0,570	0,570
	5 ⁴	0,109	0,109

Figure IV.1 illustrates the distribution of the shear stress as a function of the ratio z/h for a square FGM plate under sinusoidal loading.

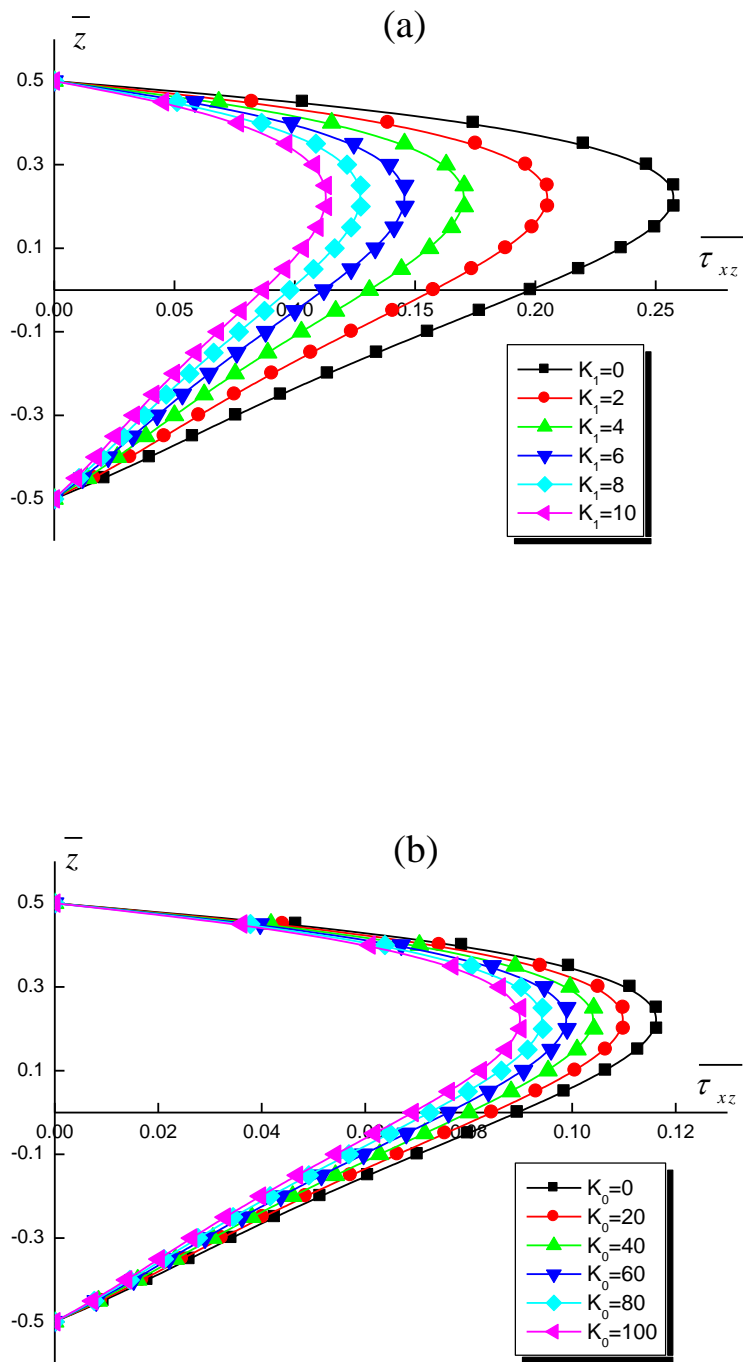
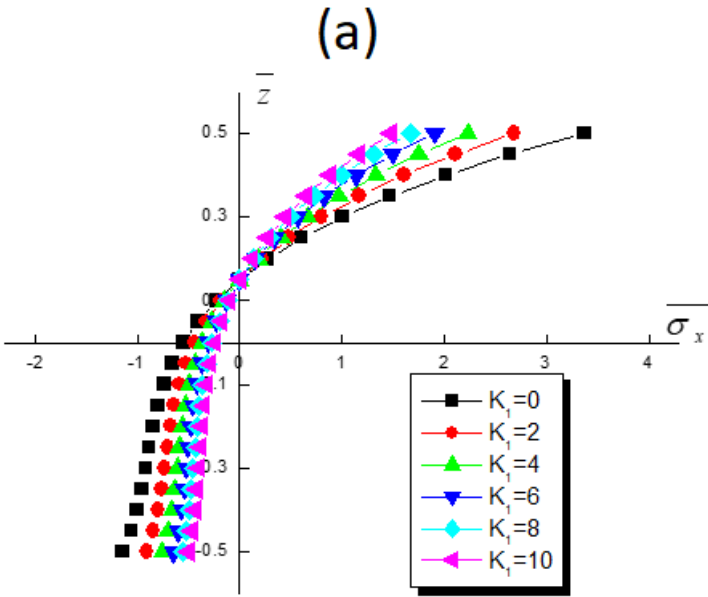


Figure IV. 1: Variation of transverse shear stress as a function of z/h for a square FGM plate on elastic supports with $a/h=10$, $p=2$: (a) $K_0=10$; (b) $K_i=10$.

The distinction between the curves in **Figures IV.1.a** and **IV.1.b** is evident. It can be observed that the transverse shear stress gradually increases with the decrease of K_0 or K_1 , indicating that increasing the elastic modulus of the foundation can enhance the stiffness of the plate.

Additionally, the distribution of transverse shear stress through the thickness of the plate is not parabolic, as is typically known for homogeneous plates. The maximum shear stress value is obtained at the surfaces ($z/h=\pm 0.5$) and not in the middle of the plate ($z/h=0$), as is the case for homogeneous materials (composed of a single material).

Figures IV.2 show the distribution of longitudinal normal stress as a function of the ratio z/h for a square FGM plate under sinusoidal loading.



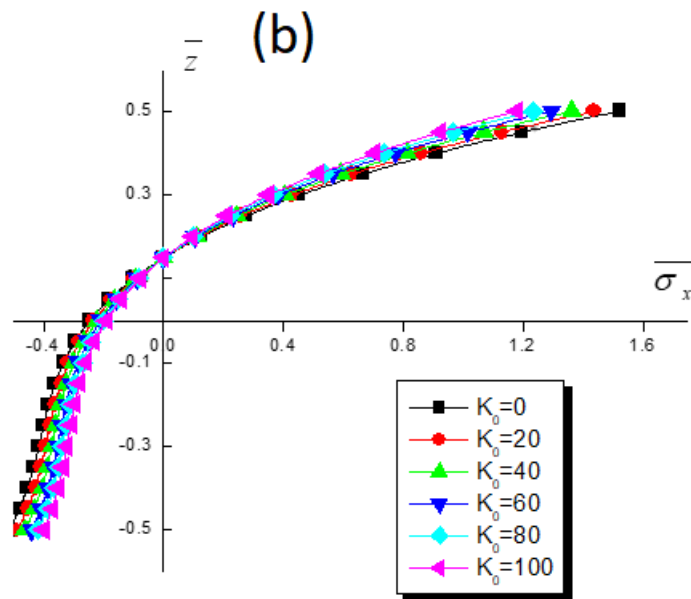


Figure IV. 2: Variation of normal stress as a function of $z/hz/h$ for a square FGM plate on elastic supports with $a/h=10$, $p=2$, (a) $K_0 = 10$. (b) $K_1 = 10$

Based on the results illustrated in Figures IV.2, it can be observed that:

- The stresses are in a state of compression and reach their minimum values in the lower half (metal-rich side).
- The stresses are zero at $z/h=0.151$. Beyond this point, they transition to a state of tension and become significantly higher compared to the compressive stresses in the upper half (ceramic-rich side).
- The maximum values of normal compressive and tensile stresses are found at the extreme lower and upper fibers of the plate, respectively.
- The elastic foundation has a significant effect on the maximum values of the normal stress σ_x . As evident, the normal stress gradually increases with the decrease of K_0 or K_1 .

Figure IV.3 depicts the distribution of the tangential stress as a function of the ratio z/h for a square FGM plate under sinusoidal loading. From the results illustrated in Figure IV.3, it can be observed that the tangential stress is maximal at certain points on the upper and lower surfaces of the FGM plate. It is zero at $\bar{z} = 0,151$

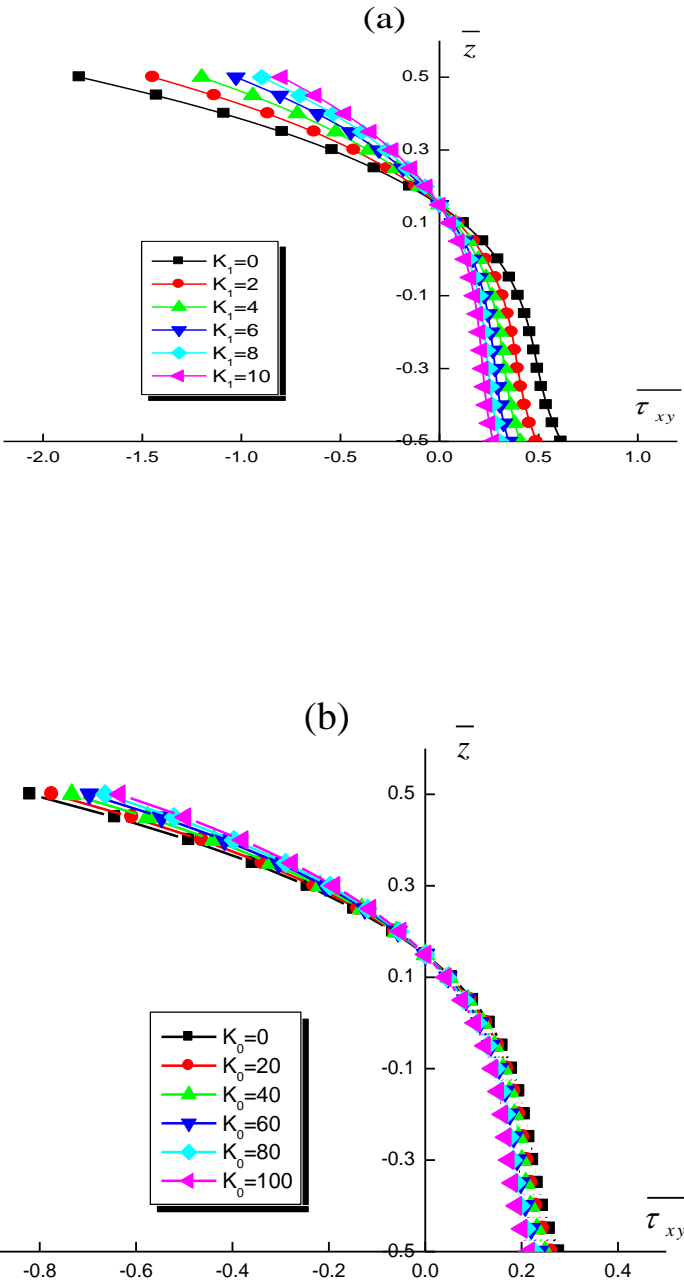


Figure IV. 3: Variation of the shear stress as a function of z/h for a square FGM plate on elastic supports with $a/h=10$, $p=2$: (a) $K_0=10$; (b) $K_1=10$.

IV.1.2. Dynamic Analysis of Macroscopic Functionally Graded Material (FGM) Plates

A plate AL/Al₂O₃ composed of Aluminum (as metal) and Alumina (as ceramic) is considered. The material characteristics such as Young's modulus and the mass density of Aluminum are $E_m = 70GPA$ et $\rho_m = 2702Kg/m^3$, while those of Alumina are $E_c = 380GPA$, $\rho_c = 3800Kg/m^3$. The Poisson's ratio is assumed constant throughout the thickness of the plate, with a value of 0.3. The different nondimensional parameters used are:

Dimensionless frequency parameters:

$$\omega^* = \omega \frac{a^2}{h\pi} \sqrt{\frac{12\rho}{E}} ; \hat{\omega} = \omega h \sqrt{\frac{\rho_c}{E_c}} ; \bar{\omega} = \omega \frac{a^2}{h} \sqrt{\frac{\rho_c}{E_c}} ; \tilde{\omega} = \omega h \sqrt{\frac{\rho_m}{E_m}} ; \bar{\omega} = \omega \frac{a^2}{h} \sqrt{\frac{\rho_m}{E_m}}$$

Foundation parameters:

$$K_0 = k_0 a^4 / D \quad K_1 = k_1 a^2 / D$$

Where

$$D_{11} = \frac{E_m h^3}{(12 - (1 - \nu_m))}$$

A- Perfectly Supported FG Plate

Table IV.4 presents the first five dimensionless fundamental frequencies ω^* of a simply supported isotropic square plate, with simply supported boundary conditions ($a/h=1000$ and $a/h=5$). The results obtained are compared to those published by (Manna, 2005), (Leissa, 1973), (Liew and al., 1993), (Raju and al., 1980).

It is noted that the obtained results correlate well with the results of the other mentioned studies.

Table IV. 4:The first five dimensionless fundamental frequencies ω^* of a simply supported

a/h	Source	Mode				
		1	2	3	4	5
1000	(Manna, 2005)	2.000	5.000	5.000	8.000	10.000
	(Manna, 2005)	2.000	5.000	5.000	8.000	10.000
	(Manna, 2005)	2.000	5.000	5.000	8.000	10.000
	(Leissa, 1973)	2.000	5.000	5.000	8.000	10.000
	(Liew, and al, 1993)	2.000	5.000	5.000	8.000	10.000
	Present	2.0965	5.2413	5.2413	8.3861	10.4826
5	(Manna, 2005)	1.768	3.868	3.868	5.596	6.615
	(Manna, 2005)	1.768	3.868	3.868	5.594	6.611
	(Manna, 2005)	1.807	4.000	4.000	5.807	6.867
	(Liew and al., 1993)	1.768	3.866	3.866	5.588	6.601
	(Raju and al, 1980)	1.768	3.876	3.876	5.600	6.683
	Present	1.8459	4.0225	4.0225	5.8021	6.8463

Table IV.5 shows the values obtained for the first two nondimensional fundamental frequencies $\hat{\omega}$ of square Al/Al₂O₃ plates for different values of the length-to-thickness ratio and the power index P. Using the current theory and other theories.

Analysis of this table reveals that the current theory offers excellent accuracy in determining the frequencies of FGM plates. Additionally, it was found that the nondimensional frequencies $\hat{\omega}$ of FGM plates decreased as the value of the power index increased.

Table IV. 5: The first two nondimensional fundamental frequencies ω of square Al/Al₂O₃ plate

Mode	a/h	Method	p				
			0	0.5	1	4	10
1	2	Quasi-3D (Matsunaga, 2008)	0.9400	0.8233	0.7477	0.5997	0.5460
		S-FSDT (Thai & Choi, 2013)	0.9265	0.8062	0.7333	0.6116	0.5644
		Present	0.9157	0.8017	0.7258	0.5815	0.5277
	5	Quasi-3D (Matsunaga, 2008)	0.2121	0.1819	0.1640	0.1383	0.1306
		S-FSDT (Thai & Choi, 2013)	0.2112	0.1805	0.1631	0.1397	0.1324
		Present	0.2103	0.1801	0.1625	0.1372	0.1291
	10	Quasi-3D (Matsunaga, 2008)	0.0578	0.0492	0.0443	0.0381	0.0364
		S-FSDT (Thai & Choi, 2013)	0.0577	0.0490	0.0442	0.0382	0.0366
		Present	0.0576	0.0489	0.0441	0.0380	0.0362
2	2	Quasi-3D (Matsunaga, 2008)	1.7406	1.5425	1.4078	1.1040	0.9847
		S-FSDT (Thai & Choi, 2013)	1.7045	1.4991	1.3706	1.1285	1.0254
		Present	1.6774	1.4876	1.3509	1.0542	0.9387
	5	Quasi-3D (Matsunaga, 2008)	0.4658	0.4040	0.3644	0.3000	0.2790
		S-FSDT (Thai & Choi, 2013)	0.4618	0.3978	0.3604	0.3049	0.2856
		Present	0.4584	0.3963	0.3580	0.2951	0.2732
	10	Quasi-3D (Matsunaga, 2008)	0.1381	0.1180	0.1063	0.0905	0.0859
		S-FSDT (Thai & Choi, 2013)	0.1376	0.1173	0.1059	0.0911	0.0867
		Present	0.1372	0.1171	0.1056	0.0899	0.0852

Table IV.6 illustrates the first four nondimensional frequencies ω of a rectangular FGM plate, with geometric ratios of 5, 10, and 20, and a power law index varying from 0 to 10. The plate was composed of aluminum as metal and alumina as ceramic. Using equation (III.1) to evaluate the Young's modulus and the density of the plate, the first four nondimensional frequencies ω obtained from this theory were compared to those provided by (Hosseini-Hashemi and al, 2011) based on FSDT, (Reddy,2000) based on TSDT, and (Thai and al, 2013) based on SSDT.

Table IV. 6: The first four nondimensional frequencies $\bar{\omega}$ of a rectangular plate ($b/a=2$)

a/h	Mode (m, n)	Method	P						
			0	0.5	1	2	5	8	10
5	1 (1,1)	(Hosseini-Hashemi and al, 2011)	3.4409	2.9322	2.6473	2.4017	2.2528	2.1985	2.1677
		(Reddy,2000)	3.4412	2.9347	2.6475	2.3949	2.2272	2.1697	2.1407
		(Thai and al, 2013)	3.4416	2.9350	2.6478	2.3948	2.2260	2.1688	2.1403
		Present	3.4315	2.9285	2.6411	2.4875	2.2203	2.1609	2.1303
	2 (1,2)	(Hosseini-Hashemi and al, 2011)	5.2802	4.5122	4.0773	3.6953	3.4492	3.3587	3.3094
		(Reddy,2000)	5.2813	4.518	4.0781	3.6805	3.3938	3.2964	3.2514
		(Thai and al, 2013)	5.2822	4.5187	4.0787	3.6804	3.3914	3.2947	3.2506
		Present	5.2592	4.5039	4.0635	3.6638	3.3782	3.2769	3.2283
	3 (1,3)	(Hosseini-Hashemi and al, 2011)	8.0710	6.9231	6.2636	5.6695	5.2579	5.1045	5.0253
		(Reddy,2000)	8.0749	6.9366	6.2663	5.6390	5.1425	4.9758	4.9055
		(Thai and al, 2013)	8.0772	6.9384	6.2678	5.6391	5.1378	4.9727	4.9044
		Present	8.0257	6.9052	6.2333	5.6012	5.1074	4.9328	4.8553
	4 (2,1)	(Hosseini-Hashemi and al, 2011)	9.7416	8.6926	7.8711	7.1189	6.5749	5.9062	5.7518
		(Reddy,2000)	10.1164	8.7138	7.8762	7.0751	6.4074	6.1846	6.0954
		(Thai and al, 2013)	10.1201	8.7167	7.8787	7.0756	6.4010	6.1806	6.0942
		Present	10.0415	8.6657	7.8257	7.0171	6.3536	6.1196	6.0200

10	1 (1,1)	(Hosseini-Hashemi and al, 2011)	3.6518	3.0983	2.7937	2.5386	2.3998	2.3504	2.3197
		(Reddy,2000)	3.6518	3.0990	2.7937	2.5364	2.3916	2.3411	2.3110
		(Thai and al, 2013)	3.6519	3.0991	2.7937	2.5364	2.3912	2.3408	2.3108
		Present	3.6488	3.0972	2.7917	2.5342	2.3895	2.3384	2.3078
	2 (1,2)	(Hosseini-Hashemi and al, 2011)	5.7693	4.8997	4.4192	4.0142	3.7881	3.7072	3.6580
		(Reddy,2000)	5.7694	4.9014	4.4192	4.0090	3.7682	3.6846	3.6368
		(Thai and al, 2013)	5.7697	4.9016	4.4194	4.0089	3.7673	3.6839	3.6365
		Present	5.7622	4.8969	4.4145	4.0036	3.7632	3.6780	3.6290
	3 (1,3)	(Hosseini-Hashemi and al, 2011)	9.1876	7.8145	7.0512	6.4015	6.0247	5.8887	5.8086
		(Reddy,2000)	9.1880	7.8189	7.0515	6.3886	5.9765	5.8341	5.7575
		(Thai and al, 2013)	9.1887	7.8194	7.0519	6.3885	5.9742	5.8324	5.7566
		Present	9.1702	7.8007	7.0399	6.3754	5.9640	5.8180	5.7383
	4 (2,1)	(Hosseini-Hashemi and al, 2011)	11.8310	10.0740	9.0928	8.2515	7.7505	7.5688	7.4639
(Reddy,2000)		11.8315	10.0810	9.0933	8.2309	7.6731	7.4813	7.3821	
(Thai and al, 2013)		11.8326	10.0818	9.0940	8.2306	7.6696	7.4787	7.3808	
Present		11.8024	10.0627	9.0743	8.2091	7.6527	7.4552	7.3511	
20	1 (1,1)	(Hosseini-Hashemi and al, 2011)	3.7123	3.1456	2.8352	2.5777	2.4425	2.3948	2.3642
		(Reddy,2000)	3.7123	3.1458	2.8352	2.5771	2.4403	2.3923	2.3619
		(Thai and al, 2013)	3.7123	3.1458	2.8353	2.5771	2.4401	2.3922	2.3618

		Present	3.7115	3.1453	2.8347	2.5765	2.4397	2.3915	2.3610
2 (1,2)	(Hosseini-Hashemi and al, 2011)	5.9198	5.0175	4.5228	4.1115	3.8939	3.8170	3.7681	
	(Reddy,2000)	5.9199	5.0180	4.5228	4.1100	3.8884	3.8107	3.7622	
	(Thai and al, 2013)	5.9199	5.0180	4.5228	4.1100	3.8881	3.8105	3.7621	
	Present	5.9179	5.0167	4.5215	4.1086	3.8870	3.8089	3.7600	
3 (1,3)	(Hosseini-Hashemi and al, 2011)	9.5668	8.1121	7.3132	6.6471	6.2903	6.1639	6.0843	
	(Reddy,2000)	9.5669	8.1133	7.3132	6.6433	6.2760	6.1476	6.0690	
	(Thai and al, 2013)	9.5671	8.1135	7.3133	6.6432	6.2753	6.1471	6.0688	
	Present	9.5618	8.1102	7.3099	6.6395	6.2725	6.1429	6.0635	
4 (2,1)	(Hosseini-Hashemi and al, 2011)	12.4560	10.5660	9.5261	8.6572	8.1875	8.0207	7.9166	
	(Reddy,2000)	12.4562	10.5677	9.5261	8.6509	8.1636	7.9934	7.8909	
	(Thai and al, 2013)	12.4565	10.5680	9.5263	8.6508	8.1624	7.9925	7.8905	
	Present	12.4477	10.5624	9.5336	8.6446	8.1576	7.9856	7.8816	

B- The perfect FG plates resting on an elastic foundation (Winkler-Pasternak)

Table IV.7 presents the fundamental nondimensional frequencies « $\tilde{\omega}$ » of square FG plates varying according to the thickness-to-length ratios "h/a", the power index "p", and the stiffness parameters of the Winkler-Pasternak foundation (K_0, K_I). According to (Baferani and al,2011) and (Shahsavari and al, 2018), the current results are compared to those presented previously. The agreement between the current results and those of existing models in the literature is evident in the table, confirming their adequacy.

Table IV. 7: Fundamental nondimensional frequencies « $\tilde{\omega}$ » of isotropic and square FG plates resting on Winkler-Pasternak foundations.

K_0	K_1	h / a	Théorie	p				
				0	0.5	1	2	5
0	0	0.05	(Baferani and al., 2011)	0.0290	0.0249	0.0227	0.0209	0.0197
			(Shahsavari and al., 2018)	0.0291	0.0248	0.0226	0.0206	0.0195
			Présente	0.0293	0.0249	0.0224	0.0208	0.0196
		0.1	(Baferani and al., 2011)	0.1134	0.0975	0.0891	0.0819	0.0767
			(Shahsavari and al., 2018)	0.1135	0.0970	0.0882	0.0806	0.0755
			Présente	0.1133	0.0971	0.0884	0.0803	0.0756
		0.15	(Baferani and al., 2011)	0.2454	0.2121	0.1939	0.1778	0.1648
			(Shahsavari and al., 2018)	0.2459	0.2109	0.1916	0.1746	0.1622
			Présente	0.2455	0.2111	0.1919	0.1749	0.1629
		0.2	(Baferani and al., 2011)	0.4154	0.3606	0.3299	0.3016	0.2765
			(Shahsavari and al., 2018)	0.4168	0.3586	0.3260	0.2961	0.2722
			Présente	0.4169	0.3589	0.3265	0.2967	0.2733
100	0	0.05	(Baferani and al., 2011)	0.0298	0.0258	0.0238	0.0221	0.0210
			(Shahsavari and al., 2018)	0.0298	0.0257	0.0236	0.0218	0.0208
			Présente	0.0299	0.0257	0.0238	0.0219	0.0209
		0.1	(Baferani and al., 2011)	0.1162	0.1012	0.0933	0.0867	0.0821
			(Shahsavari and al., 2018)	0.1163	0.1006	0.0923	0.0853	0.0809
			Présente	0.1170	0.1009	0.0923	0.0853	0.0809
		0.15	Baferani, Saidi et Ehteshami, (2011)	0.2519	0.2204	0.2036	0.1889	0.1775
			(Shahsavari and al., 2018)	0.2522	0.2190	0.2010	0.1855	0.1745
			Présente	0.2526	0.2199	0.2011	0.1855	0.1746
		0.2	(Baferani and al., 2011)	0.4273	0.3758	0.3476	0.3219	0.2999
			(Shahsavari and al., 2018)	0.4284	0.3734	0.3431	0.3159	0.2950
			Présente	0.4287	0.3738	0.3440	0.3160	0.2967

100	100	0.05	(Baferani and al., 2011)	0.0411	0.0395	0.0388	0.0386	0.0388
			(Shahsavari and al., 2018)	0.0411	0.0393	0.0386	0.0383	0.0385
			Présente	0.0411	0.0393	0.0386	0.0383	0.0385
		0.1	(Baferani and al., 2011)	0.1619	0.1563	0.1542	0.1535	0.1543
			(Shahsavari and al., 2018)	0.1616	0.1551	0.1525	0.1512	0.1521
			Présente	0.1620	0.1553	0.1526	0.1519	0.1530
		0.15	(Baferani and al., 2011)	0.3560	0.3460	0.3422	0.3412	0.3427
			(Shahsavari and al., 2018)	0.3551	0.3421	0.3367	0.3342	0.3358
			Présente	0.3552	0.3426	0.3370	0.3350	0.3358
		0.2	(Baferani and al., 2011)	0.6162	0.6026	0.5978	0.5970	0.5993
			(Shahsavari and al., 2018)	0.6137	0.5940	0.5856	0.5815	0.5843
			Présente	0.6140	0.5950	0.5860	0.5820	0.5850

C- Perfect and imperfect FG plates resting on the Winkler-Pasternak elastic foundation

The results of our analysis on porosity in the material of the FG plate are presented in this section. We examined two models of micro-void distribution and included them in our study.

Table IV.8 data illustrate the effects of porosity and Winkler-Pasternak foundation on the nondimensional frequency parameters " $\bar{\omega}$ " of square FG plates with " $p=1$ ". Our findings indicate that increasing porosity as a volume fraction has minimal impact on the " $\bar{\omega}$ " frequency parameter values of the non-uniform model. Additionally, we observed an inverse relationship between the nondimensional frequency parameter " $\bar{\omega}$ " and the porosity index " ξ " for uniform porosity models. However, for non-uniform porosities, the nondimensional frequency " $\bar{\omega}$ " increases with " ξ " even surpassing the frequency of a perfect plate. In conclusion, the highest values of the nondimensional frequency " $\bar{\omega}$ " are obtained for plates resting on an elastic foundation with a coefficient $(K_0, K_1) = 100$

Table IV. 8: Variations of the frequency parameters $\langle \bar{\omega} \rangle$ of perfect and imperfect square FG plates with respect to the stiffness of Winkler-Pasternak foundations ($p=1$).

(K_0, K_1)	h / a	ξ	Even porosity	Uneven porosity	Perfect
(0,0)	0.05	0.05	8.8876	9.7668	9.035
		0.1	8.7762	9.0476	
		0.15	8.5676	9.0576	
		0.2	8.8828	9.8856	
	0.1	0.05	8.7792	8.9408	8.839
		0.1	8.5535	8.8470	
		0.15	8.4598	8.8882	
		0.2	8.3058	8.9006	
	0.15	0.05	8.5531	8.6029	8.555
		0.1	8.2761	8.5456	
		0.15	8.1248	8.5494	
		0.2	7.9539	8.5542	
	0.2	0.05	8.0635	8.1795	8.189
		0.1	7.9385	8.1800	
		0.15	7.8015	8.1815	
		0.2	7.6450	8.1835	
(100,0)	0.05	0.05	9.3248	9.4560	9.445
		0.1	9.2032	9.4752	
		0.15	9.0696	9.4960	
		0.2	8.9192	9.5176	
	0.1	0.05	9.1372	9.2608	9.276
		0.1	9.0216	9.2770	
		0.15	8.8948	9.2950	
		0.2	8.7532	9.3142	
	0.15	0.05	8.8538	8.9654	8.960
		0.1	8.7480	8.9797	
		0.15	8.6328	8.9939	
		0.2	8.5037	9.0108	
	0.2	0.05	8.5095	8.6080	8.698
		0.1	8.4160	8.6195	
		0.15	8.3157	8.6325	
		0.2	8.1995	8.6455	
(100,100)	0.05	0.05	15.6217	15.5755	15.535
		0.1	15.8274	15.7115	
		0.15	16.0589	15.8576	
		0.2	16.3146	16.0115	
	0.1	0.05	15.4170	15.3577	15.326
		0.1	15.6250	15.4950	
		0.15	15.8600	15.6390	
		0.2	16.1210	15.7900	
	0.15	0.05	15.1180	15.0520	14.924

		0.1	15.3340	15.1860	14.574
		0.15	15.5730	15.3260	
		0.2	15.8380	15.4730	
	0.2	0.05	14.7730	14.6990	
		0.1	14.9930	14.8300	
		0.15	15.2360	14.9660	
		0.2	15.5060	15.1080	

IV.1.2. Dynamic analysis of free FG nano-plates at the nanoscale

A- Perfectly Supported Nano-FG Plate

Table IV.9 compares the results obtained for the first four nondimensional frequencies $\bar{\omega}$ of rectangular nano-plates (with aspect ratios $b/a=2$ and $a/h=10$) simply supported as a function of the power index P and the non-local parameter μ .

Our observations reveal that increasing μ has a significant effect on the nondimensional frequencies $\bar{\omega}$. Furthermore, it is important to note that the nondimensional frequencies $\bar{\omega}$ show an inverse relationship with the power index P in our results.

Table IV. 9:The first four nondimensional frequencies $\bar{\omega}$ of rectangular nano-plates (with (b/a=2 et a/h=10)

μ	Mode (m,n)	P						
		0	0,5	1	2	5	8	10
0	1(1,1)	3.6488	3.0972	2.7917	2.5342	2.3895	2.3384	2.3078
	2(1,2)	5.7622	4.8969	4.4145	4.0036	3.7632	3.6780	3.6290
	3(1,3)	9.1702	7.8007	7.0399	6.3754	5.9640	5.8180	5.7383
	4(2,1)	11.8024	10.0627	9.0743	8.2091	7.6527	7.4552	7.3511
0,1	1(1,1)	3,6511	3,0991	2,7935	2,5358	2,3910	2,3398	2,3094
	2(1,2)	5,7679	4,9018	4,4189	4,0076	3,7669	3,6817	3,6326
	3(1,3)	9,1850	7,8203	7,0512	6,3856	5,9735	5,8274	5,7475
	4(2,1)	11,8273	10,0838	9,0344	8,2264	7,6688	7,4709	7,3666
0,2	1(1,1)	3,6579	3,1048	2,7987	2,5405	2,3954	2,3442	2,3135
	2(1,2)	5,7851	4,9164	4,4321	4,0195	3,7781	3,6926	3,6434
	3(1,3)	9,2296	7,8583	7,0855	6,4167	6,0026	5,8557	5,7755
	4(2,1)	11,9027	10,1482	9,1514	8,2789	7,7177	7,5186	7,4135
0,3	1(1,1)	3,6693	3,1145	2,8074	2,5484	2,4029	2,3515	2,3207
	2(1,2)	5,8141	4,9410	4,4543	4,0396	3,7970	3,7111	3,6617
	3(1,3)	9,3055	7,9229	7,1437	6,4694	6,0519	5,9039	5,8230
	4(2,1)	12,0317	10,2582	9,2506	8,3686	7,8014	7,6001	7,4939
0,4	1(1,1)	3,6854	3,1282	2,8197	2,5596	2,4135	2,3618	2,3309
	2(1,2)	5,8554	4,9761	4,4860	4,0684	3,8240	3,7375	3,6877
	3(1,3)	9,4150	8,0161	7,2278	6,5455	6,1231	5,9733	5,8915
	4(2,1)	12,2196	10,4184	9,3950	8,4993	7,9232	7,7187	7,6109

B- Perfect and imperfect FG nano-plates resting on the Winkler-Pasternak elastic foundation

Table IV.10 highlights the influence of the Winkler-Pasternak foundation, the non-local parameter, and the porosity distribution on the nondimensional frequency $\bar{\omega}$ of square FG nano-plates with P=1 and a geometric ratio h/a =0.1. The obtained results reveal the combined impact of these factors on the nondimensional frequency $\bar{\omega}$ of the plates.

Table IV. 10: Variations of the frequency parameters " ω " of perfect and imperfect square FG nano-plates with respect to the stiffness of Winkler-Pasternak foundations ($\rho=1$) and ($h/a=0.1$).

(K_0, K_1)	μ	ξ	Even porosity	Uneven porosity	Perfet
(0,0)	0	0.05	8.7792	8.9408	9.030
		0.1	8.5535	8.8470	
		0.15	8.4598	8.8882	
		0.2	8.3058	8.9006	
	0.1	0.05	8.7893	8.9509	9.130
		0.1	8.5635	8.8570	
		0.15	8.4698	8.8982	
		0.2	8.3158	8.9106	
	0.2	0.05	8.7903	8.9609	9.143
		0.1	8.5735	8.8671	
		0.15	8.4735	8.9082	
		0.2	8.3258	8.9206	
	0.3	0.05	8.8003	8.9709	9.149
		0.1	8.5835	8.8771	
		0.15	8.4835	8.9182	
		0.2	8.3358	8.9306	
(100,0)	0	0.05	9.3248	9.4560	9.276
		0.1	9.2032	9.4752	
		0.15	9.0696	9.4960	
		0.2	8.9192	9.5176	
	0.1	0.05	9.3348	9.4660	9.298
		0.1	9.2132	9.4852	
		0.15	9.0796	9.5060	
		0.2	8.9292	9.5276	

	0.2	0.05	9.3448	9.4760	9.301
		0.1	9.2232	9.4952	
		0.15	9.0896	9.5860	
		0.2	8.9392	9.5376	
	0.3	0.05	9.3448	9.4760	9.311
		0.1	9.2232	9.4952	
		0.15	9.0896	9.5860	
		0.2	8.9392	9.5376	
(100,100)	0	0.05	15.6210	15.5700	15.326
		0.1	15.8270	15.7100	
		0.15	16.0580	15.8570	
		0.2	16.3140	16.0100	
	0.1	0.05	15.6214	15.5710	15.420
		0.1	15.8370	15.7200	
		0.15	16.0680	15.8670	
		0.2	16.3244	16.0111	
	0.2	0.05	15.6314	15.5810	15.430
		0.1	15.8470	15.7300	
		0.15	16.0780	15.8870	
		0.2	16.3344	16.0411	
	0.3	0.05	15.6414	15.5910	15.444
		0.1	15.8570	15.7400	
		0.15	16.0880	15.8970	
		0.2	16.3444	16.0511	

Figure IV.4 illustrates the variation of the first five modes of the nondimensional frequency ω^* of simply supported isotropic square FG plates as a function of modes for different values of the geometric ratio a/h .

The plots in Figure IV.4 show that the frequency ω^* increases with the increase in mode.

It can also be observed that the variation of frequency ω^* differs depending on the geometric ratio a/h . This indicates that the geometry of the plate significantly influences the vibration frequency.

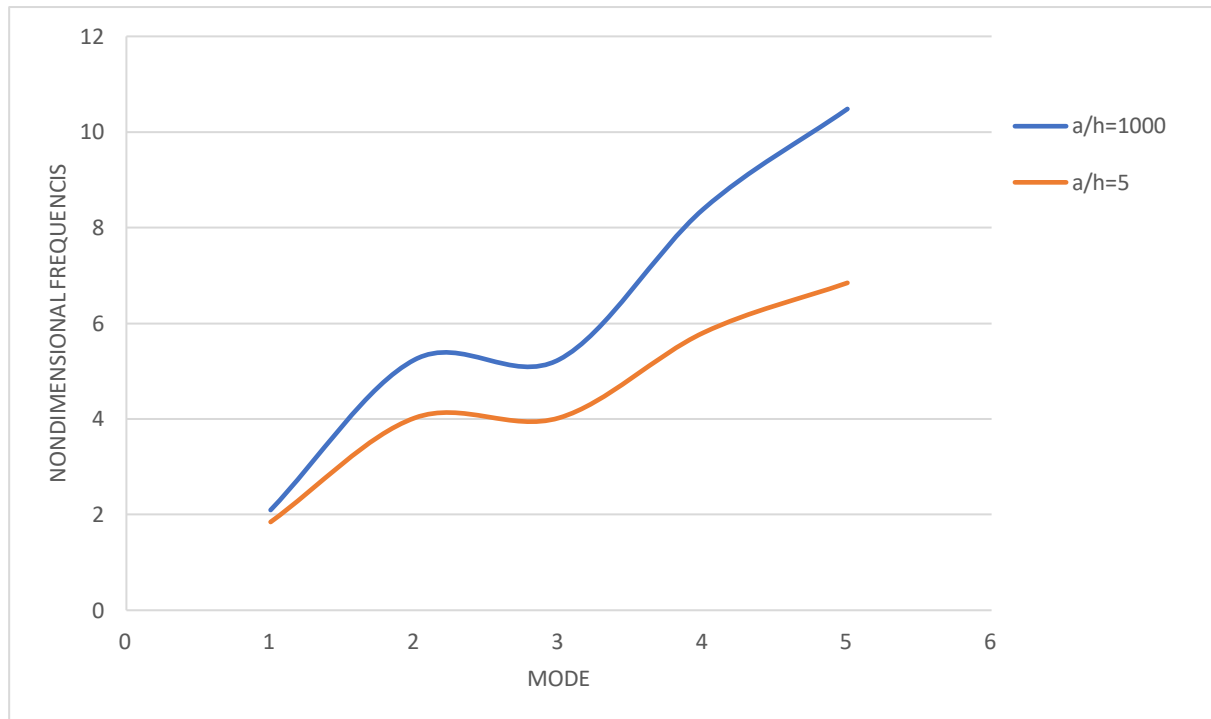


Figure IV. 4: The variation of the first five modes of the nondimensional frequency ω^* of simply supported isotropic square FG plates.

The variation of the nondimensional frequency $\hat{\omega}$ of AL/AL₂O₃ FG square plates as a function of the power index parameter is presented in **Figure IV.5**. A decrease in the nondimensional frequency is observed with an increase in the power index parameter (P) for all geometric ratios a/h . The plots indicate that the change in the nondimensional frequency of FG plates is strongly influenced by the ratio a/h . For moderately thick plates ($a/h=10$), the effect of the parameter (P) on the frequency is less pronounced than for thick plates $a/h=2$. This suggests that the ratio a/h of the plate plays a crucial role in accurately predicting the vibrational behavior of the plates.

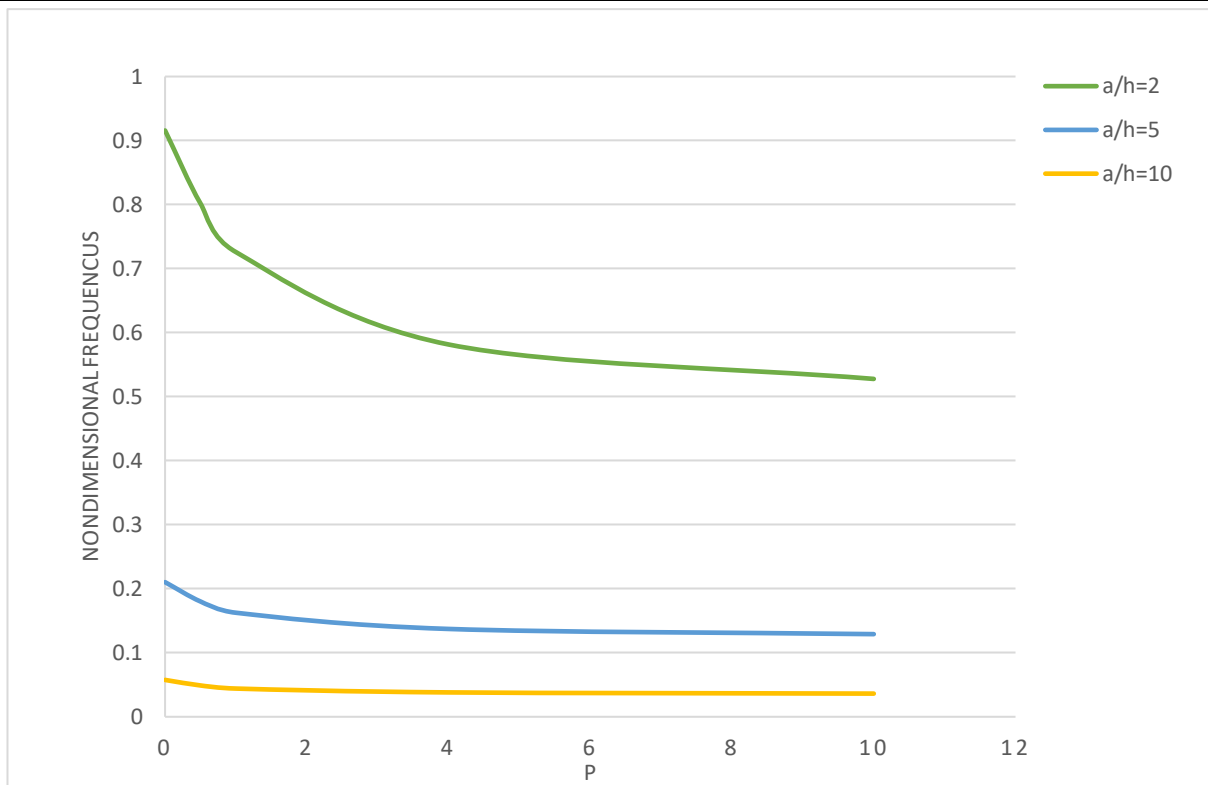


Figure IV. 5: The variation of the nondimensional frequency $\hat{\omega}$ of AL/AL₂O₃ FG square plates as a function of the power index parameter.

Figure IV.6 illustrates the relationship between the nondimensional frequency " $\bar{\omega}$ " of the perfect rectangular FG plate and the power index "p" for various a/h ratios. It is noted that the highest frequencies are observed for the thin plate with an a/h ratio of 20

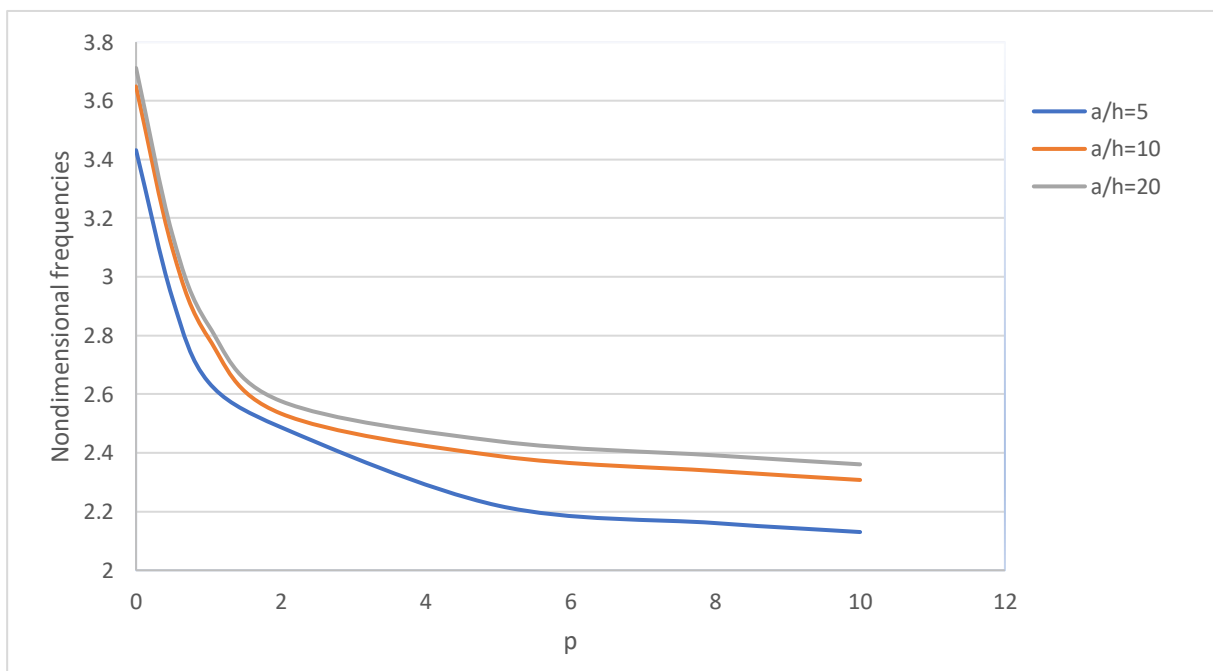


Figure IV. 6: The variation of the nondimensional frequency $\bar{\omega}$ of rectangular FG plates as a function of the power index parameter.

Figure IV.7 illustrates the effect of the elastic foundation and the power index on the nondimensional frequency $\tilde{\omega}$ of moderately thick plates with $a/h = 10$, with a notable influence of the power index.

The results show a decrease in frequency with an increase in the power index (P). Specifically, the results indicate that the highest frequencies are associated with plates resting on a Pasternak foundation, characterized by $(K_0, K_1) = 100$. In contrast, the lowest frequencies are recorded for plates without a foundation, where $(K_0, K_1) = 0$. However, the results for the Winkler foundation show slightly higher frequencies compared to plates without a foundation. This highlights the significant impact of the foundation nature on the vibrational properties of moderately thick plates.

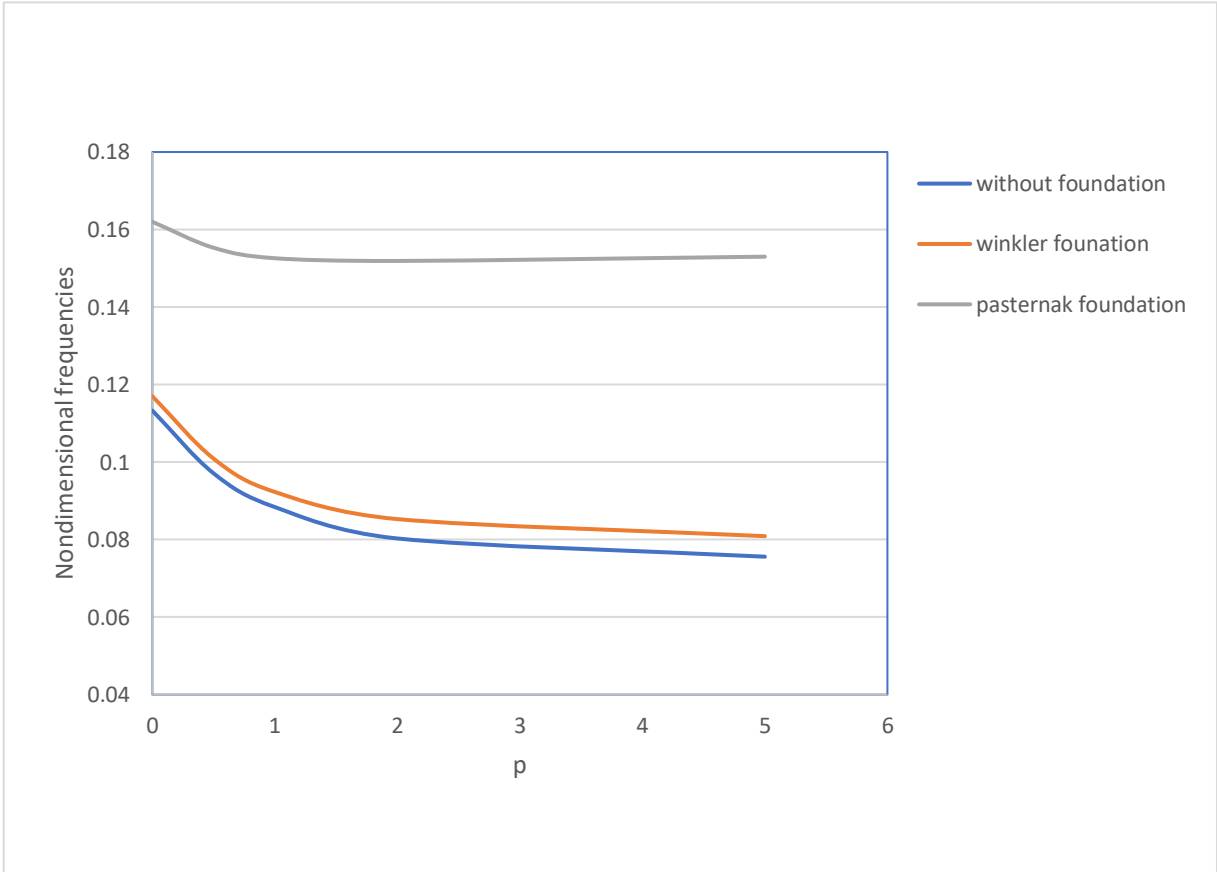


Figure IV. 7:the effect of the elastic foundation and the power index on the nondimensional frequency $\tilde{\omega}$ of plates with $a/h = 10$.

The variation of the nondimensional frequency " $\bar{\omega}$ " of imperfect FG plates with $h/a = 10$, resting on a Pasternak elastic foundation $(K_0, K_1) = 100$, as a function of the porosity index, is presented in **Figures IV.8** and **IV.9**. The results indicate that the frequency " $\bar{\omega}$ " increases with an increase in the porosity index ξ , whether the porosity distribution is even or uneven. It is observed that the frequency is slightly higher in the case of uneven porosity compared to even porosity.

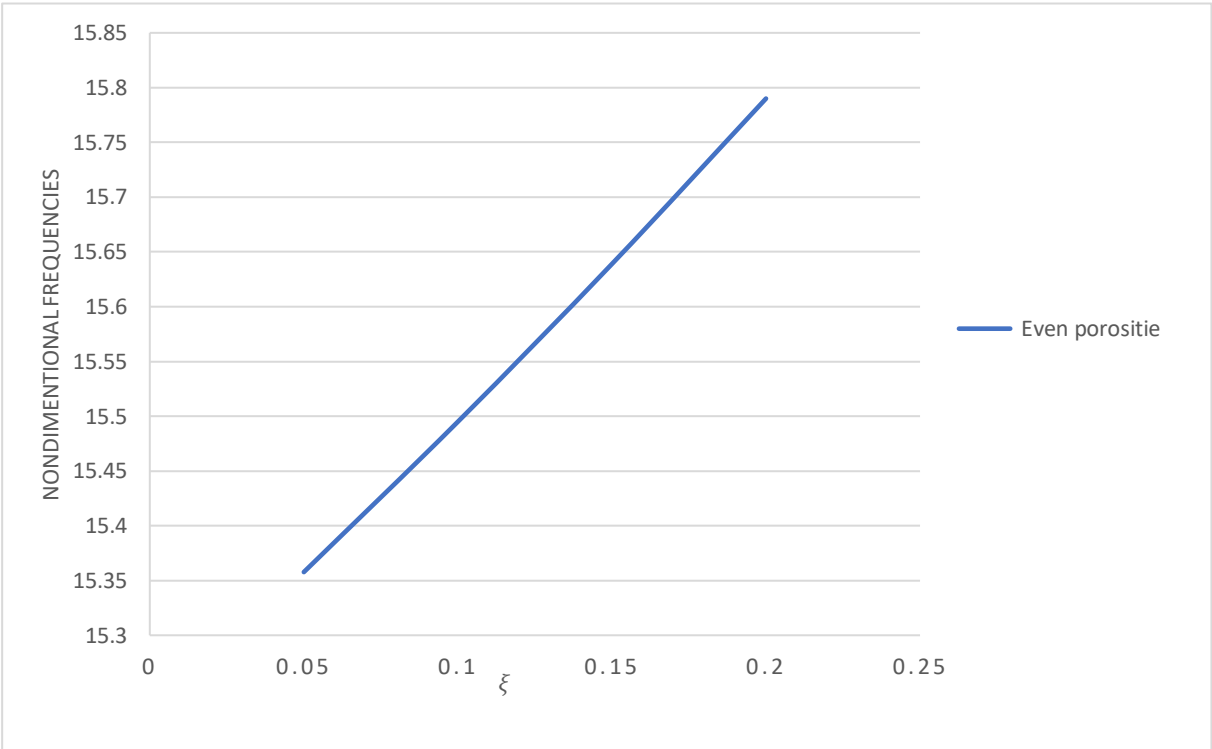


Figure IV. 8:The variation of the nondimensional frequency $\bar{\omega}$ of imperfect FG plates, resting on a Pasternak elastic foundation as a function of the porosity index for even porosities.

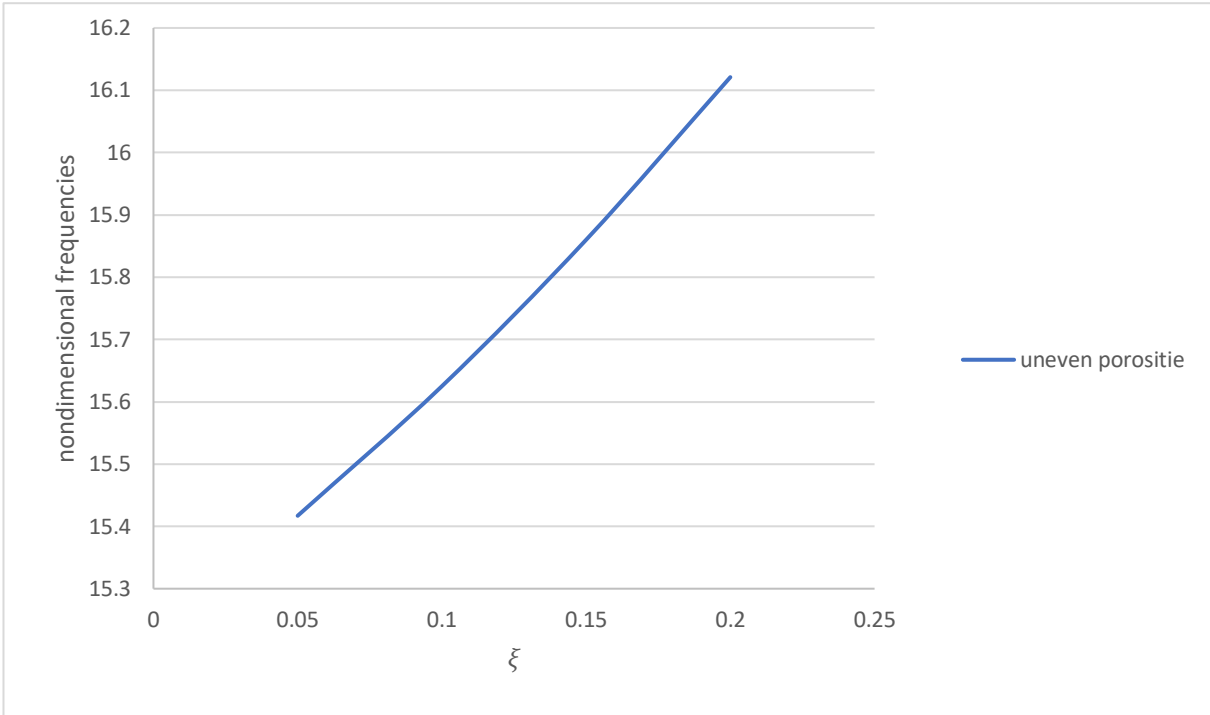


Figure IV. 9: The variation of the nondimensional frequency " $\bar{\omega}$ " of imperfect FG plates, resting on a Pasternak elastic foundation as a function of the porosity index for uneven porosities

Figure IV.10 illustrates the variation of the nondimensional frequency of both perfect and imperfect FG plates resting on a Pasternak elastic foundation, as a function of different porosity variations with a porosity index of 0.2.

According to the curves, it can be observed that the frequency is inversely proportional to the geometric ratio h/a . It is also evident that different porosity distributions result in different frequencies. These results emphasize the importance of considering porosity in the analysis of plates resting on a Pasternak elastic foundation.

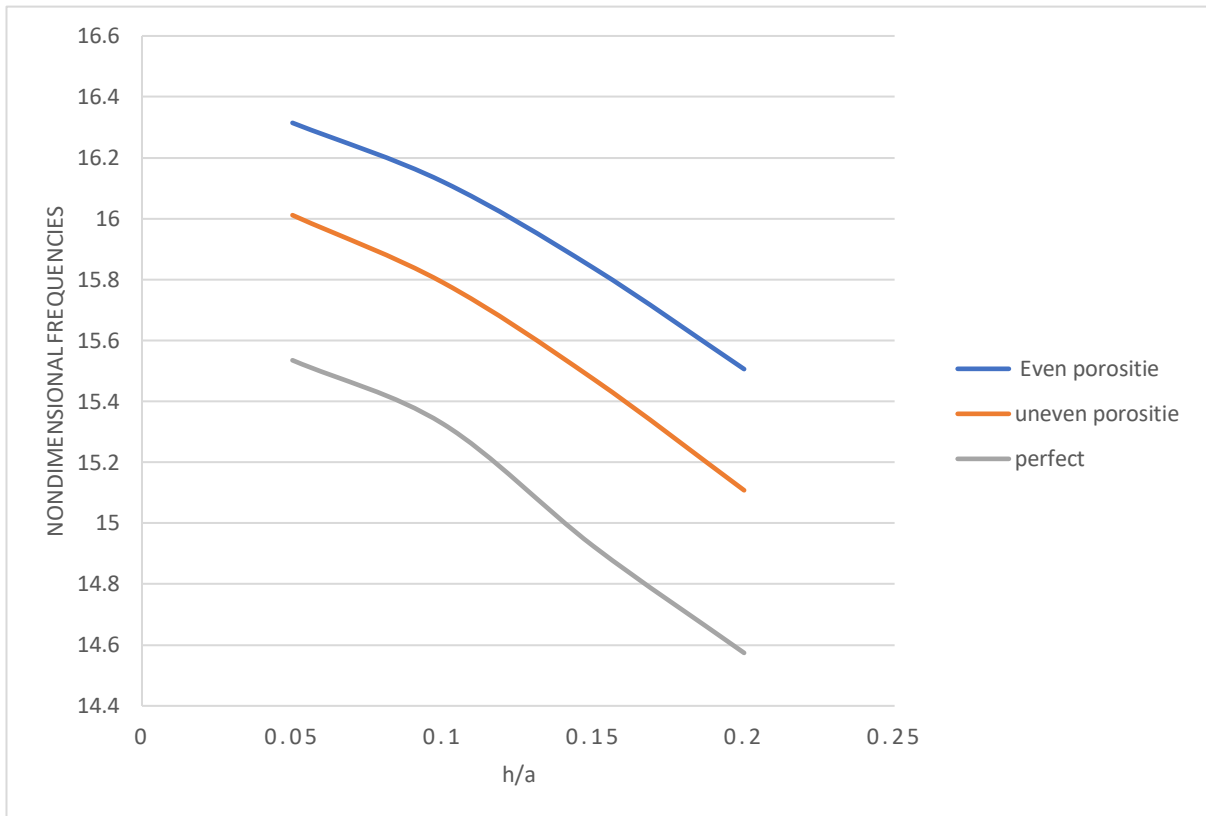


Figure IV. 10:the variation of the nondimensional frequency $\bar{\omega}$ of perfect and imperfect FG plates resting on a Pasternak elastic foundation, as a function of different porosity variations with $\xi = 0.2$.

The analysis of **figures IV.11** and **IV.12** highlights the significant impact of the non-local parameter on the vibrational behavior of functionally graded nano-plates. It is noteworthy that the variation in nondimensional frequency is directly related to the power index, suggesting that the mechanical properties of nano-plates can be finely tuned by modifying this parameter. Our work with an extended range of values μ (from 0 to 2.5) in figure IV.9 provides an in-depth understanding of non-local theory and its influence on the dynamics of nano-scale structures.

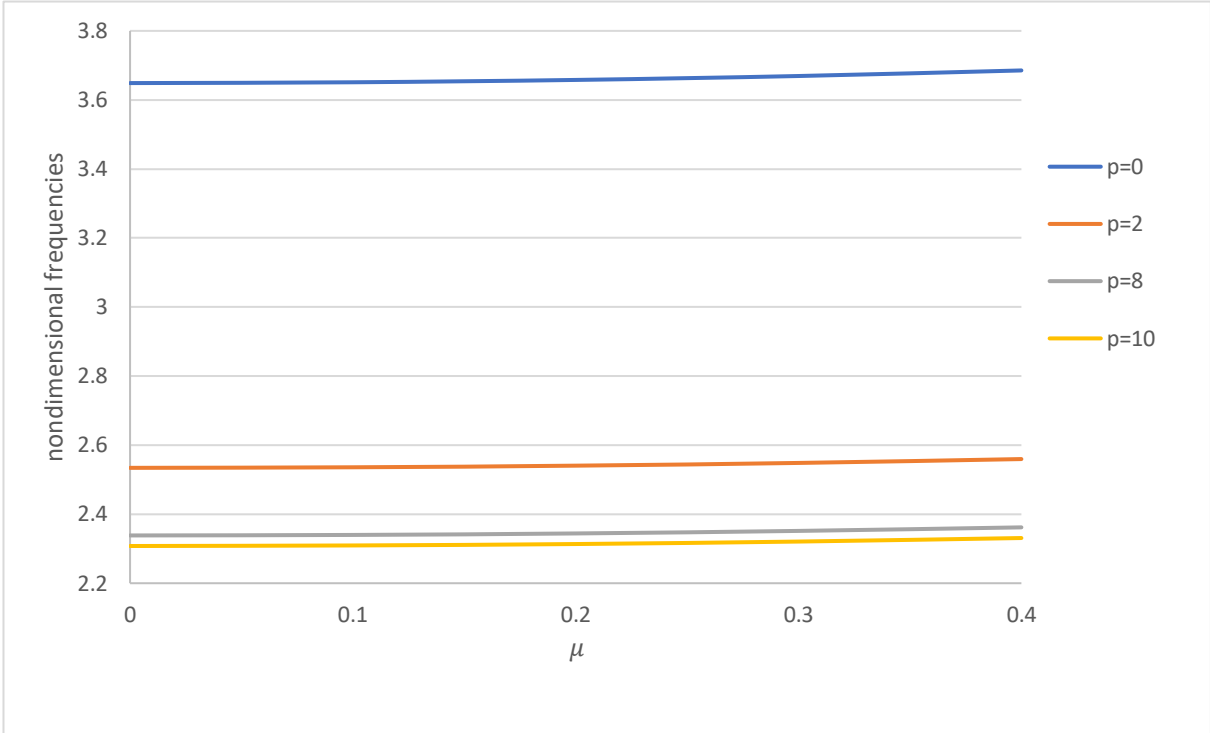


Figure IV. 11 The effect of non-local parameter (with μ values less than 0.5) on the variation of nondimensional frequencies of nano-plates without a foundation for different power index values.

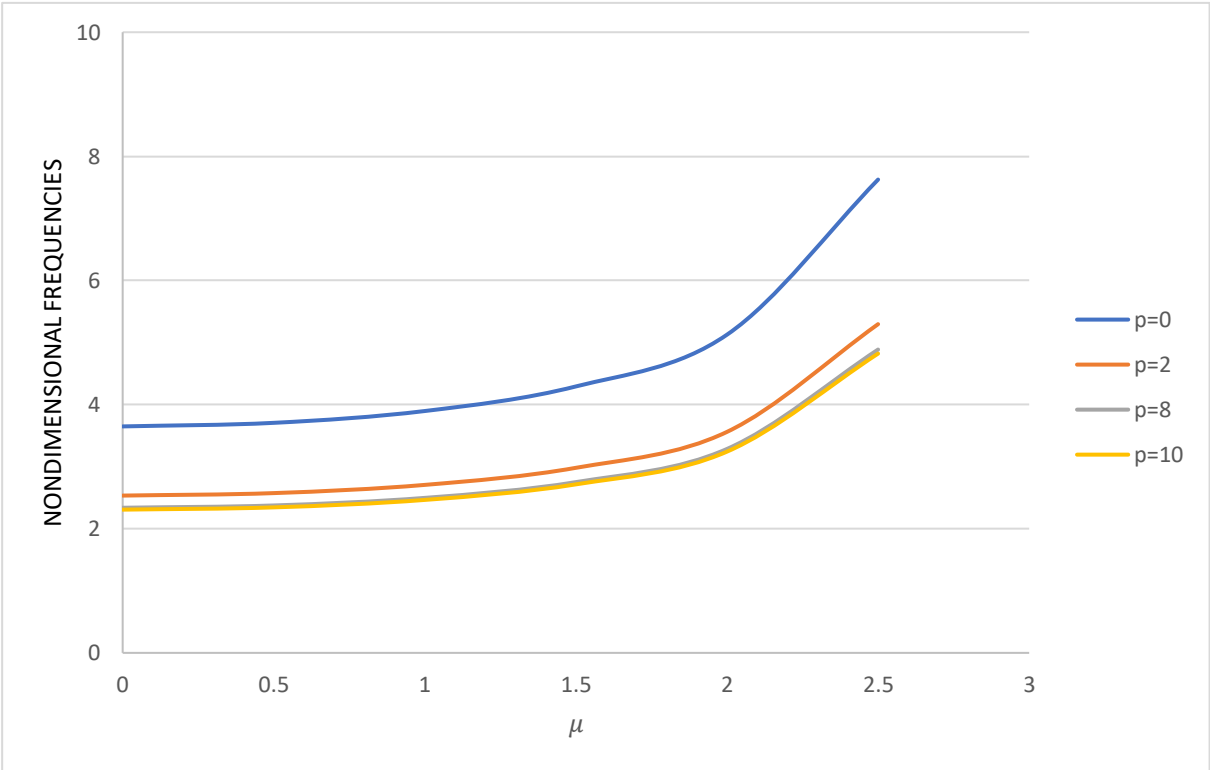


Figure IV. 12: The effect of non-local parameter (with μ values ranging from 0 to 2.5) on the variation of nondimensional frequencies of nano-plates without a foundation for different power index values.

Figure IV.13 illustrates the variation of the nondimensional frequency of the nano-plates ($h/a=0.1$). resting on different types of foundations. These data are analyzed based on non-local parameters, with a fixed porosity index of 0.2, and power index $p=1$.

The Pasternak elastic foundation type yields higher nondimensional frequency results compared to the other types of foundations studied. This suggests that this foundation offers better performance and greater stiffness in supporting the nano-plates.

Results for the Winkler foundation are lower than those for the Pasternak foundation but higher than those without a foundation.

Nano-plates without a foundation display the lowest nondimensional frequency results. This highlights the crucial importance of an appropriate foundation in enhancing the performance of nanoscale structures and reinforcing their dynamic response.

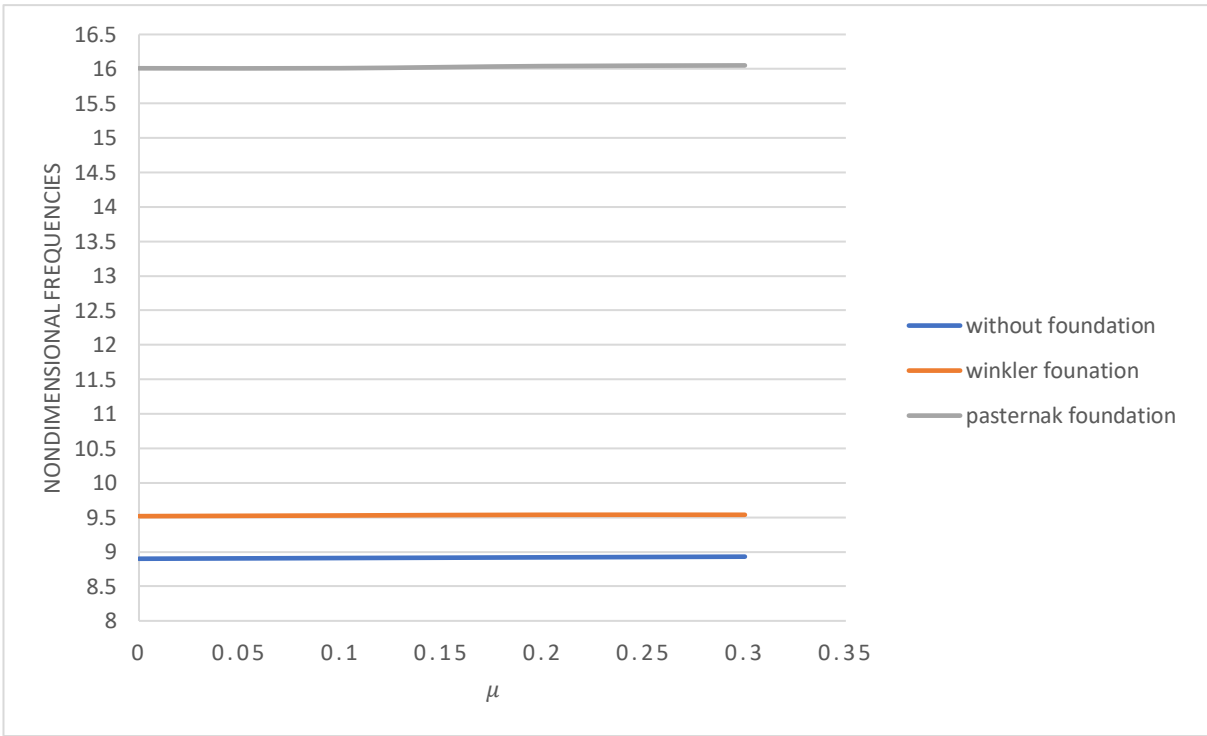


Figure IV. 13: the variation of the dimensionless frequency of nano-plates ($h/a=0.1$). based on different types of foundations. depending on non-local parameters, (with $\xi = 0.2$, $p = 1$).

IV.2. Conclusion:

In this chapter, the analysis of free vibrations of functionally graded (FG) plates has been conducted at different scales, macroscopic and nanometric, using an improved version of the first-order shear deformation theory (FSDT).

The mechanical properties of FG plates have been examined, considering a through-thickness variation following a power law tailored to include the effect of micro-voids. The accuracy and efficiency of the model have been confirmed through comparison with other established theories, demonstrating good agreement in all cases studied.

The Pasternak foundation theory approach has proven to be the most effective in explaining the stiffness of FG plates compared to Winkler foundations. It emerges from this analysis that several parameters, such as the non-local parameter, the volume fraction exponent, the porosity parameter, as well as geometric ratios and types of foundations, exert a significant influence on the dynamic response of functionally graded nanoplates.

GENERAL CONCLUSION

GENERAL CONCLUSION

Throughout the duration of this thesis, our exploration traversed the intricate landscape of structural mechanics, where we intricately applied the First Order Shear Deformation Theory (FSDT) with four unknowns to meticulously analyze the behavior of a functionally graded metal-ceramic nano plate (P-FGM). This investigation was not merely confined to theoretical realms but extended to practical applications, as the plate was carefully positioned atop an elastic Winkler-Pasternak foundation, adding another layer of complexity to our analytical endeavors. Recognizing the multifaceted nature of FG plates, we embarked on a journey of comprehensive analysis, integrating a vast array of equations encompassing equilibrium, compatibility, and structure-related boundary conditions into our calculations. Through painstaking scrutiny, we unearthed a treasure trove of insights, each shedding light on the intricate interplay of factors governing the behavior of these composite structures.

The ramifications of our findings were far-reaching, touching upon fundamental aspects of material science and structural engineering. Notably, we observed that the position within the plate's thickness emerged as a pivotal factor influencing its material characteristics, thereby exerting a profound influence on its mechanical and thermal behavior. This nuanced understanding enabled us to discern the intricate relationship between material composition and structural response, paving the way for optimized design methodologies in the realm of composite materials.

Furthermore, our investigation delved deep into the realm of porosity, revealing its profound impact on the mechanical properties of FG plates. The presence and size of porosities within the material matrix emerged as critical determinants of structural integrity, with microvoids notably altering deflection patterns and stress distributions in simply supported configurations. This newfound awareness of the role of porosity in composite materials represents a significant advancement in our understanding of material behavior under varying loading conditions.

Additionally, our examination illuminated the pivotal role played by the shear layer within the Pasternak foundation in shaping the dynamic response of FG plates. The intricate interplay between foundation characteristics and plate dynamics was laid bare, with the shear layer emerging as a key mediator of vibration frequencies and mode shapes. This insight into the

GENERAL CONCLUSION

dynamic behavior of FG plates offers invaluable guidance for the design and optimization of structures subjected to dynamic loading conditions.

In conclusion, our comprehensive analysis, spanning theoretical derivations and practical applications, has yielded profound insights into the behavior of functionally graded plates resting on Winkler-Pasternak foundations. By unraveling the complex interplay of material composition, porosity, and foundation characteristics, we have laid the groundwork for advanced design methodologies that promise enhanced structural performance and resilience in a diverse array of engineering applications.

Bibliographic references

Bibliographic references

- ADDOU Farouk Yahia. (2021). *Analyse statique et dynamique des structures FGM : formulation théorique et application dans le domaine de génie civil*. Repéré à univ-sba.dz
- Akhavan, H., Hashemi, S. H., Taher, H. R. D., Alibeigloo, A., & Vahabi, S. (2009). Exact solutions for rectangular Mindlin plates under in-plane loads resting on Pasternak elastic foundation. Part II: Frequency analysis. *Computational Materials Science*, 44(3).
<https://doi.org/10.1016/j.commatsci.2008.07.001>
- Al-Basyouni, K. S., Tounsi, A., & Mahmoud, S. R. (2015). Size dependent bending and vibration analysis of functionally graded micro beams based on modified couple stress theory and neutral surface position. *Composite Structures*, 125. <https://doi.org/10.1016/j.compstruct.2014.12.070>
- Amara, K., Tounsi, A., Mechab, I., & Adda-Bedia, E. A. (2010). Nonlocal elasticity effect on column buckling of multiwalled carbon nanotubes under temperature field. *Applied Mathematical Modelling*, 34(12). <https://doi.org/10.1016/j.apm.2010.03.029>
- Ashwinkumar, A. K. (2017). Review on functionally graded materials and various theories. International research. *engineering and technology*.
- Avcar, M. (2016). Effects of material non-homogeneity and two parameter elastic foundation on fundamental frequency parameters of timoshenko beams. Dans *Acta Physica Polonica A* (Vol. 130). <https://doi.org/10.12693/APhysPolA.130.375>
- Avcar, Mehmet, & Mohammed, W. K. M. (2018). Free vibration of functionally graded beams resting on Winkler-Pasternak foundation. *Arabian Journal of Geosciences*, 11(10).
<https://doi.org/10.1007/s12517-018-3579-2>
- Baferani, A. H., Saidi, A. R., & Ehteshami, H. (2011). Accurate solution for free vibration analysis of functionally graded thick rectangular plates resting on elastic foundation. *Composite Structures*, 93(7). <https://doi.org/10.1016/j.compstruct.2011.01.020>
- Bakar, W. Z. W., Basri, S., Jamaludin, S. N. S., & Sajjad, A. (2018). Functionally graded materials: An overview of dental applications. *World Journal of Dentistry*. <https://doi.org/10.5005/jp-journals-10015-1523>
- Bao, G., & Wang, L. (1995). Multiple cracking in functionally graded ceramic/metal coatings. *International Journal of Solids and Structures*, 32(19). [https://doi.org/10.1016/0020-7683\(94\)00267-Z](https://doi.org/10.1016/0020-7683(94)00267-Z)
- BENSALAH, N. , and K. A. (2022). *Vibration libre des plaques FGM en utilisant une simple Théorie de déformation d'ordre élevée (nth-HSDT)* .

Bibliographic references

- Benzair, A., Tounsi, A., Besseghier, A., Heireche, H., Moulay, N., & Boumia, L. (2008). The thermal effect on vibration of single-walled carbon nanotubes using nonlocal Timoshenko beam theory. *Journal of Physics D: Applied Physics*, 41(22). <https://doi.org/10.1088/0022-3727/41/22/225404>
- Bessaim, A., Houari, M. S. A., Tounsi, A., Mahmoud, S. R., & Bedia, E. A. A. (2013). A new higher-order shear and normal deformation theory for the static and free vibration analysis of sandwich plates with functionally graded isotropic face sheets. *Journal of Sandwich Structures and Materials*, 15(6). <https://doi.org/10.1177/1099636213498888>
- Bohidar, S. K., Sharma, R., & Mishra, P. R. (2014). Functionally Graded Materials: A Critical Review. *International Journal of Research*, 1(7).
- Bouderba, B., Houari, M. S. A., & Tounsi, A. (2013). Thermomechanical bending response of FGM thick plates resting on winkler-pasternak elastic foundations. *Steel and Composite Structures*, 14(1). <https://doi.org/10.12989/scs.2013.14.1.085>
- Bounouara, F., Benrahou, K. H., Belkorissat, I., & Tounsi, A. (2016). A nonlocal zeroth-order shear deformation theory for free vibration of functionally graded nanoscale plates resting on elastic foundation. *Steel and Composite Structures*, 20(2). <https://doi.org/10.12989/scs.2016.20.2.227>
- BOUNOUARA Fatima. (2016). *Etude du comportement mécaniques des nano plaques* .
- Chawla, K. K. (2012). *Composite materials: Science and engineering, third edition. Composite Materials: Science and Engineering, Third Edition*. (S.l.) : (s.n.). <https://doi.org/10.1007/978-0-387-74365-3>
- Chung, Y. L. , & C. S. H. The residual stress of functionally graded materials. (2001).
- Delale, F., & Erdogan, F. (1983). The crack problem for a nonhomogeneous plane. *Journal of Applied Mechanics, Transactions ASME*, 50(3). <https://doi.org/10.1115/1.3167098>
- Draoui, A., Zidour, M., Tounsi, A., & Adim, B. (2019). Static and dynamic behavior of nanotubes-reinforced sandwich plates using (FSDT). *Journal of Nano Research*, 57. <https://doi.org/10.4028/www.scientific.net/JNanoR.57.117>
- Ebrahimi, F., Mahmoodi, F., & Barati, M. R. (2017). Thermo-mechanical vibration analysis of functionally graded micro/nanoscale beams with porosities based on modified couple stress theory. *Advances in Materials Research (South Korea)*, 6(3). <https://doi.org/10.12989/amr.2017.6.3.279>
- El-Haina, F., Bakora, A., Bousahla, A. A., Tounsi, A., & Mahmoud, S. R. (2017). A simple analytical approach for thermal buckling of thick functionally graded sandwich plates. *Structural Engineering and Mechanics*, 63(5). <https://doi.org/10.12989/sem.2017.63.5.585>

Bibliographic references

- ELLALI, M. (2019). *Analyse du flambement thermique des matériaux FGM piézoélectriques (Doctoral dissertation, Université de Ain Témouchent Belhadj Bouchaib).*
- ELMASCRI, S. (2020). *Contribution à l'étude de l'effet de température sur le comportement vibratoire des structures en matériaux composites avancés* .
- Eltaher, M. A., Fouda, N., El-midany, T., & Sadoun, A. M. (2018). Modified porosity model in analysis of functionally graded porous nanobeams. *Journal of the Brazilian Society of Mechanical Sciences and Engineering*, 40(3). <https://doi.org/10.1007/s40430-018-1065-0>
- Halbe, J. (2021). *Development of a sustainable systems engineering framework for the design and assessment of sustainability visions*. . University (Canada). : (s.n.).
- Heireche, H., Tounsi, A., Benzair, A., Maachou, M., & Adda Bedia, E. A. (2008). Sound wave propagation in single-walled carbon nanotubes using nonlocal elasticity. *Physica E: Low-Dimensional Systems and Nanostructures*, 40(8). <https://doi.org/10.1016/j.physe.2007.12.021>
- Hellal, H., Bourada, M., Hebali, H., Bourada, F., Tounsi, A., Bousahla, A. A., & Mahmoud, S. R. (2021). Dynamic and stability analysis of functionally graded material sandwich plates in hygro-thermal environment using a simple higher shear deformation theory. *Journal of Sandwich Structures and Materials*, 23(3). <https://doi.org/10.1177/1099636219845841>
- Hildebrand, F. B., Reissner, E., & Thomas, G. B. (1949). Notes on the Foundations of the Theory of Small Displacements of Orthotropic Shells. *NACA TN 1833*.
- Hosseini-Hashemi, S., Fadaee, M., & Atashipour, S. R. (2011). A new exact analytical approach for free vibration of ReissnerMindlin functionally graded rectangular plates. *International Journal of Mechanical Sciences*, 53(1). <https://doi.org/10.1016/j.ijmecsci.2010.10.002>
- Hsu, M. H. (2010). Vibration analysis of orthotropic rectangular plates on elastic foundations. *Composite Structures*, 92(4). <https://doi.org/10.1016/j.compstruct.2009.09.015>
- Iakovidis, D., Gadanakis, Y., & Park, J. (2022). Farm-level sustainability assessment in Mediterranean environments: Enhancing decision-making to improve business sustainability. *Environmental and Sustainability Indicators*, 15. <https://doi.org/10.1016/j.indic.2022.100187>
- J. Wang, O. V. D. B. and J. V. (1999). Functionally Graded Materials: . *Journal of Materials Science*.
- Jalali, S. K., Beigrezaee, M. J., & Pugno, N. M. (2021). Is it always worthwhile to resolve the governing equations of plate theories for graded porosity along the thickness? *Composite Structures*, 256. <https://doi.org/10.1016/j.compstruct.2020.112960>

Bibliographic references

- Kant, T., & Swaminathan, K. (2002). Analytical solutions for the static analysis of laminated composite and sandwich plates based on a higher order refined theory. *Composite Structures*, 56(4). [https://doi.org/10.1016/S0263-8223\(02\)00017-X](https://doi.org/10.1016/S0263-8223(02)00017-X)
- Karami, B., Shahsavari, D., Janghorban, M., & Tounsi, A. (2019). Resonance behavior of functionally graded polymer composite nanoplates reinforced with graphene nanoplatelets. *International Journal of Mechanical Sciences*, 156. <https://doi.org/10.1016/j.ijmecsci.2019.03.036>
- Kaushal, S., Gupta, D., & Bhowmick, H. (2018). An approach for functionally graded cladding of composite material on austenitic stainless steel substrate through microwave heating. *Journal of Composite Materials*, 52(3). <https://doi.org/10.1177/0021998317705977>
- Kneifati, M. C. (1985). Analysis of Plates on a Kerr Foundation Model. *Journal of Engineering Mechanics*, 111(11). [https://doi.org/10.1061/\(asce\)0733-9399\(1985\)111:11\(1325\)](https://doi.org/10.1061/(asce)0733-9399(1985)111:11(1325))
- Kobayashi, H., & Sonoda, K. (1989). Rectangular mindlin plates on elastic foundations. *International Journal of Mechanical Sciences*, 31(9). [https://doi.org/10.1016/S0020-7403\(89\)80003-7](https://doi.org/10.1016/S0020-7403(89)80003-7)
- Koizumi, M. (1997). FGM activities in Japan. *Composites Part B: Engineering*, 28(1-2). [https://doi.org/10.1016/s1359-8368\(96\)00016-9](https://doi.org/10.1016/s1359-8368(96)00016-9)
- Kolahchi, R., Safari, M., & Esmailpour, M. (2016). Dynamic stability analysis of temperature-dependent functionally graded CNT-reinforced visco-plates resting on orthotropic elastomeric medium. *Composite Structures*, 150. <https://doi.org/10.1016/j.compstruct.2016.05.023>
- Lam, K. Y., Wang, C. M., & He, X. Q. (2000). Canonical exact solutions for Levy-plates on two-parameter foundation using Green's functions. *Engineering Structures*, 22(4). [https://doi.org/10.1016/S0141-0296\(98\)00116-3](https://doi.org/10.1016/S0141-0296(98)00116-3)
- Leissa, A. W. (1973). The free vibration of rectangular plates. *Journal of Sound and Vibration*, 31(3). [https://doi.org/10.1016/S0022-460X\(73\)80371-2](https://doi.org/10.1016/S0022-460X(73)80371-2)
- Li, Y., Feng, Z., Hao, L., Huang, L., Xin, C., Wang, Y., ... Peijs, T. (2020). A Review on Functionally Graded Materials and Structures via Additive Manufacturing: From Multi-Scale Design to Versatile Functional Properties. *Advanced Materials Technologies*. <https://doi.org/10.1002/admt.201900981>
- Liew, K. M., Xiang, Y., & Kitipornchai, S. (1993). Transverse vibration of thick rectangular plates-I. Comprehensive sets of boundary conditions. *Computers and Structures*, 49(1). [https://doi.org/10.1016/0045-7949\(93\)90122-T](https://doi.org/10.1016/0045-7949(93)90122-T)

Bibliographic references

- Lü, C. F., Lim, C. W., & Chen, W. Q. (2009). Exact solutions for free vibrations of functionally graded thick plates on elastic foundations. *Mechanics of Advanced Materials and Structures*, 16(8).
<https://doi.org/10.1080/15376490903138888>
- Lu, P., Zhang, P. Q., Lee, H. P., Wang, C. M., & Reddy, J. N. (2007). Non-local elastic plate theories. *Proceedings of the Royal Society A: Mathematical, Physical and Engineering Sciences*, 463(2088). <https://doi.org/10.1098/rspa.2007.1903>
- Mahamood, R. M., Akinlabi, E. T., Shukla, M., & Pityana, S. (2012). Functionally graded material: An overview. Dans *Lecture Notes in Engineering and Computer Science* (Vol. 3).
- Makwana, A. B., Panchal, K. C., & Gandhi, A. H. (2014). *Stress Analysis of Functionally Graded Material Plate with Cut-out*. *International Journal of Advanced Mechanical Engineering*.
- Manna, M. C. (2005). Free vibration analysis of isotropic rectangular plates using a high-order triangular finite element with shear. *Journal of Sound and Vibration*, 281(1-2).
<https://doi.org/10.1016/j.jsv.2004.01.015>
- Matsunaga, H. (2008). Free vibration and stability of functionally graded plates according to a 2-D higher-order deformation theory. *Composite Structures*, 82(4).
<https://doi.org/10.1016/j.compstruct.2007.01.030>
- Monaco, G. T., Fantuzzi, N., Fabbrocino, F., & Luciano, R. (2021). Critical temperatures for vibrations and buckling of magneto-electro-elastic nonlocal strain gradient plates. *Nanomaterials*, 11(1).
<https://doi.org/10.3390/nano11010087>
- Naebe, M., & Shirvanimoghaddam, K. (2016). Functionally graded materials: A review of fabrication and properties. *Applied Materials Today*. <https://doi.org/10.1016/j.apmt.2016.10.001>
- Naghdi, P. M. (1957). On the theory of thin elastic shells. *Quarterly of Applied Mathematics*, 14(4).
<https://doi.org/10.1090/qam/84284>
- Ngo, T. D., Kashani, A., Imbalzano, G., Nguyen, K. T. Q., & Hui, D. (2018). Additive manufacturing (3D printing): A review of materials, methods, applications and challenges. *Composites Part B: Engineering*. <https://doi.org/10.1016/j.compositesb.2018.02.012>
- Nguyen, H. N., Hong, T. T., Van Vinh, P., Quang, N. D., & Van Thom, D. (2019). A refined simple first-order shear deformation theory for static bending and free vibration analysis of advanced composite plates. *Materials*, 12(15). <https://doi.org/10.3390/ma12152385>
- Pasternak, P. L. (1954). On a new method of analysis of an elastic foundation by means of two foundation constants. *Cosudarstvennoe Izdatelstvo Literaturi po Stroitelstvu i Arkhitekture, Moscow, USSR*.

Bibliographic references

- Penna, R., Feo, L., Lovisi, G., & Fabbrocino, F. (2021). Hygro-thermal vibration of porous fg nano-beams based on local/nonlocal stress gradient theory of elasticity. *Nanomaterials*, *11*(4). <https://doi.org/10.3390/nano11040910>
- Penna, R., Feo, L., Lovisi, G., & Fabbrocino, F. (2022). Application of the Higher-Order Hamilton Approach to the Nonlinear Free Vibrations Analysis of Porous FG Nano-Beams in a Hygrothermal Environment Based on a Local/Nonlocal Stress Gradient Model of Elasticity. *Nanomaterials*, *12*(12). <https://doi.org/10.3390/nano12122098>
- Raju, K. K., & Hinton, E. (1980). Natural frequencies and modes of rhombic mindlin plates. *Earthquake Engineering & Structural Dynamics*, *8*(1). <https://doi.org/10.1002/eqe.4290080106>
- Reddy, J. N. (1984). A simple higher-order theory for laminated composite plates. *Journal of Applied Mechanics, Transactions ASME*, *51*(4). <https://doi.org/10.1115/1.3167719>
- Reddy, J. N. (1997). *Mechanics of laminated composite plates : theory and analysis*. NA (Vol. NA). (S.l.) : (s.n).
- Reddy, J. N., & Pang, S. D. (2008). Nonlocal continuum theories of beams for the analysis of carbon nanotubes. *Journal of Applied Physics*, *103*(2). <https://doi.org/10.1063/1.2833431>
- Reissner, E. (1945). The Effect of Transverse Shear Deformation on the Bending of Elastic Plates. *Journal of Applied Mechanics, Transactions ASME*, *12*(2). <https://doi.org/10.1115/1.4009435>
- SAID, A. (2016). *Etude et Analyse des Plaque FGM en Génie Civil* .
- Sato, M., Inoue, A., & Shima, H. (2017). Bamboo-inspired optimal design for functionally graded hollow cylinders. *PLoS ONE*, *12*(5). <https://doi.org/10.1371/journal.pone.0175029>
- Shahsavari, D., Shahsavari, M., Li, L., & Karami, B. (2018). A novel quasi-3D hyperbolic theory for free vibration of FG plates with porosities resting on Winkler/Pasternak/Kerr foundation. *Aerospace Science and Technology*, *72*. <https://doi.org/10.1016/j.ast.2017.11.004>
- Sobhy, M. (2013). Buckling and free vibration of exponentially graded sandwich plates resting on elastic foundations under various boundary conditions. *Composite Structures*, *99*. <https://doi.org/10.1016/j.compstruct.2012.11.018>
- Sofiyev, A. H., & Avcar, M. (2010). The Stability of Cylindrical Shells Containing an FGM Layer Subjected to Axial Load on the Pasternak Foundation. *Engineering*, *02*(04). <https://doi.org/10.4236/eng.2010.24033>
- Thai, H. T., & Choi, D. H. (2013). A simple first-order shear deformation theory for the bending and free vibration analysis of functionally graded plates. *Composite Structures*, *101*. <https://doi.org/10.1016/j.compstruct.2013.02.019>

Bibliographic references

- Thai, H. T., & Vo, T. P. (2013). A new sinusoidal shear deformation theory for bending, buckling, and vibration of functionally graded plates. *Applied Mathematical Modelling*, 37(5).
<https://doi.org/10.1016/j.apm.2012.08.008>
- Thakur, M. S. H., Islam, M., Monisha, N. J., Bose, P., Munshi, M. A. M., & Pial, T. H. (2021). Atomistic modelling of functionally graded Cu - Ni alloy and its implication on the mechanical properties of nanowires. Dans *AIP Conference Proceedings* (Vol. 2324).
<https://doi.org/10.1063/5.0037478>
- Timoshenko, S. , & W.-K. S. (1959). *Theory of plates and shells* (Vol. Vol. 2, pp. 240-246). New York: McGraw-hill. : (s.n).
- Touratier, M. (1991). An efficient standard plate theory. *International Journal of Engineering Science*, 29(8). [https://doi.org/10.1016/0020-7225\(91\)90165-Y](https://doi.org/10.1016/0020-7225(91)90165-Y)
- Valencia, F. J., Aurora, V., Ramírez, M., Ruestes, C. J., Prada, A., Varas, A., & Rogan, J. (2022). Probing the Mechanical Properties of Porous Nanoshells by Nanoindentation. *Nanomaterials*, 12(12). <https://doi.org/10.3390/nano12122000>
- Wang, K., Cheng, J. F., Sun, W. J., & Xue, H. S. (2012). An approach for increase of reinforcement content in particle rich zone of centrifugally cast SiCP/Al composites. *Journal of Composite Materials*, 46(9). <https://doi.org/10.1177/0021998311414070>
- Wang, L., Hou, Y., Zhang, L., & Liu, G. (2017). A combined static-and-dynamics mechanics analysis on the bridge deck pavement. *Journal of Cleaner Production*, 166.
<https://doi.org/10.1016/j.jclepro.2017.08.034>
- Wang, Y. H., Tham, L. G., & Cheung, Y. K. (2005). Beams and plates on elastic foundations: A review. *Progress in Structural Engineering and Materials*. <https://doi.org/10.1002/pse.202>
- Wattanasakulpong, N., & Ungbhakorn, V. (2014). Linear and nonlinear vibration analysis of elastically restrained ends FGM beams with porosities. *Aerospace Science and Technology*, 32(1).
<https://doi.org/10.1016/j.ast.2013.12.002>
- Youcef, D. O., Kaci, A., Benzair, A., Bousahla, A. A., & Tounsi, A. (2018). Dynamic analysis of nanoscale beams including surface stress effects. *Smart Structures and Systems*, 21(1).
<https://doi.org/10.12989/sss.2018.21.1.065>
- Zarga, D., Tounsi, A., Bousahla, A. A., Bourada, F., & Mahmoud, S. R. (2019). Thermomechanical bending study for functionally graded sandwich plates using a simple quasi-3D shear deformation theory. *Steel and Composite Structures*, 32(3).
<https://doi.org/10.12989/scs.2019.32.3.389>

Bibliographic references

- Zenkour, A. M. (2006). Generalized shear deformation theory for bending analysis of functionally graded plates. *Applied Mathematical Modelling*, 30(1).
<https://doi.org/10.1016/j.apm.2005.03.009>
- Zhang, C., Chen, F., Huang, Z., Jia, M., Chen, G., Ye, Y., ... Lavernia, E. J. (2019). Additive manufacturing of functionally graded materials: A review. *Materials Science and Engineering: A*, 764. <https://doi.org/10.1016/j.msea.2019.138209>
- Zidi, M., Houari, M. S. A., Tounsi, A., Bessaim, A., & Mahmoud, S. R. (2017). A novel simple two-unknown hyperbolic shear deformation theory for functionally graded beams. *Structural Engineering and Mechanics*, 64(2). <https://doi.org/10.12989/sem.2017.64.2.145>

